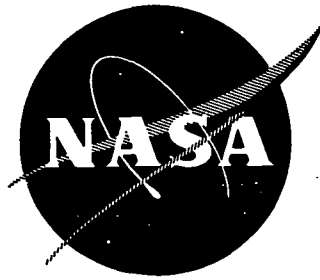


N 7 2 3 1 4 9 6



CASE FILE  
COPY

METALLIC POSITIVE EXPULSION DIAPHRAGMS

by  
D. Gleich

ARDE, INC.

Prepared for:

NATIONAL AERONAUTICS AND SPACE ADMINISTRATION  
NASA Lewis Research Center  
Contract NAS 3-12026  
R. F. Lark, Project Manager

1. Report No. NASA CR-72775		2. Government Accession No.		3. Recipient's Catalog No.	
4. Title and Subtitle  METALLIC POSITIVE EXPULSION DIAPHRAGMS				5. Report Date January 1972	
				6. Performing Organization Code	
7. Author(s)  D. Gleich				8. Performing Organization Report No. ARDE 46002	
9. Performing Organization Name and Address ARDE, INC. 19 Industrial Avenue Mahwah, New Jersey 07430				10. Work Unit No.	
				11. Contract or Grant No. NAS 3-12026	
12. Sponsoring Agency Name and Address National Aeronautics and Space Administration Washington, D. C. 20546				13. Type of Report and Period Covered Contractor Report	
				14. Sponsoring Agency Code	
15. Supplementary Notes Project Manager, R. F. Lark, Materials & Structures Division, NASA Lewis Research Center					
16. Abstract  <p>High-cycle life ring-reinforced hemispherical type positive expulsion diaphragm performance was demonstrated by room temperature fluid expulsion tests of 13" diameter, 8 mil thick stainless steel configurations. A maximum of eleven (11) leak-free, fluid expulsions were achieved by a 25° cone angle diaphragm hoop-reinforced with .110" cross-sectional diameter wires. This represents a 70% improvement in diaphragm reversal cycle life compared to results previously obtained. The reversal tests confirmed analytic predictions for diaphragm cycle life increases due to increasing values of diaphragm cone angle, radius to thickness ratio and material strain to necking capacity.</p> <p>Practical fabrication techniques were demonstrated for forming close-tolerance, thin corrugated shells and for obtaining closely controlled reinforcing ring stiffness required to maximize diaphragm cycle life. A non-destructive inspection technique for monitoring large local shell bending strains was developed.</p>					
17. Key Words (Suggested by Author(s))  Diaphragm, high cycle-life diaphragm, metallic diaphragm, positive expulsion diaphragm, ring-reinforced diaphragm			18. Distribution Statement  Unclassified - unlimited		
19. Security Classif. (of this report)  Unclassified		20. Security Classif. (of this page)  Unclassified		21. No. of Pages	
				22. Price*  \$3.00	

\* For sale by the National Technical Information Service, Springfield, Virginia 22151

## FOREWORD

This report is submitted by ARDE, INC. in fulfillment of contract NAS 3-12026 and covers the period from July 1968 to March 1971. The principal investigator was David Gleich.

Guidance and many helpful suggestions were provided throughout the program by the NASA Project Manager, R. F. Lark of the Materials & Structures Division, Lewis Research Center.

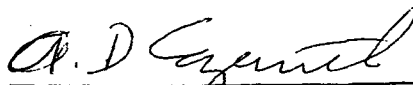
Prepared by:



---

David Gleich

Approved by:



---

A. D. Cozewith

## CONTENTS

### Page No.

SUMMARY. . . . .	
1.0 INTRODUCTION. . . . .	1
2.0 DESCRIPTION OF THE RING REINFORCED DIAPHRAGM. . . . .	3
3.0 TECHNICAL DISCUSSION. . . . .	5
3.1 Stainless Steel Diaphragm Design . . . . .	5
3.2 Stainless Steel Diaphragm Fabrication. . . . .	28
3.3 Stainless Steel Diaphragm Cycle Tests. . . . .	38
3.4 Evaluation of Stainless Steel Ring Reinforced Diaphragm Reversal Test Results. . . . .	79
3.5 Description of Aluminum Diaphragm and Cryogenic Testing Effort . . . . .	83
4.0 CONCLUSIONS AND RECOMMENDATIONS . . . . .	87
4.1 Conclusions. . . . .	87
4.2 Recommendations. . . . .	88
5.0 REFERENCES. . . . .	91
6.0 APPENDICES. . . . .	93
6.1 Appendix 1 - Diaphragm Actuation Pressure Relation .	95
6.2 Appendix 2 - Diaphragm Cycle Life Variables. . . . .	98
6.3 Appendix 3 - Diaphragm Reversal Testing Documentation . . . . .	102
7.0 DISTRIBUTION LIST . . . . .	142



## LIST OF FIGURES

<u>Figure No.</u>		<u>Page No.</u>
1	Metallic Positive Expulsion Diaphragm. . . .	3a
2	Diaphragm Reversal . . . . .	4
3	Summary - Ring Reinforced Diaphragm Design Criteria . . . . .	7
4	Sketch of Modified Hemispherical Diaphragm Shell. . . . .	8
5	Typical Copper Braze Joint . . . . .	11
6	13" S. S. Diaphragm Assembly Type A (17 1/2° Cone Angle) . . . . .	14
7	Shell-13" S. S. Diaphragm Type A' (17 1/2° Cone Angle) . . . . .	15
8	13" SST Diaphragm Assembly Type A' (25° Cone Angle) . . . . .	16
9	Shell-13" SST Diaphragm Type A' (25° Cone Angle) . . . . .	17
10	Diamond-Shaped Shell Buckles . . . . .	18
11	Diaphragm Shell Buckling Mode. . . . .	20
12	13" SST Diaphragm Assembly Type B' (25° Cone Angle) . . . . .	21
13	Small Intermediate Reinforcing Wire Diaphragm Configuration Design Criterion . .	22
14	Influence of Ring Centroid Location on Ring and Shell Compression. . . . .	24
15	13" SST Diaphragm Assembly Type C' (25° Cone Angle) . . . . .	25
16	Shell-13" SST Diaphragm 25° Cone Angle - Type C' Corrugated for .094 Dia. Wires . . .	26
17	13" SST Diaphragm Assembly Type D' (25° Cone Angle) . . . . .	27
18	13" SST Diaphragm Assembly Type D' (25° Cone Angle). . . . .	29
19	13" SST Diaphragm Assembly Type A' (17 1/2° Cone Angle) . . . . .	30
20	Ring Sizing Die for D 3745 . . . . .	34

LIST OF FIGURES

<u>Figure No.</u>		<u>Page No.</u>
21	Bladder Ring Tack Welding Fixture for (NASA Lewis) . . . . .	35
22	Test Diaphragm Assembly (Helium Leak Test) . . .	36
23	Water Actuating Rig - 13" Diaphragm-Water Cycling Test . . . . .	40
24	13" Diaphragm Water Cycling Test Rig . . . . .	41
25	25° Cone Angle Diaphragm D 3745, S/N #1 After First and Tenth Reversals. . . . .	45
26	25° Cone Angle Diaphragm D 3745, S/N #1 After Eleventh Reversal. . . . .	46
27	13" SST Diaphragm Water Reversal Test Reversal Test Reversal #1. . . . .	48
28	13" SST Diaphragm Water Reversal Test Reversal #1. . . . .	49
29	13" SST Diaphragm Water Reversal Test Reversal #2. . . . .	50
30	13" SST Diaphragm Water Reversal Test Reversal #4. . . . .	51
31	Diaphragm Contour at Wire Number 1 During First Reversal . . . . .	55
32	Diaphragm Contour at Failure Region After Fourth Reversal. . . . .	56
33	Actuation $\Delta P$ Trace P/N D 3745, S/N #2 (Reversal #1). . . . .	57
34	13" SST Diaphragm Reversals 1 & 5. . . . .	60
35	13" SST Diaphragm After Reversal #8. . . . .	61
36	Actuation $\Delta P$ Trace, P/N D 3745, S/N 3 (Reversal #8). . . . .	62
37	13" SST Diaphragm After Reversal #6. . . . .	65
38	Actuation $\Delta P$ Trace, P/N D 3747, S/N #1 (Reversal #5). . . . .	66
39	Diaphragm Contour in Vicinity of First Wire During First Reversal. . . . .	68
40	13" SST Diaphragm Reversals 1 & 4. . . . .	69

# LIST OF FIGURES

<u>Figure No.</u>		<u>Page No.</u>
41	Actuation $\Delta P$ Trace, P/N D 3767, S/N #1 (Reversal #1) . . . . .	71
42	13" SST Diaphragm Reversals 1 & 8. . . . .	72
43	13" SST Diaphragm Water Reversal Test Reversal #12 . . . . .	74
44	Actuation $\Delta P$ Trace, P/N D 3745, S/N #2 (Reversal #1) . . . . .	76
45	Actuation $\Delta P$ Trace, P/N D 3804, S/N #1 (Reversal #1) . . . . .	77
46	13" SST Diaphragm Reversals 1 & 3... . . . .	78
47	Actuation $\Delta P$ Trace, P/N D 3805, S/N #1 (Reversal #3) . . . . .	80
48	13" SST Diaphragm Water Reversal Test Reversal #6. . . . .	81
49	13" Diaphragm Cryogenic Cycling Test Schematic	85
A-1	Diaphragm Actuation Pressure Loads and Forces	96
A-2	Wire Spacing Considerations. . . . .	101
TP-100	"Test Plan for Room Temperature Cycle Testing of 13" Stainless Steel Diaphragms". . . . .	103
TOP-100	"Operation Procedures for Diaphragm Water Actuation Test" . . . . .	109
TOP-101	"Operational Procedure for Diaphragm Water Cycling Test" . . . . .	113
TP-201	"Test Plan for Cryogenic Cycle Test of Stainless Steel Positive Expulsion Diaphragms". . . . .	117
TP-202	"Test Plan for Cryogenic Cycle Test of Aluminum Positive Expulsion Diaphragm" . . . . .	122
TOP-200	"Operational Procedures for Diaphragm Cryogenic Cycle Test" . . . . .	127
WS-200	"LH <sub>2</sub> Cycle Testing of 13" Metallic Diaphragms"	133
AC-200	"Acceptance Criteria 200, 13" Diaphragm Cryo- genic Cycling Test Rig" . . . . .	138

## LIST OF TABLES

<u>Table No.</u>		<u>Page No.</u>
I	13" Ring Reinforced Modified Hemispherical Type Stainless Steel Diaphragm Design Configurations . . . . .	12
2	List of 13" Stainless Steel Diaphragms Fabricated . . . . .	31
3	Summary of 13" Stainless Steel Diaphragm Cycle Test Results . . . . .	43
4	Reinforcing Wire Diameter Reduction Due to Diaphragm Reversal (P/N D 3745, S/N#2) . . . .	53
5	Reinforcing Wire Diameter Reduction Due to Diaphragm Reversal (P/N D 3745, S/N#3) . . . .	63
6	Reinforcing Wire Diameter Reduction Due to Diaphragm Reversal (P/N D 3747, S/N#1) . . . .	67
7	Diaphragm Reversal Cycle Life Correlation. . .	82

# METALLIC POSITIVE EXPULSION DIAPHRAGMS

by

D. Gleich

## SUMMARY

A design and experimental program was performed to define and demonstrate increased cycle life ring reinforced modified hemispherical type metallic positive expulsion diaphragms for cryogenic fluid service. Design, analysis, diaphragm fabrication and room temperature diaphragm fluid expulsion testing efforts were conducted. The experimental results showed that metal positive expulsion diaphragms having improved cycle-life performance can be designed and fabricated.

Room temperature fluid expulsion tests of 13" nominal diameter, 8 mil thick stainless steel wire reinforced hemispherical-type diaphragms, utilizing water as the fluid and  $\text{GN}_2$  as the pressurants, demonstrated a maximum of eleven (11) leak-free complete diaphragm reversals. This represents a 70% improvement compared to test results heretofore obtained under Air Force sponsorship. The 13" diaphragm experimental results, together with other test data, confirmed analytic predictions of diaphragm reversal cycle life. Four (4) diaphragms of the maximum cycle life configuration were delivered to NASA for testing and evaluation.

Practical fabrication techniques needed for high cycle life diaphragm construction were demonstrated. A non-destructive inspection method utilizing dental wax molds and photomicrographs was developed for monitoring large-diaphragm shell local bending strains. These techniques should also have application to other types of shell structures.

Means for still further increasing the reversal cycle life of hemispherical type ring reinforced metallic positive expulsion diaphragms have been identified. Significantly increased cycle life (in excess of twenty reversals, for example) should be realized through the use of aluminum and Hastelloy B materials for diaphragm construction because of their much greater strain-to-necking capacity compared with stainless steel.

## 1.0 INTRODUCTION

### 1.1 Background

There is a need for reliable, non-porous and lightweight cryogenic propellant storage and positive expulsion systems for a variety of missions. A key technology area which must be demonstrated in order to meet this requirement is a reliable positive expulsion diaphragm for cryogenic service. Development of suitable non-metallic or combined plastic-metallic diaphragms (or bladders) has met with indifferent success due to reliability, compatibility and porosity problems, as well as other factors. Metallic diaphragms offer a solution to these problems.

Hemispherical-type ring-reinforced multicycle metallic diaphragms have been successfully demonstrated in size ranges from 6 inches to 6 feet in diameter, references 7 to 11. In addition, installation of these devices, by welding, into a tank to produce a reliable, leak-tight, lightweight, positive expulsion tank assembly has also been accomplished, references 7 and 9 to 12. This type of positive expulsion tank assembly has been successfully proven by ground and flight tests under severe operational environments, including high g fields and hot gas actuation.

Maximum multicycle capability demonstrated by hemispherical type ring reinforced metallic positive expulsion diaphragms up to the present time, has been six to seven diaphragm reversals. Many present and contemplated missions require a larger number of reversal cycles because of ground checkout and projected reuse needs. The primary goal of the present program (directed toward this anticipated need) was to develop an increased cycle life diaphragm of the metallic ring reinforced hemispherical type configuration for moderate cycle life requirements. A 13" nominal diameter diaphragm size was selected for this program.

### 1.2 Program Description

The program objective was to define, develop and verify ring reinforced hemispherical type metallic diaphragm configurations which would provide significant increases in diaphragm reversal cycle life compared to those previously obtained. The program consisted initially of a nine (9) task effort which included both stainless steel and aluminum diaphragm design, fabrication and cycle testing. Room temperature as well

as cryogenic testing were specified. The program was subsequently revised by deleting the all-aluminum diaphragm and cryogenic testing effort in order to utilize available funding to identify and develop high cycle life stainless steel diaphragm configurations.

Thirteen inch (13") nominal diameter, 8 mil thick stainless steel hemispherical-type ring-reinforced diaphragms were designed, fabricated and tested at room temperature to determine cycle life. Both smooth and corrugated shell diaphragms were investigated. Reinforcing wire size and spacing, as well as diaphragm equator region cone angles were varied to determine the affects of these parameters on diaphragm cycle-life. The  $17\frac{1}{2}^{\circ}$  cone angle configuration of the type previously demonstrated on contract AF 33(615)-11314 was used as a reference datum point. Nine (9) diaphragms were reversal tested. Four (4) diaphragms of the highest cycle life configuration were delivered to NASA-Lewis for testing and evaluation.

## 2.0 DESCRIPTION OF THE RING REINFORCED DIAPHRAGM

The metallic positive expulsion diaphragm considered herein, reference 13, consists of a thin, one-piece hemispherical type shell which is reinforced by hoop wires (Figure 1). The function of the hoop reinforcement is to prevent random buckling and to control the diaphragm rolling mode during reversal and fluid expulsion. When such a hoop reinforced diaphragm is housed inside a tank (Figure 2) and fluid is stored on the concave side of the diaphragm, the application of a pressure on the convex side of the diaphragm, that exceeds the fluid pressure by about 2 to 13 psig will cause the diaphragm to invert at its apex and pass through successive positions (e.g. positions 1-6 in Figure 2) until the diaphragm is completely inverted and the fluid is expelled. Controlled rim-rolling deformation modes, wherein the diaphragm begins to invert at its rim, as well as combination rim-and-apex rolling modes, can also be achieved.

In order to accomplish the program objective of obtaining increased cycle life, the strain per cycle imparted to the diaphragm during the reversals described above must be a small fraction of the total strain-to-necking capability of the diaphragm material. Diaphragm strain can be reduced by such means as lowering diaphragm stiffness and by better control of the diaphragm deformation mode during reversal (e.g. prevention of random buckling and cocking). The need for maintaining low diaphragm stiffness and the requirement of attaining stable, controlled diaphragm deformation are conflicting requirements and compromises must be made.

The efforts and accomplishments made to define and resolve this problem are discussed in the next section.



## 2.0 DESCRIPTION OF THE RING REINFORCED DIAPHRAGM

The metallic positive expulsion diaphragm considered herein, reference 13, consists of a thin, one-piece hemispherical type shell which is reinforced by hoop wires (Figure 1). The function of the hoop reinforcement is to prevent random buckling and to control the diaphragm rolling mode during reversal and fluid expulsion. When such a hoop reinforced diaphragm is housed inside a tank (Figure 2) and fluid is stored on the concave side of the diaphragm, the application of a pressure on the convex side of the diaphragm, that exceeds the fluid pressure by about 2 to 13 psig will cause the diaphragm to invert at its apex and pass through successive positions (e.g. positions 1-6 in Figure 2) until the diaphragm is completely inverted and the fluid is expelled. Controlled rim-rolling deformation modes, wherein the diaphragm begins to invert at its rim, as well as combination rim-and-apex rolling modes, can also be achieved.

In order to accomplish the program objective of obtaining increased cycle life, the strain per cycle imparted to the diaphragm during the reversals described above must be a small fraction of the total strain-to-necking capability of the diaphragm material. Diaphragm strain can be reduced by such means as lowering diaphragm stiffness and by better control of the diaphragm deformation mode during reversal (e.g. prevention of random buckling and cocking). The need for maintaining low diaphragm stiffness and the requirement of attaining stable, controlled diaphragm deformation are conflicting requirements and compromises must be made.

The efforts and accomplishments made to define and resolve this problem are discussed in the next section.

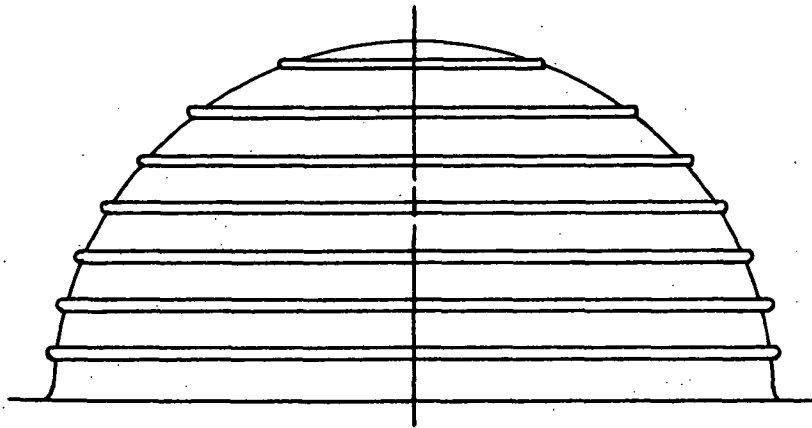


Figure 1  
Metallic Positive  
Expulsion Diaphragm

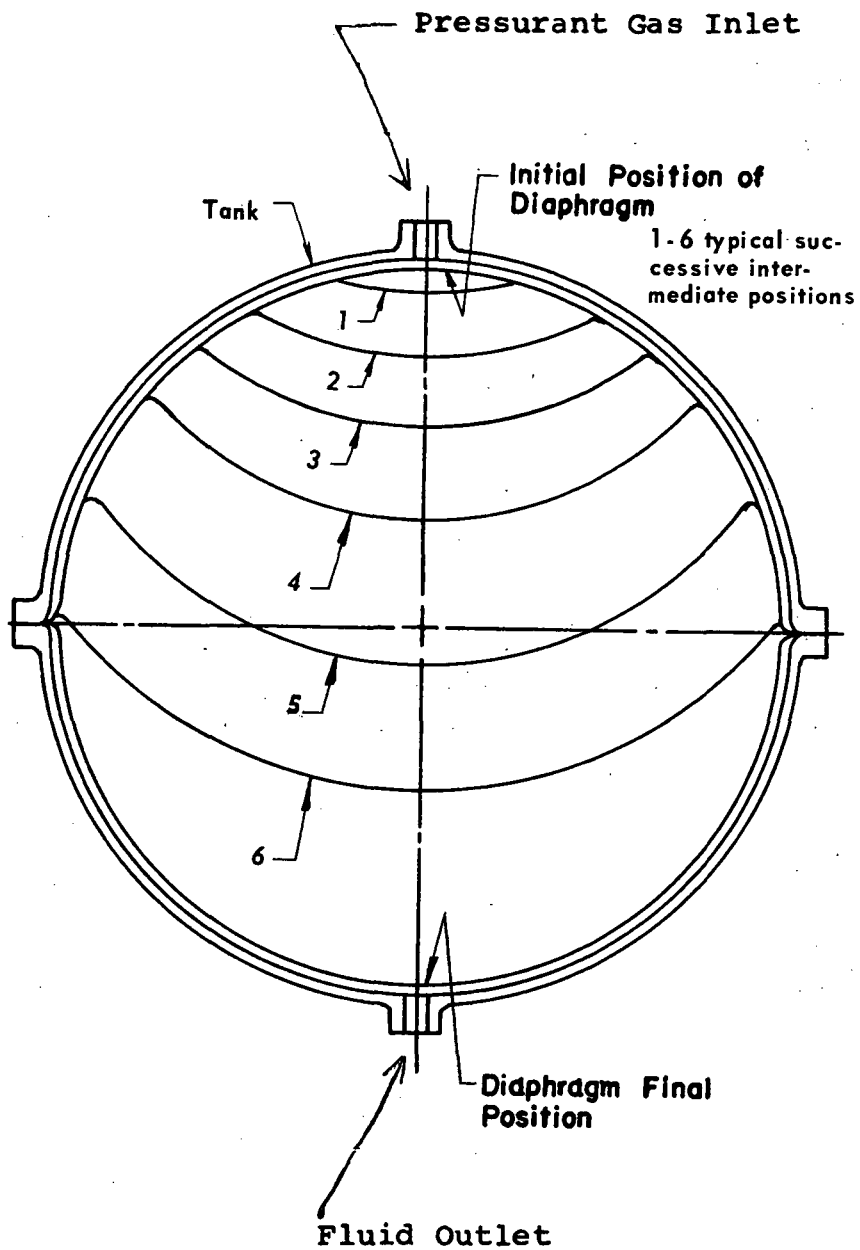


Figure 2  
Typical Diaphragm Reversal Mode

### 3.0 TECHNICAL DISCUSSION

This section describes the technical effort and accomplishments, presents analytical and test data, details problem areas encountered during the program and discusses approaches taken to resolve these problems. The program effort included the design and fabrication of stainless steel diaphragms, design and fabrication of diaphragm reversal test rigs and specification of test procedures and test programs, as well as a limited effort devoted to defining fabrication techniques for aluminum diaphragms. Room temperature reversal testing was performed to determine the cycle life of the stainless steel diaphragm test specimens.

#### 3.1 Stainless Steel Diaphragm Design

##### 3.1.1 Structural Design Considerations

The ring reinforced hemispherical type expulsion diaphragm structural design considerations involve the selection of shell thickness, contour and reinforcing wire size and spacing, as well as, the wire-to-shell joint configuration.

The shell is made as thin as possible to reduce bending strains and also to lower the actuation pressure requirements during diaphragm reversal testing. The size and spacing of the shell reinforcement (stiffeners) was selected to control the diaphragm deformation mode and preclude random buckling.

A satisfactory design is one which exhibits lower actuation pressures than critical buckling pressures for the complete diaphragm reversal cycle. The actuation pressures are the pressure differences across the diaphragm required to roll the diaphragm through each wire in the deformation mode similar to the one sketched on Figure 2. The critical buckling pressures are the lower of the pressures required to produce either overall or local compressive instability of the stiffened shell structure. Reinforcing wire interference during diaphragm deflection must also be avoided. The reinforcing wires must be spaced far enough apart so that rolling through only one wire at a time can take place without inducing rolling through adjacent wires. Finally, membrane stresses in the shell and reinforcing wires due to actuation pressures or high axial "g" fields must be below yield point values and the diaphragm stiffness, as measured by the actuation pressures, must be high enough to prevent uncontrolled cocking due to the destabilizing effect of high lateral "g" fields.

As is often the case, trade offs have to be made. For low shell bending strain and actuation pressure, the shell should have a small thickness and the reinforcing wires have a small cross-section and be spaced far apart. This reduces the diaphragm buckling resistance. For increased buckling resistance, shell thickness and wire cross-section need to be increased and wire spacing reduced. Further compromise is required when the wire spacing needed to preclude buckling for a given wire size and shell thickness is small enough to lead to wire interference during diaphragm reversal.

The stiffener ring to shell brazed joint configuration is designed to develop the full strength of the stiffener and to produce minimum strain concentration during diaphragm reversal. To accomplish this, the braze meniscus is made as small as possible. In addition, a high strength, ductile braze material (copper) is used to accommodate the large strains imposed on the joint by diaphragm deformation. These aspects are discussed in somewhat more detail in Sections 3.1.3 and 3.2 which follow.

The ring reinforced diaphragm structural design criteria, heretofore developed by ARDE and discussed above is summarized on Figure 3, together with some design formulae. The relations for buckling pressures and shell span length for bending effects decay are well known and are reported in the literature, references 1, 2 and 14 to 17. The actuation pressure relation (verified by tests) is detailed in Appendix 1, Section 6.1.

The actuation pressures for a true hemispherical shaped diaphragm have singularities at the pole and the equator as seen from the formula given in Figure 3. It takes an infinite actuation pressure to reverse the diaphragm at angular coordinates  $\alpha = 0$  and  $\pi/2$ . The difficulty is avoided at the pole region by locating the uppermost reinforcing wire at angular coordinate,  $\alpha > 0$ . At the equator, a conical transition region, Figure 4, is employed to eliminate the singularity there. The cone also reduces the bending strain in this maximum strain area since the angle turned through by the diaphragm in this region during reversal is reduced compared to that required for the true hemispherical shape. In addition, the cone permits closer wire spacing without wire interference problems leading to better deflection mode control and suppression

1. Actuation pressure,  $P_A < P_{cr}$ , where  $P_{cr}$  = minimum external pressure for either local or overall compressive instability of the ring reinforced diaphragm.

For Design:

$$P_A = \frac{2\sigma_y}{(R/t)^{3/2} \sin \alpha} \left\{ 1 + k \frac{(d/R)^3 (R/t)^2}{\sin \alpha} \right\} \begin{cases} k = \pi/8 \text{ for ring elastic} \\ k = 2/3 \text{ for ring plastic} \end{cases}$$

$$P_{cr,s} \approx \frac{\sqrt{Rt}}{L} E (t/R)^2 \text{ --- Buckling of shell between rings}$$

$$P_{cr,r} = \frac{3EI}{L (R \sin \alpha)^3} \text{ --- Buckling of ring plus effective shell}$$

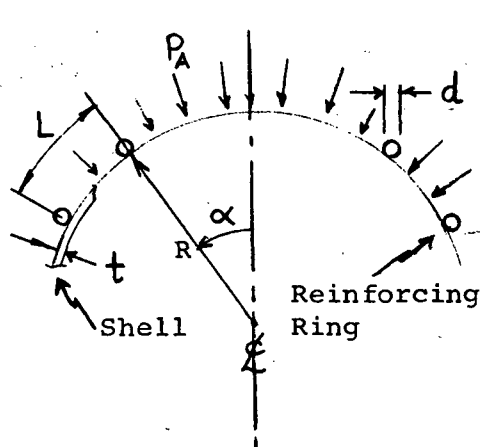
$$P_{cr,o} \approx K E (t/R)^2 + \frac{3EI_r}{(R \sin \alpha)^3 L} \text{ --- Approximate value for overall instability}$$

$$K = .2 \text{ sphere}$$

$$K = .1 \text{ cylinder}$$

Takes into account imperfections and built in eccentricities

2. Shell and ring membrane stresses  $<$  yield point values.
3.  $P_A > 2P_D$ , where  $P_D$  is equivalent "destabilizing pressure" for side "g" load.
4. Chose minimum reinforcing wire spacing,  $L_{min}$ , so that:
  - a) wires pass each other without interference during diaphragm reversal
  - b) Diaphragm rolls through only one wire at a time ( $L_{min} \approx 1.5\sqrt{Rt}$ )
5. Reinforcing ring to shell joint to have minimum braze meniscus and develop full strength of ring.



- $d$  = Ring cross-section diameter
- $E$  = Young's Modulus of shell and ring material
- $I$  = Moment of Inertia (ring & effective shell)
- $I_r$  = Moment of Inertia (ring)
- $L$  = Ring Spacing
- $P_A$  = Actuation Pressure (difference between pressurant and contained fluid pressure)
- $P_{cr,s}, P_{cr,r}, P_{cr,o}$  = critical buckling pressures
- $R$  = Shell radius
- $t$  = Shell thickness
- $\alpha$  = Angular coordinate
- $\sigma_y$  = Yield stress of shell and ring material

#### SUMMARY

#### RING REINFORCED DIAPHRAGM DESIGN CRITERIA

Figure 3

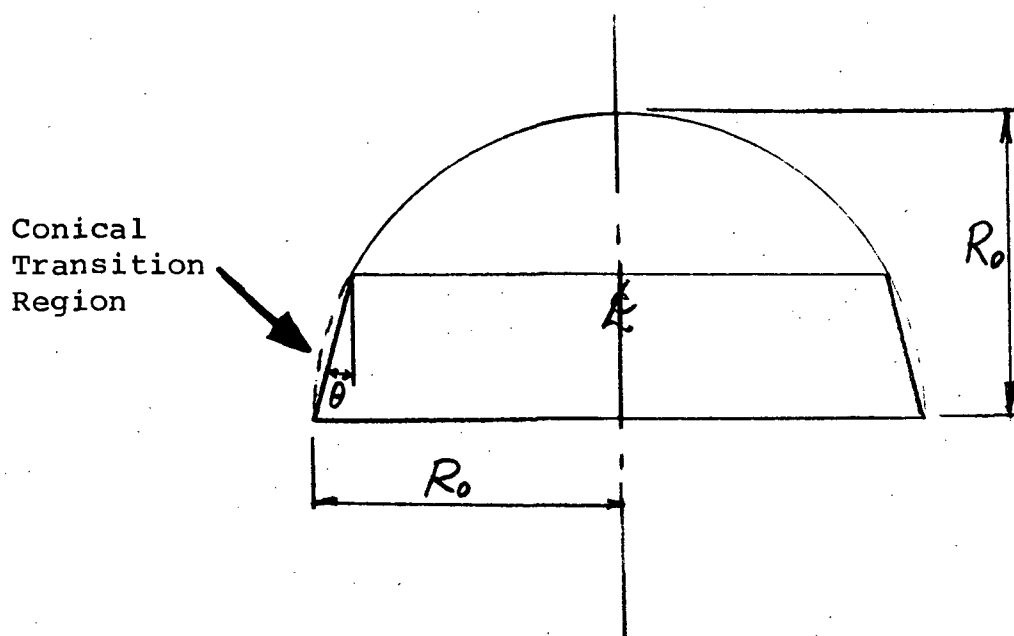


Figure 4

Sketch of Modified Hemispherical  
Diaphragm Shell

of random buckling of the diaphragm. The magnitude of the cone angle is, therefore, an important parameter in determining diaphragm reversal cycle life,  $N$ . The larger the cone angle, all other things being equal, the higher the diaphragm reversal cycle life. In the limit, as  $\theta \rightarrow \pi/2$ , the cone degenerates into a flat plate and the reversal cycle life theoretically approaches an infinite value since, at this limit, one is cycling the flat plate at very small bending strain amplitudes. This result for cone angle  $\theta \rightarrow \pi/2$  can also be deduced from the reversal cycle life relation for a given diaphragm material,  $N$  proportional to  $\left\{ \frac{(R/t) \sin \theta}{(\pi - 2\theta)^2} \right\}$ , which is derived in Appendix 2, Section 6.2.

The structural requirements leading to large cone angles for high cycle life diaphragms have to be traded off with packaging considerations and volumetric and expulsion efficiency requirements. These latter requirements generally tend to limit cone angle to relatively small values unless the tank in which the diaphragm is mounted is contoured to "fit" the diaphragm shape. Cone angles  $\theta$  up to  $17\ 1/2^\circ$  have been successfully used up to the present time with maximum cycle life demonstrated for the  $17\ 1/2^\circ$  cone angle configuration. Diaphragm cone angles of  $25^\circ$  and  $17\ 1/2^\circ$  have been used in this program in order to demonstrate the anticipated significant increase in cycle life compared to the best results obtained heretofore. The  $25^\circ$  cone angle for the modified hemispherical type ring reinforced diaphragm was considered a reasonable compromise between the high cycle life and packaging requirements.

### 3.1.2 Material Selection

The materials selected for construction of the stainless steel diaphragms on this program were the same as those previously demonstrated by ARDE under Contract AF 33(657)-11314, reference 18. Diaphragm shell and reinforcing ring materials were annealed AISI 321 and AISI 308L stainless steels, respectively. Copper braze was used to attach the reinforcing rings to the diaphragm shell.

The shell and ring materials are compatible with cryogenic fluids and have about 35-40% strain to necking capability at room  $LN_2$  and  $LH_2$  temperatures. The stabilized 321 stainless steel has a relatively low work hardening rate compared to the unstabilized grades. Carbide precipitation on slow cooling down during annealing or brazing from about  $2000^\circ F$  to room temperature is prevented for the stabilized 321 shell material and minimized



by the use of extra low carbon 308L wire. All these factors contribute towards increasing diaphragm cycle life. In addition, the selected shell and ring materials can be readily formed, brazed, welded and machined.

The brazed joint required in this application must exhibit considerable ductility, be compatible with cryogenic fluids, have a minimum meniscus to avoid strain amplification during diaphragm reversal, be strong enough to develop the full strength of the ring stiffener, and must not degrade the parent material by virtue of substantial penetration or diffusion into the shell wall.

Test results have demonstrated that both copper and gold brazed joints can very readily meet these requirements, references 7 to 12 and 18. The brazed joint has been shown to be stronger than the parent material; failures occur in the diaphragm shell material. Copper was chosen for use in the present program since compatibility with cryogenic fluids of interest was no problem and copper braze offered a cost advantage. A typical copper braze joint is shown in Figure 5.

### 3.1.3 Stainless Steel Diaphragm Design Configurations

Thirteen inch (13") nominal diameter ring reinforced stainless steel diaphragms having both smooth and corrugated shells with  $17\frac{1}{2}^\circ$  and  $25^\circ$  cone angles and various reinforcing wire sizes and spacings were designed. These diaphragms were subsequently built and reversal tested, as detailed in Sections 3.2 and 3.3, to identify and demonstrate a high cycle life configuration.

Table I below lists and briefly describes all the diaphragm variations designed. The design approaches and rationale as well as the design details for each diaphragm are discussed in this section. Unless otherwise noted, the structural design criteria used were those previously detailed in Section 3.1.1 and summarized in Figure 3.

#### 3.1.3.1 $17\frac{1}{2}^\circ$ Cone Angle Smooth Shell Diaphragm With .094" $\varnothing$ Reinforcing Wires (P/N D 3769)

This first stainless steel diaphragm configuration, shown on Figure 6, was used as a baseline reference design. It is a scale down of the highest (6-7 reversal) cycle life 23" stainless steel diaphragm previously demonstrated by Arde under Contract AF 33(615)-11314.



COPPER BRAZE

NOTE:

1. Complete lack of diffusion with parent material.
2. Small well-bonded braze area with good fillet

150 X Magnification

Sodium Cyanide Etch

Figure 5  
Typical Copper Braze Etch

**TABLE I - 13" RING REINFORCED MODIFIED  
HEMISPHERICAL TYPE STAINLESS STEEL  
DIAPHRAGM DESIGN CONFIGURATIONS**

P/N	Cone Angle	Shell Type	Reinforcing Wire Cross-Section Diameter	Shell Thickness	Remarks
D3769	17 1/2°	Smooth	.094"	.008"	Reference design-scaled down of 23" diaphragm previously demonstrated on contract AF33(615) 11314; First diaphragm design configuration
D3745	25°	Smooth	.094" $\emptyset$ *	.088"	Second diaphragm design configuration
D3747	25°	Smooth	.094" and .047"	.008"	Smaller intermediate wire design; third diaphragm design configuration
D3767	25°	Corrugated	.094"	.008"	Fourth diaphragm design configuration
D3798	25°	Smooth	.125"	.008"	Heavy wire variation Fifth diaphragm design configuration
D3804	25°	Smooth	.110"	.008"	Highest cycle life configuration; last 25° cone angle design configuration
D3805	17 1/2°	Smooth	.110" $\emptyset$	.008"	Last 17 1/2° cone angle design configuration

\*Circular

Twenty (20) .094"  $\emptyset$  wires spaced .45" apart were used for hoop reinforcement as detailed on Figure 6.

The 17 1/2° cone angle 13" modified hemispherical smooth diaphragm shell is described on Figure 7. A direct diameter to thickness scale-down from the previously demonstrated 23" diameter and 10 mil thick diaphragm ( $D/t = 2300$ ) would require a 13" diaphragm shell thickness of  $13/2300$ , or about 6 mils. Fabrication considerations and sheet availability problems led to the selection of eight (8) mils  $\pm 1$  mil as the 13" diaphragm shell thickness.

The reinforcing wires are tack welded to the shell to hold them in place prior to brazing. Burn through (holes) sometimes occur due to the tack welding operation. Although appropriate fabrication processing techniques can minimize this problem, the possibility of burn through increases as the shell thickness and shell diameter to thickness ratio increases. In addition, six (6) mil nominal thickness sheet was not available at the time it would be required. Rerolling, grinding or chemical milling available 8 or 10 mil thick sheet to 6 mil thickness presented the technical difficulty of thickness control and, in addition, was considered too costly.

#### 3.1.3.2 25° Cone Angle Smooth Shell Diaphragm with .094" $\emptyset$ Reinforcing Wires (P/N D 3745)

Figures 8 and 9 define this first 25° cone angle design configuration which has twenty four (24) .094"  $\emptyset$  reinforcing wires spaced .33" apart on the smooth modified hemispherical type diaphragm shell. The design is patterned after its 17 1/2° counterpart previously described in section 3.1.3.1. The larger 25° cone angle permits the use of more and closer spaced reinforcing wires leading to better control of the diaphragm deflection mode compared to the 17 1/2° variation. The bending strain is also reduced for the 25° cone angle design as discussed in section 3.3.1.

#### 3.1.3.3 25° Cone Angle Smooth Shell Diaphragm with .094" $\emptyset$ and .047" $\emptyset$ Reinforcing Wires (P/N D3747)

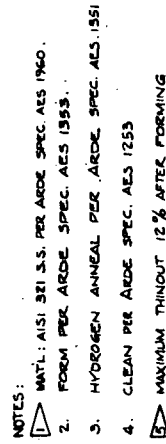
In a previous program, reference 18, it had been noticed that the diaphragm shell buckled locally in "diamond-shaped" buckles between reinforcing rings, as sketched on figure 10. These buckles, not present during initial diaphragm reversals, appeared only after the third or fourth diaphragm reversal. The



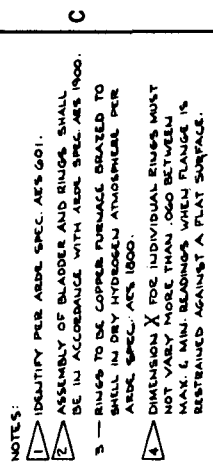
- NOTES:**

**NOTES:**

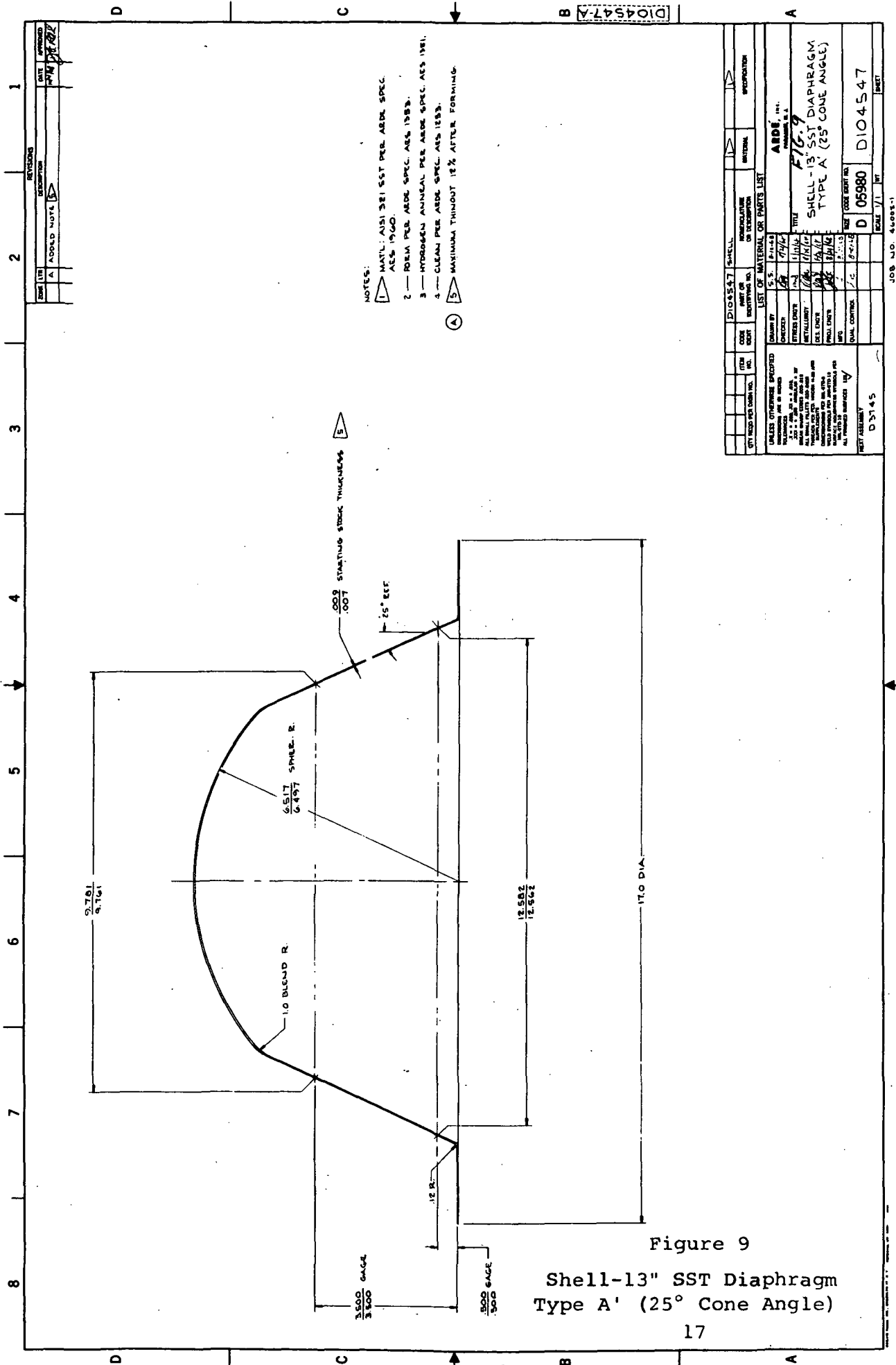
**NOTES:**

[illegible]

15

[illegible]

16





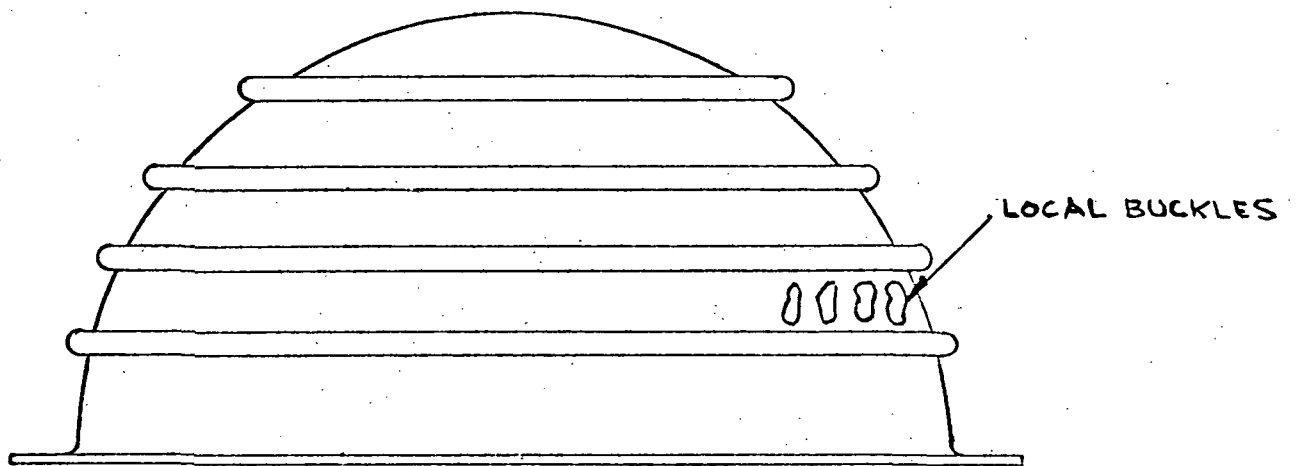


Figure 10  
Diamond-Shaped Shell Buckles

buckles reduced diaphragm cycle life since they increased the local bending strain in proportion to the amplitude of the buckles. Failure after subsequent reversals would generally occur in the buckled diaphragm shell high strain region.

This diaphragm shell buckling phenomenon may be explained by consideration of the diaphragm model sketched on figure 11. The reinforcing ring, initially at point A with radius  $r_A$ , is compressed in going through positions A" and A' with radii  $r_{A''}$  and  $r_{A'}$ , respectively, during the diaphragm reversal. The maximum ring compression per reversal occurs at mid position A". The final radius  $r_{A'}$  is  $<$  initial radius  $r_A$  due to work hardening. The diaphragm shell, which is attached to the ring, is similarly compressed during diaphragm reversal. This ring and shell compression, verified by measurements, continues and increases during each reversal. After several reversals, the diaphragm shell compressive strain reaches the critical value and the shell buckles locally between stiffener rings in the observed diamond pattern.

In an attempt to suppress the aforementioned shell buckles and thus increase diaphragm reversal cycle life, an intermediate smaller reinforcing ring was used between the larger rings. The smaller intermediate ring, acting with the shell, would tend to suppress the diamond pattern shell buckles between the larger rings. Even if the smaller ring buckled and became out of round, it was anticipated that the shell buckling amplitudes between larger rings would be less than they would have been without the smaller intermediate ring.

This intermediate small reinforcing wire diaphragm design approach was used to design the third 25° cone angle diaphragm configuration. The diaphragm assembly design is detailed on figure 12. The smooth diaphragm shell configuration used (figure 9), is the same as employed for P/N D3745 previously discussed. Nine (9) .047"Ø smaller intermediate reinforcing rings are used between the eighteen (18) .094"Ø larger reinforcing rings as shown on figure 12. All reinforcing wires are spaced .27" apart. The diameter and spacing of the wires was chosen to provide increased local buckling resistance.

The structural design model, sketched on figure 13, consisted of the shell element plus the two(2) .094"Ø rings and the .047"Ø intermediate ring. The structure was treated as a beam column on a distributed elastic foundation plus the local hoop spring supports provided by the rings. The shell span used for the intermediate wire design ( $\lambda = .54"$ ) which is twice the

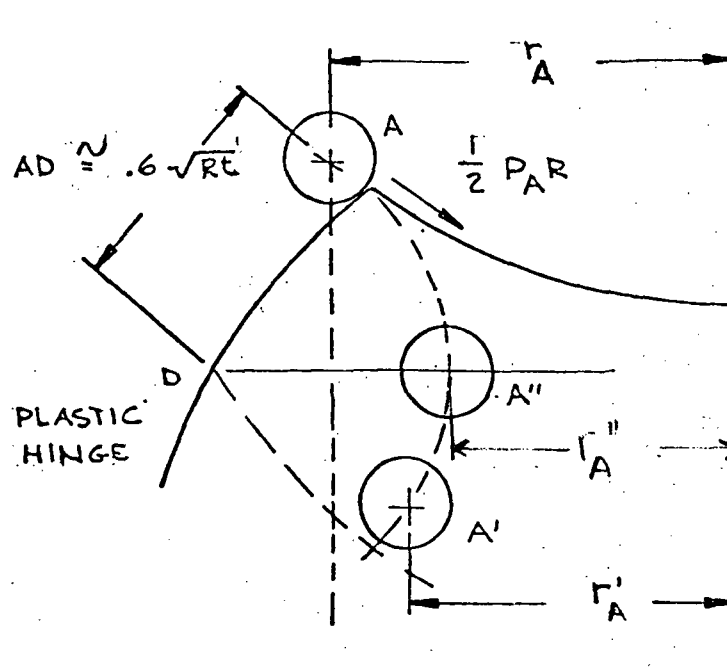


Figure 11  
Diaphragm Shell Buckling Model

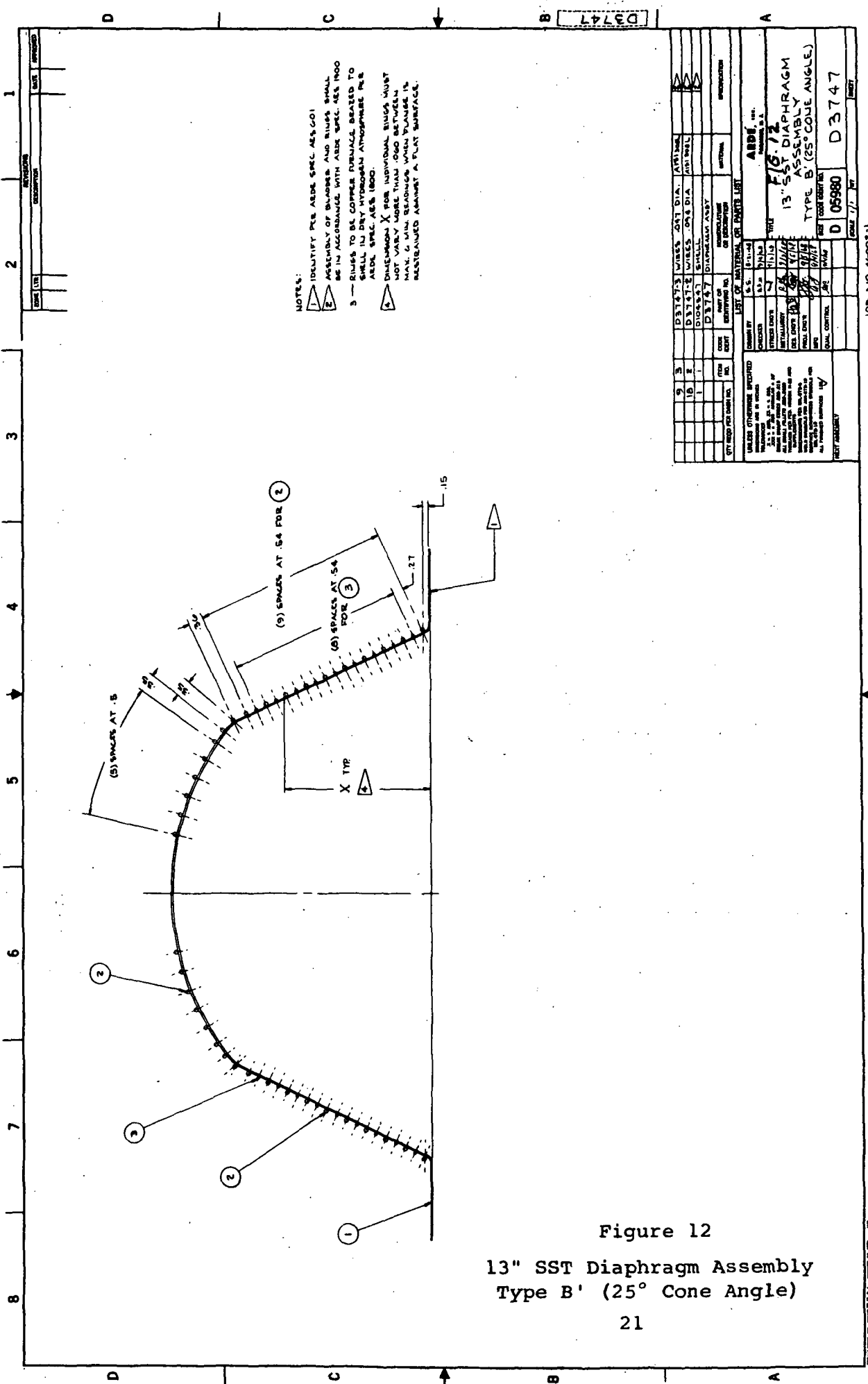
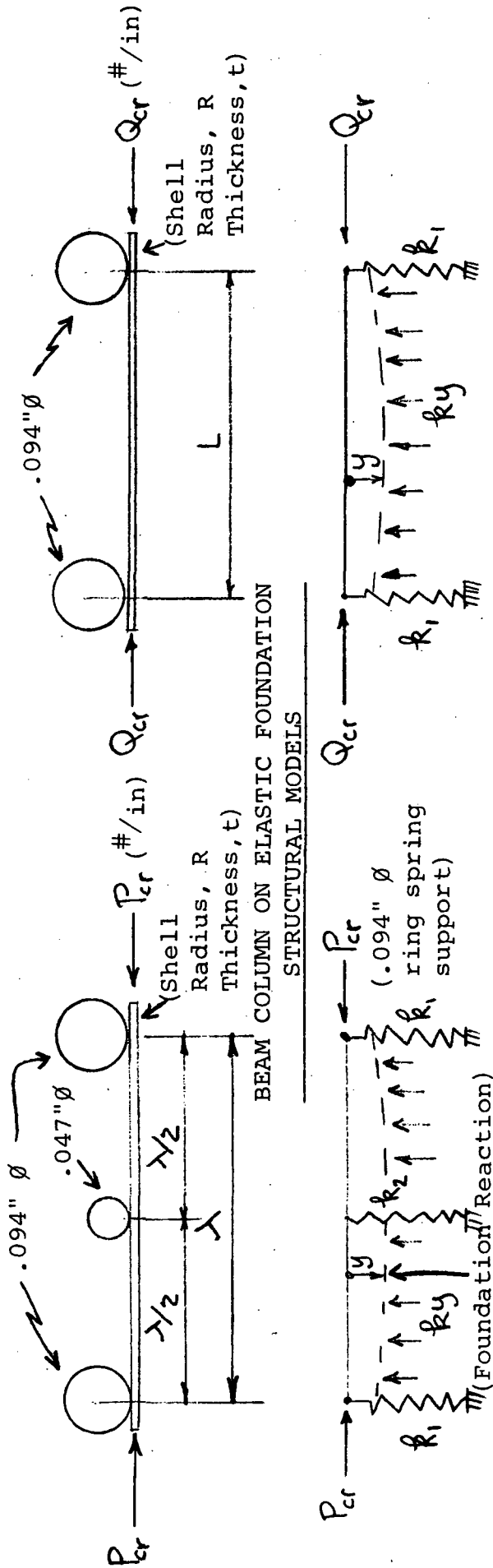


Figure 12  
13" SST Diaphragm Assembly  
Type B' (25° Cone Angle)



DESIGN CRITERION:

- 1) Select length  $\lambda$  so that  $P_{cr} > Q_{cr}$
- 2) Length  $\lambda$  to be large enough to prevent wire interference during diaphragm reversal.

Figure 13

Small Intermediate Reinforcing Wire  
Diaphragm Configuration Design Criterion

wire spacing, was chosen so as to provide a greater buckling load compared to the  $L=.33$ " span with the two (2)  $.094"$   $\emptyset$  wires used for the constant wire  $25^\circ$  cone angle diaphragm configuration (P/N D3745). This buckling load comparison is detailed on figure 13.

#### 3.1.3.4 $25^\circ$ Cone Angle Corrugated Shell Diaphragm With $.094"$ $\emptyset$ Reinforcing Wires (P/N D3767)

The objective of the corrugated shell configuration was to reduce the ring compression and therefore the compressive loads in the diaphragm shell between rings as the diaphragm reverses. This compressive strain reduction is the result of locating the centers of the reinforcing ring cross-sections in the diaphragm shell median surface (instead of being displaced from it as in the smooth shell designs). For a smooth shell configuration with a reinforcing ring tangent at A as shown on figure 14 (a), the ring radius is reduced by an amount  $\Delta r = \delta_1 + \delta_2$  during a reversal. The component " $\delta_1$ " is due to the offset of the ring center from the shell. If the ring center is "on" the diaphragm shell median surface, the " $\delta_1$ " component goes to zero and the decrease in ring radius is less severe, i.e.,  $\Delta r = \delta_2$  (figure 14 (b)). As discussed previously in section 3.1.3.3, this reduction in compressive strain will postpone the onset of "diamond pattern" buckling and thus increase the diaphragm reversal cycle life.

The  $25^\circ$  cone angle corrugated diaphragm assembly configuration is shown on figure 15 and the corrugated shell is detailed on figure 16. The corrugated design reinforcing wire size and spacing was made the same as the  $.094"$   $\emptyset$  wire size smooth  $25^\circ$  cone angle diaphragm (figure 8) so as to provide a meaningful comparison of the effect of the corrugated configuration on diaphragm cycle life.

#### 3.1.3.5 $25^\circ$ Cone Angle Smooth Shell Diaphragm with $.125"$ $\emptyset$ Reinforcing Wires (P/N D3798)

This smooth shell  $25^\circ$  cone angle configuration, shown on figure 17, utilizes larger than usual reinforcing wire size (twenty  $1/8"$   $\emptyset$  wires at  $.43$ " spacing). The diaphragm shell (figure 9) is the same type used for the other  $25^\circ$  smooth shell configurations.

The purpose of the larger diameter reinforcing wires was to obtain better control of the diaphragm deflection mode during reversal (minimize cocking tendency with the possibility

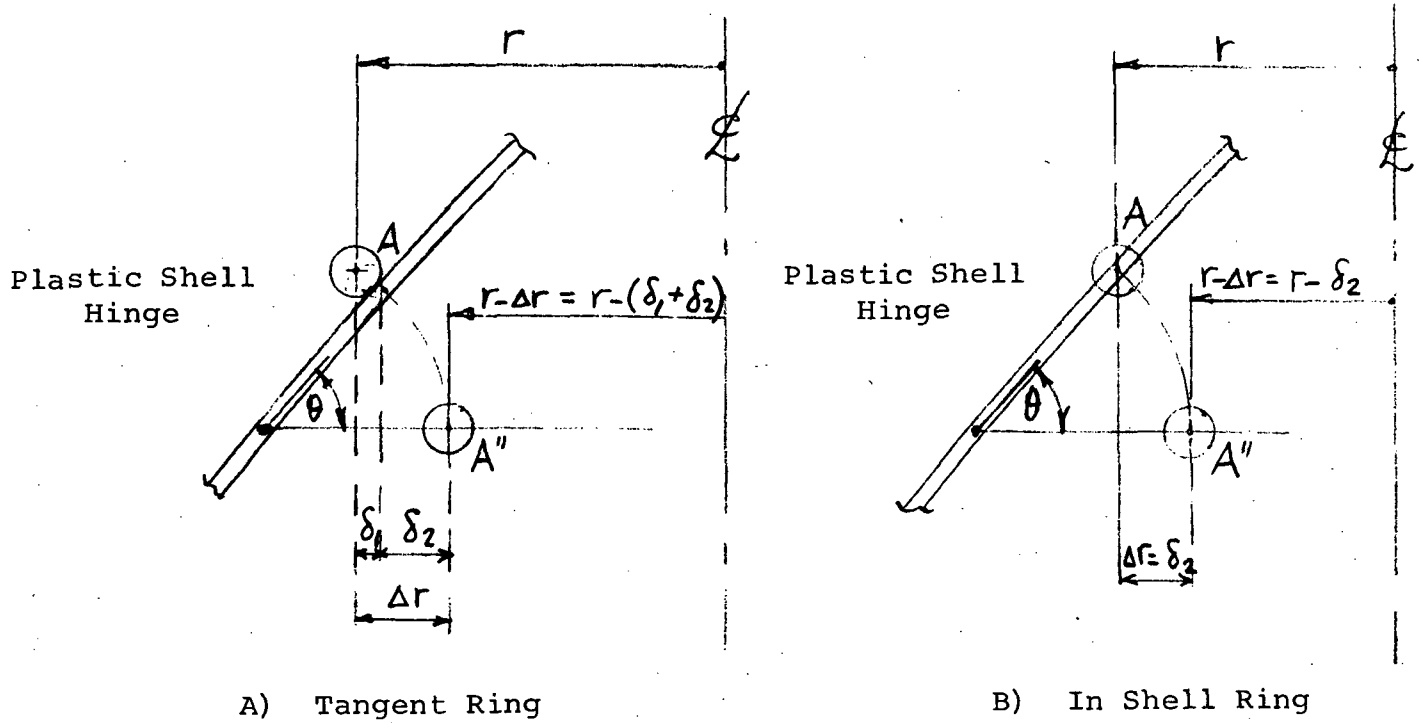


Figure 14

Influence of Ring Centroid Location on Ring  
and Shell Compression

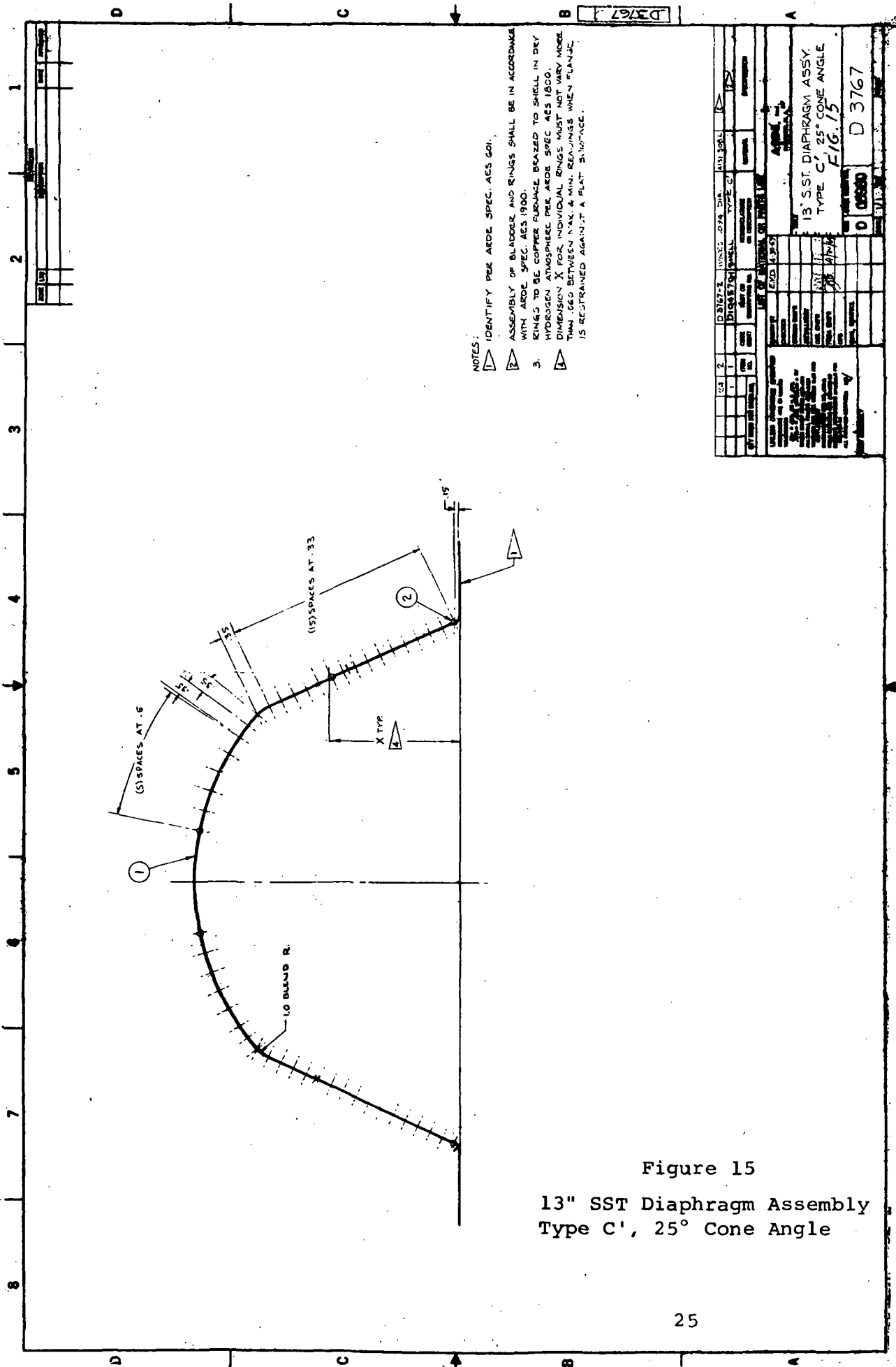
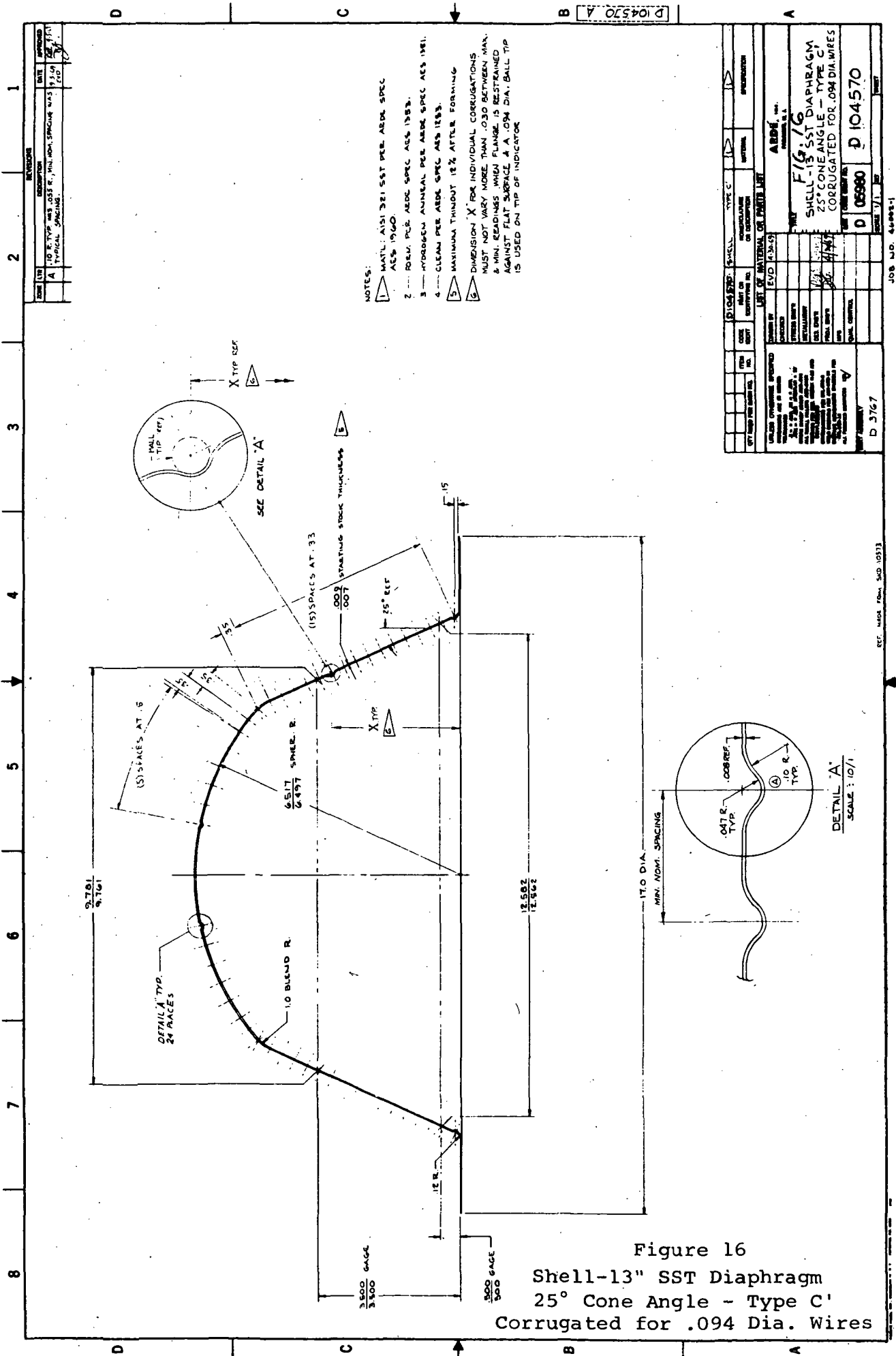


Figure 15  
13" SST Diaphragm Assembly  
Type C', 25° Cone Angle







of concomitant wire interference and increased shell bending strain). Although desirable from a diaphragm deflection mode control point of view, larger size reinforcing wires increase the restraint to shell rotation during diaphragm motion. This leads to increased shell bending strain and hence reduced diaphragm reversal cycle life. The final choice of reinforcing wire cross-sectional diameter is usually a trade off between these two conflicting effects.

#### 3.1.3.6 25° Cone Angle Smooth Shell Diaphragm with .110"Ø Reinforcing Wires (P/N D3804)

This 25° cone angle smooth shell diaphragm configuration, detailed on figures 18 and 9, demonstrated the highest cycle life in diaphragm reversal tests. The .110"Ø reinforcing ring size used was midway between the .094"Ø and .125"Ø hoop stiffeners employed on the previous designs. A trade off was made therefore between increased diaphragm deflection mode control of the largest (.125"Ø) reinforcing wires and the reduced bending restraint strain of the smallest (.094"Ø) reinforcing wires as discussed in detail in the preceeding section 3.1.3.5.

#### 3.1.3.7 17 1/2° Cone Angle Smooth Shell Diaphragm with .110"Ø Reinforcing Wires (P/N D3805)

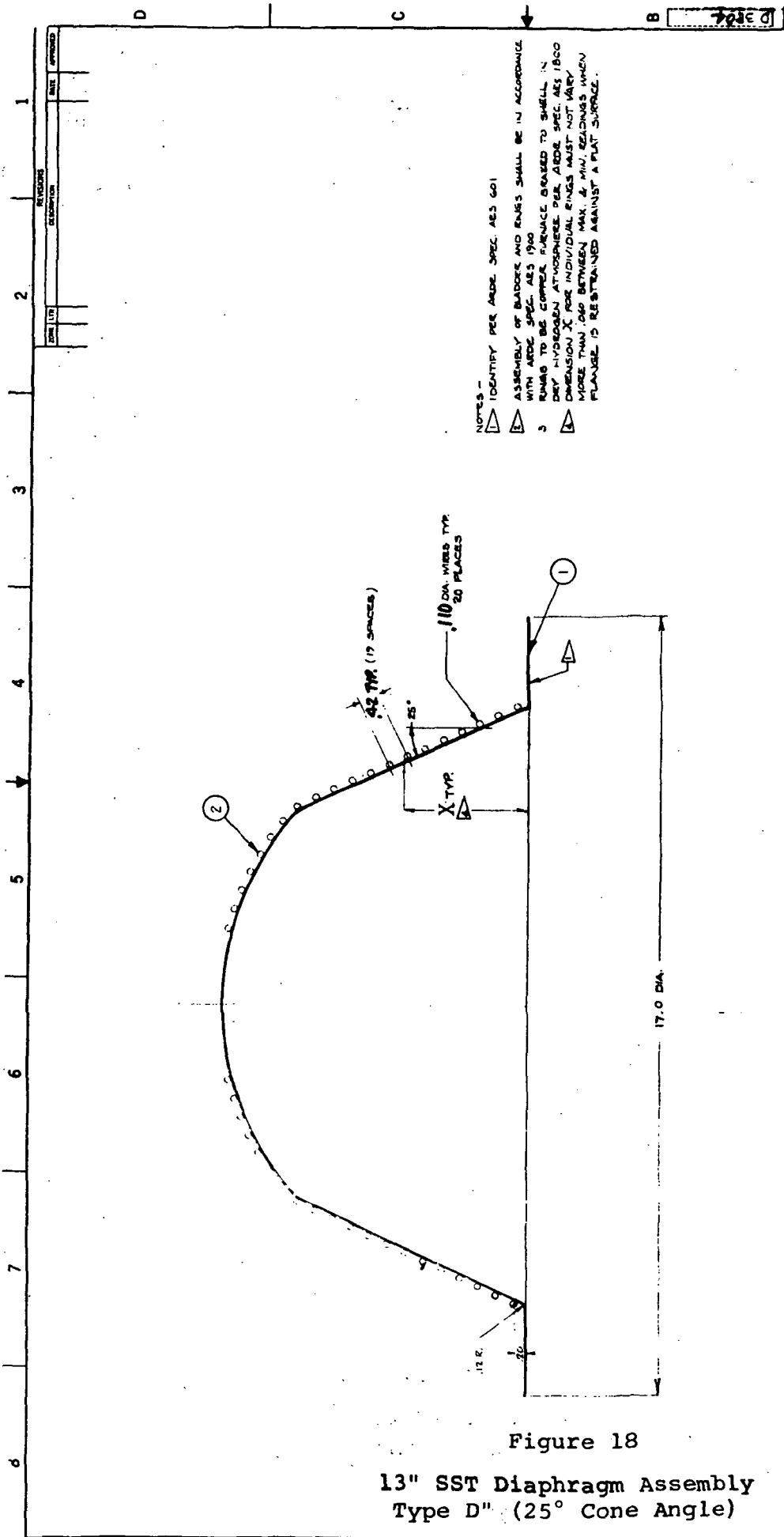
Figures 19 and 7 define this 17 1/2° cone angle smooth shell diaphragm configuration. The .110"Ø reinforcing rings are used again as a compromise between diaphragm deflection mode control and shell bending restraint requirements.

### 3.2 Stainless Steel Diaphragm Fabrication

Ring reinforced hemispherical type stainless steel diaphragm fabrication consists of four (4) primary operations as listed below.

- a) Shell forming
- b) Reinforcing ring fabrication
- c) Tack welding the reinforcing rings to the shell
- d) Furnace brazing the reinforcing rings to the shell to complete the diaphragm assembly.

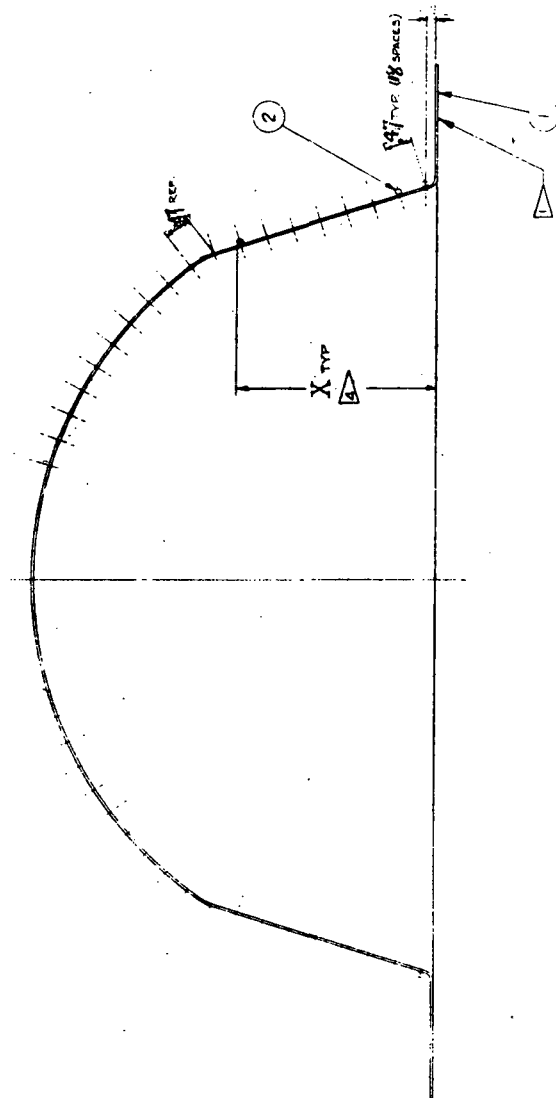
In process inspections were performed during fabrication (from the raw material stage to completion of construction). Helium leak checks were made with a mass spectrometer after wire tack welding and subsequent to furnace brazing. A special leak check



- NOTES -
- 1. IDENTIFY PER ARMO SPEC. AES 601
  - 2. ASSEMBLY OF BARRAGE AND RINGS SHALL BE IN ACCORDANCE WITH ARMO SPEC. AES 1900
  - 3. RINGS TO BE COMPACTED TO SPEC. AES 1800
  - 4. DRY HYDRANT ATTACHMENT PER ARMO SPEC. AES 1800
  - 5. CONNECTION X FOR INDIVIDUAL RINGS MUST NOT VARY MORE THAN .100 BETWEEN MAX. & MIN. SECTIONS WHEN PLACED TO REST AGAINST A PLAT SURFACE.

10	2	3	4	5	6	7	8	9	10	11	12	13	14	15	16	17	18	19	20	21	22	23	24	25	26	27	28	29	30	31	32	33	34	35	36	37	38	39	40	41	42	43	44	45	46	47	48	49	50	51	52	53	54	55	56	57	58	59	60	61	62	63	64	65	66	67	68	69	70	71	72	73	74	75	76	77	78	79	80	81	82	83	84	85	86	87	88	89	90	91	92	93	94	95	96	97	98	99	100
<p>1. IDENTIFY PER ARMO SPEC. AES 601</p> <p>2. ASSEMBLY OF BARRAGE AND RINGS SHALL BE IN ACCORDANCE WITH ARMO SPEC. AES 1900</p> <p>3. RINGS TO BE COMPACTED TO SPEC. AES 1800</p> <p>4. DRY HYDRANT ATTACHMENT PER ARMO SPEC. AES 1800</p> <p>5. CONNECTION X FOR INDIVIDUAL RINGS MUST NOT VARY MORE THAN .100 BETWEEN MAX. &amp; MIN. SECTIONS WHEN PLACED TO REST AGAINST A PLAT SURFACE.</p>										<p>1. IDENTIFY PER ARMO SPEC. AES 601</p> <p>2. ASSEMBLY OF BARRAGE AND RINGS SHALL BE IN ACCORDANCE WITH ARMO SPEC. AES 1900</p> <p>3. RINGS TO BE COMPACTED TO SPEC. AES 1800</p> <p>4. DRY HYDRANT ATTACHMENT PER ARMO SPEC. AES 1800</p> <p>5. CONNECTION X FOR INDIVIDUAL RINGS MUST NOT VARY MORE THAN .100 BETWEEN MAX. &amp; MIN. SECTIONS WHEN PLACED TO REST AGAINST A PLAT SURFACE.</p>										<p>1. IDENTIFY PER ARMO SPEC. AES 601</p> <p>2. ASSEMBLY OF BARRAGE AND RINGS SHALL BE IN ACCORDANCE WITH ARMO SPEC. AES 1900</p> <p>3. RINGS TO BE COMPACTED TO SPEC. AES 1800</p> <p>4. DRY HYDRANT ATTACHMENT PER ARMO SPEC. AES 1800</p> <p>5. CONNECTION X FOR INDIVIDUAL RINGS MUST NOT VARY MORE THAN .100 BETWEEN MAX. &amp; MIN. SECTIONS WHEN PLACED TO REST AGAINST A PLAT SURFACE.</p>										<p>1. IDENTIFY PER ARMO SPEC. AES 601</p> <p>2. ASSEMBLY OF BARRAGE AND RINGS SHALL BE IN ACCORDANCE WITH ARMO SPEC. AES 1900</p> <p>3. RINGS TO BE COMPACTED TO SPEC. AES 1800</p> <p>4. DRY HYDRANT ATTACHMENT PER ARMO SPEC. AES 1800</p> <p>5. CONNECTION X FOR INDIVIDUAL RINGS MUST NOT VARY MORE THAN .100 BETWEEN MAX. &amp; MIN. SECTIONS WHEN PLACED TO REST AGAINST A PLAT SURFACE.</p>																																																																					

Figure 18  
13" SST Diaphragm Assembly  
Type D" (25° Cone Angle)



NOTES:

- 1 IDENTIFY PER ARDE SPEC. AELS 601
- 2 ASSEMBLY OF BLADDER & RINGS SHALL BE IN ACCORDANCE WITH ARDE SPEC. AELS 1900
- 3 RINGS TO BE COPPER FURNACE BRAZED TO SHELL IN DRY HYDROGEN ATMOSPHERE PER ARDE SPEC. AELS 1000.
- 4 DIMENSION X FOR INDIVIDUAL RINGS MUST NOT VARY MORE THAN .050 BETWEEN MAX. & MIN. READINGS WHEN FLANGE IS RESTRAINED AGAINST A FLAT SURFACE.

Figure 19

13" SST Diaphragm Assembly  
Type A' (17 1/2° Cone Angle)

DESIGN NO. 13-19		REV. 1	
DATE 10/1/55		BY 10/1/55	
DRAWN BY 10/1/55		CHECKED BY 10/1/55	
APPROVED BY 10/1/55		10/1/55	
LIST OF REVISIONS ON PRINTS LIST		ARDE, INC.	
REVISION NO. 1		FIG. 19	
REVISION NO. 2		13" SST DIAPHRAGM ASSEMBLY	
REVISION NO. 3		TYPE A' (17 1/2° CONE ANGLE)	
REVISION NO. 4		D 05980	
REVISION NO. 5		D 3805	
REVISION NO. 6		10/1/55	
REVISION NO. 7		10/1/55	
REVISION NO. 8		10/1/55	
REVISION NO. 9		10/1/55	
REVISION NO. 10		10/1/55	
REVISION NO. 11		10/1/55	
REVISION NO. 12		10/1/55	
REVISION NO. 13		10/1/55	
REVISION NO. 14		10/1/55	
REVISION NO. 15		10/1/55	
REVISION NO. 16		10/1/55	
REVISION NO. 17		10/1/55	
REVISION NO. 18		10/1/55	
REVISION NO. 19		10/1/55	
REVISION NO. 20		10/1/55	
REVISION NO. 21		10/1/55	
REVISION NO. 22		10/1/55	
REVISION NO. 23		10/1/55	
REVISION NO. 24		10/1/55	
REVISION NO. 25		10/1/55	
REVISION NO. 26		10/1/55	
REVISION NO. 27		10/1/55	
REVISION NO. 28		10/1/55	
REVISION NO. 29		10/1/55	
REVISION NO. 30		10/1/55	
REVISION NO. 31		10/1/55	
REVISION NO. 32		10/1/55	
REVISION NO. 33		10/1/55	
REVISION NO. 34		10/1/55	
REVISION NO. 35		10/1/55	
REVISION NO. 36		10/1/55	
REVISION NO. 37		10/1/55	
REVISION NO. 38		10/1/55	
REVISION NO. 39		10/1/55	
REVISION NO. 40		10/1/55	
REVISION NO. 41		10/1/55	
REVISION NO. 42		10/1/55	
REVISION NO. 43		10/1/55	
REVISION NO. 44		10/1/55	
REVISION NO. 45		10/1/55	
REVISION NO. 46		10/1/55	
REVISION NO. 47		10/1/55	
REVISION NO. 48		10/1/55	
REVISION NO. 49		10/1/55	
REVISION NO. 50		10/1/55	
REVISION NO. 51		10/1/55	
REVISION NO. 52		10/1/55	
REVISION NO. 53		10/1/55	
REVISION NO. 54		10/1/55	
REVISION NO. 55		10/1/55	
REVISION NO. 56		10/1/55	
REVISION NO. 57		10/1/55	
REVISION NO. 58		10/1/55	
REVISION NO. 59		10/1/55	
REVISION NO. 60		10/1/55	
REVISION NO. 61		10/1/55	
REVISION NO. 62		10/1/55	
REVISION NO. 63		10/1/55	
REVISION NO. 64		10/1/55	
REVISION NO. 65		10/1/55	
REVISION NO. 66		10/1/55	
REVISION NO. 67		10/1/55	
REVISION NO. 68		10/1/55	
REVISION NO. 69		10/1/55	
REVISION NO. 70		10/1/55	
REVISION NO. 71		10/1/55	
REVISION NO. 72		10/1/55	
REVISION NO. 73		10/1/55	
REVISION NO. 74		10/1/55	
REVISION NO. 75		10/1/55	
REVISION NO. 76		10/1/55	
REVISION NO. 77		10/1/55	
REVISION NO. 78		10/1/55	
REVISION NO. 79		10/1/55	
REVISION NO. 80		10/1/55	
REVISION NO. 81		10/1/55	
REVISION NO. 82		10/1/55	
REVISION NO. 83		10/1/55	
REVISION NO. 84		10/1/55	
REVISION NO. 85		10/1/55	
REVISION NO. 86		10/1/55	
REVISION NO. 87		10/1/55	
REVISION NO. 88		10/1/55	
REVISION NO. 89		10/1/55	
REVISION NO. 90		10/1/55	
REVISION NO. 91		10/1/55	
REVISION NO. 92		10/1/55	
REVISION NO. 93		10/1/55	
REVISION NO. 94		10/1/55	
REVISION NO. 95		10/1/55	
REVISION NO. 96		10/1/55	
REVISION NO. 97		10/1/55	
REVISION NO. 98		10/1/55	
REVISION NO. 99		10/1/55	
REVISION NO. 100		10/1/55	

fixture was used in these operations.

The type and number of 13" diameter stainless steel diaphragms built during the program are listed in Table 2 below.

Table 2 - List of 13" Stainless Steel Diaphragms Fabricated

P/N	S/N	Cone Angle	Referenced Figure No.	Remarks
D3745	1	25°	8	Tooling Check Out Unit
	2	25°	8	Tooling Check Out Unit
	3	25°	8	Reversal test Unit
D3747	1	25°	12	Reversal test Unit
D3798	1	25°	17	Reversal test Unit
D3767	1	25°	15	Reversal test Unit
D3769	1	17 1/2°	6	Reversal test Unit
D3805	1	17 1/2°	19	Reversal test Unit
D3804	1	25°	18	Reversal test Unit
	2	25°	18	NASA delivery Unit
	3	25°	18	NASA delivery Unit
	4	25°	18	NASA delivery Unit
	5	25°	18	NASA delivery Unit

### 3.2.1 Diaphragm Shell Forming

Smooth contour 13" diameter stainless steel modified hemispherical type diaphragm shells (figures 7 and 9) were fabricated by hydroforming, starting from flat sheet 7 to 9 mils. thick. Two (2) hydroforming passes with an intermediate hydrogen anneal were used. The corrugated diaphragm shell (figure 16) was formed by a combination hydroforming and spinning technique, again using 7 to 9 mils thick sheet stock as the starting material. A smooth

shell was first formed by hydroforming, followed by an intermediate hydrogen anneal. The shell was then mounted on a split mandril which was grooved corresponding to the specified corrugated configuration. The corrugations were then spun in the smooth shell using this mandril tool.

The technique developed for forming the corrugated shells was very successful. Dimensional control and consistency of the corrugated contour and wall thickness were exceedingly good for this very thin and flexible sheet metal part. This fabrication method should have application to other types of corrugated shell-like parts.

### 3.2.2 Reinforcing Ring Fabrication and Tack Welding to Diaphragm Shell

Two basic approaches previously demonstrated for reinforcing ring fabrication and tack welding of the rings to the diaphragm shell were undertaken:

- a) Rings rounded and sized using a sizing die and tack welded to the shell utilizing a tacking fixture
- b) Rings hand fabricated and hand tack welded to the shell.

Although the use of ring sizing and tack welding tooling (method "a" above) results in better dimensional control and minimizes the possibility of tack welding burn through the shell, it was not used to fabricate the diaphragm assemblies constructed in this program. Hand fabrication techniques (method "b" above) used to build the first reversal test rig checkout diaphragms, were found to be very satisfactory. All blue print dimensions were met and no tack welding burn through holes or leaks were encountered. It was therefore decided to use the hand fabrication methods for the balance of the diaphragms which were successfully built to blueprint specifications. For large quantity production however, the tooling fabrication method has obvious cost and schedule advantages.

#### 3.2.2.1 Ring Fabrication and Tack Welding Using Tooling

The main features of this fabrication technique are outlined below. Starting material was AISI 304L weld wire in coil or rod form.

- a) Roll wire to approximate ring circular

diameter. Cut ring short (2-5% less than first prescribed diameter) and butt weld ends together. Grind butt weld flush to complete the circular ring preform. Repeat these operations for the total number of rings required.

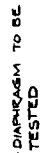
- b) Assemble smaller diameter ring preforms on ring sizing die. Stretch rings on sizing die to round and final size to prescribed diameters. The ring sizing die for diaphragm P/N D3745 (figure 8) is shown on figure 20. A tapered rod is hydraulically actuated to move downward in the split sizing die center which forces the die to displace radially outwards. This outward die deflection stretches and sizes the rings mounted on the machined cylindrical die surfaces.
- c) Assemble wires and diaphragm shell in the tack welding fixture (figure 21) and tack weld wires to the shell. The stainless steel diaphragm shell is forced outwards by internally pressurizing the neoprene bladders (TE 10153-6). The pressure force is reacted at the reinforcing rings which are positioned and supported by the grooved clamp jaws (-18 or -19 and -20 or -21) attached to the spider leg supports (-14). A split copper electrode shell (-5) contacts the inside stainless steel diaphragm surface. The other tack welding electrode, connected to the power supply, completes the circuit for tack welding the wires to the shell when it is pressed up against the reinforcing ring. The tack welding fixture is mounted on a moveable welding positioner to facilitate tack welding. This tacking technique provides rounding of parts, precise positioning of the reinforcing wires, proper clamping pressure for tack welding and precise control of the other tack welding parameters.
- d) Visually and dimensionally inspect part. Helium leak check using mass spectrometer and leak check fixture (figure 22).

#### 3.2.2.2 Hand Fabrication Method









36

DB NO 46002-2

The hand fabrication method for reinforcing ring fabrication and tack welding the rings to the shell starts, as before, with AISI 308 L weld wire in coil or rod form. The primary fabrication steps are as follows.

- a) Cut wire to approximate length required. Roll wire to approximate ring circular diameter.
- b) Fit wire to shell and maintain its position by use of spacer blocks.
- c) Cut ring to final fit length and butt weld ring ends together. Grind weld flush.
- d) Tack weld wire to shell using a two(2) copper electrode system. Aligned copper electrodes are pressed together between the stainless steel shell inside surface and the stainless steel ring outer surface. Condenser discharge power is applied for tack welding.
- e) Repeat operations for the number of rings required.
- f) Visually and dimensionally inspect and helium leak check.

#### 3.2.2.3 Diaphragm Assembly Fabrication Using Non-Standard Reinforcing Wire Sizes

As aforementioned, diaphragm reinforcing rings are made from AISI 308 L circular cross-section weld wire. This weld wire is available in standard sizes ranging from 1/32 inch diameter to 1/2 inch diameter. The wire comes in coil or straight rod form up to 1/4 inch diameter and in straight rod form over 1/4 inch diameter. The standard size increments are 1/32 inch diameter for the smaller diameter wires and 1/16 inch diameter for the larger diameter wires. The attempt is generally made to use the available standard reinforcing wire sizes for diaphragm designs. However, in order to maximize diaphragm cycle life, non-standard wire sizes may be required as was the case for the .110"Ø reinforcing wire diaphragm configurations previously discussed in sections 3.1.3.6 and 3.1.3.7. In this instance, the .110"Ø wires used were midway between the standard wire sizes of .094"Ø and .125"Ø.

A wire fabrication technique was evolved to

construct non-standard size reinforcing rings. This technique is economical and suitable for a small or large number of parts. The fabrication method starts with the procurement of straight weld rod to the nearest larger standard diameter. This larger diameter standard size rod is then centerless ground down to the desired non-standard cross-sectional diameter. The ground rod is then fabricated into reinforcing rings utilizing either the tooling or hand fabrication techniques detailed in sections 3.2.2.1 and 3.2.2.2. Additional intermediate butt welds may be needed in the ring construction depending upon the length of the reinforcing ring required and the length of the ground rod. The length of the ground rod is fixed by the stroke of available grinding machines.

In applying this method to the two (2) non-standard size (.110"Ø) reinforcing ring configurations (figures 18 and 19) one started with the procurement of available three (3) foot lengths of standard AISI 308L, 1/8"Ø straight weld rod. The 1/8"Ø rod was centerless ground down to .110±.001 inch cross-sectional diameter X 30 inches long straight rod with a 32 finish. The .110"Ø ground rod was then hand fabricated into reinforcing rings. Intermediate butt welds were required in order to form the larger reinforcing rings on the equator cone region of the 13 inch opening diameter diaphragms.

With the development and successful demonstration of this wire fabrication technique, reinforcing wire stiffness may thus be "finely tuned" to diaphragm shell stiffness as required to produce high cycle life ring reinforced diaphragm configurations. Technical, cost and schedule limitations heretofore imposed by availability of the desired wire size in less than special mill run quantities have been eliminated.

### 3.2.3 Furnace Brazing

The reinforcing wires of the diaphragms fabricated on this program were permanently attached to the shells by copper furnace brazing in a dry hydrogen atmosphere to complete the diaphragm assembly. The tack welds previously made functioned as the brazing fixture. The braze material was applied in the form of oxygen free copper wire. The brazing temperature used was 2020-2050°F.

## 3.3 Stainless Steel Diaphragm Cycle Tests

### 3.3.1 Test Objective

The 13" stainless steel diaphragm configurations,

designed and built as detailed in sections 3.1 and 3.2, were cycle tested at room temperature. The diaphragms were completely turned inside out upon themselves (reversed) as described in section 2, one complete reversal following the other. Reversal cycle testing was continued until leakage across the diaphragm was observed. The purpose of these tests was to provide the data needed to define and verify high reversal cycle life diaphragm configurations. Test results from earlier design configurations were used as a guide in developing the final highest cycle life diaphragm configuration.

### 3.3.2 Test Description

Diaphragms (defined in figures 6,8,12,15,17,18,19) were reversed (cycled) at room temperature per ARDE Test Plan 100 (TP-100) "Test Plan for Room Temperature Cycle Testing of 13" Stainless Steel Diaphragms". This test plan is given in Appendix 3, section 6.3.

The diaphragms were reversed as follows:

- a) Water was used as the pressurant to reverse the diaphragm per schematic SKD 10504 (figure 23) utilizing Test Operational Procedure 100 (TOP-100) "Operation Procedures for Diaphragm Water Actuation Test". TOP-100 is detailed in Appendix 3, section 6.3. This "open configuration" with the diaphragm exposed during reversal, provided ready access to the diaphragm for direct observation and measurement.
- b) Alternatively, gaseous helium (GHe) was used as the pressurant to reverse the diaphragm and expel  $H_2O$ , or  $H_2O$  used as the pressurant to expel GHe per schematic SKD 10505 (figure 24) utilizing Test Operational Procedure 101 (TOP-101) "Operational Procedure for Diaphragm Water Cycling Test". TOP-101 is contained in Appendix 3, section 6.3. This test rig configuration provided for continuous diaphragm cycling without rig dis-assembly (if desired).

Diaphragms were GHe leak checked with a mass spectrometer prior and subsequent to each reversal per (TOP-100) and/or (TOP-101) utilizing the special leak check fixture (figure 22) or the reversal test rigs (figures 23 and 24). Photographic coverage was provided at all stages of testing. Other measurements

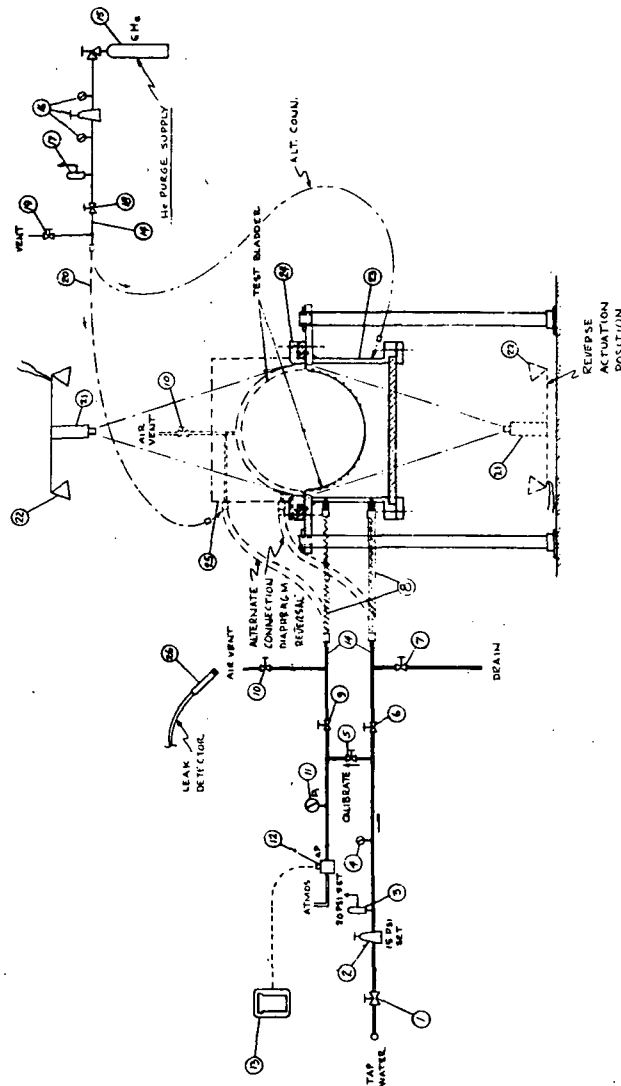
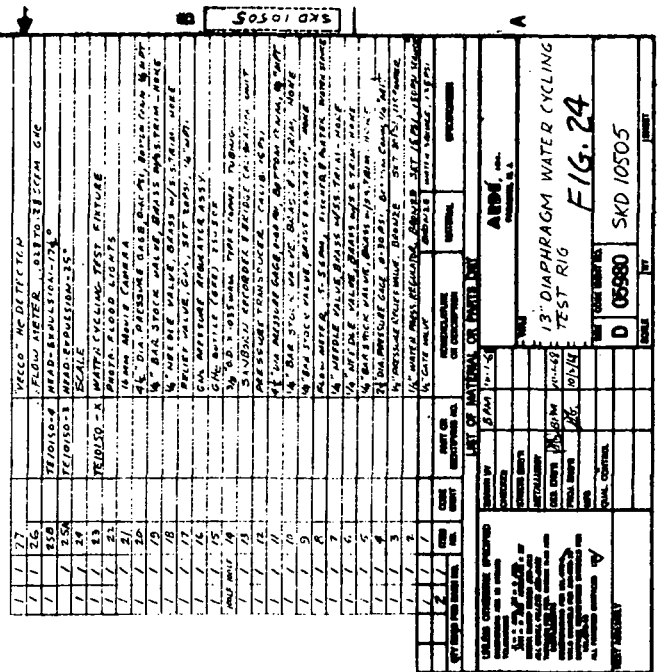


Figure 23  
Water Actuating Rig  
13" Diaphragm-Water Cycling Test

ITEM NO.		DESCRIPTION		QUANTITY		UNIT		REMARKS	
1	1	24	1	1	1	1	1	1	1
2	1	24	1	1	1	1	1	1	1
3	1	24	1	1	1	1	1	1	1
4	1	24	1	1	1	1	1	1	1
5	1	24	1	1	1	1	1	1	1
6	1	24	1	1	1	1	1	1	1
7	1	24	1	1	1	1	1	1	1
8	1	24	1	1	1	1	1	1	1
9	1	24	1	1	1	1	1	1	1
10	1	24	1	1	1	1	1	1	1
11	1	24	1	1	1	1	1	1	1
12	1	24	1	1	1	1	1	1	1
13	1	24	1	1	1	1	1	1	1
14	1	24	1	1	1	1	1	1	1
15	1	24	1	1	1	1	1	1	1
16	1	24	1	1	1	1	1	1	1
17	1	24	1	1	1	1	1	1	1
18	1	24	1	1	1	1	1	1	1
19	1	24	1	1	1	1	1	1	1
20	1	24	1	1	1	1	1	1	1
21	1	24	1	1	1	1	1	1	1
22	1	24	1	1	1	1	1	1	1
23	1	24	1	1	1	1	1	1	1
24	1	24	1	1	1	1	1	1	1
25	1	24	1	1	1	1	1	1	1
26	1	24	1	1	1	1	1	1	1
27	1	24	1	1	1	1	1	1	1
28	1	24	1	1	1	1	1	1	1
29	1	24	1	1	1	1	1	1	1
30	1	24	1	1	1	1	1	1	1
31	1	24	1	1	1	1	1	1	1
32	1	24	1	1	1	1	1	1	1
33	1	24	1	1	1	1	1	1	1
34	1	24	1	1	1	1	1	1	1
35	1	24	1	1	1	1	1	1	1
36	1	24	1	1	1	1	1	1	1
37	1	24	1	1	1	1	1	1	1
38	1	24	1	1	1	1	1	1	1
39	1	24	1	1	1	1	1	1	1
40	1	24	1	1	1	1	1	1	1
41	1	24	1	1	1	1	1	1	1
42	1	24	1	1	1	1	1	1	1
43	1	24	1	1	1	1	1	1	1
44	1	24	1	1	1	1	1	1	1
45	1	24	1	1	1	1	1	1	1
46	1	24	1	1	1	1	1	1	1
47	1	24	1	1	1	1	1	1	1
48	1	24	1	1	1	1	1	1	1
49	1	24	1	1	1	1	1	1	1
50	1	24	1	1	1	1	1	1	1
51	1	24	1	1	1	1	1	1	1
52	1	24	1	1	1	1	1	1	1
53	1	24	1	1	1	1	1	1	1
54	1	24	1	1	1	1	1	1	1
55	1	24	1	1	1	1	1	1	1
56	1	24	1	1	1	1	1	1	1
57	1	24	1	1	1	1	1	1	1
58	1	24	1	1	1	1	1	1	1
59	1	24	1	1	1	1	1	1	1
60	1	24	1	1	1	1	1	1	1
61	1	24	1	1	1	1	1	1	1
62	1	24	1	1	1	1	1	1	1
63	1	24	1	1	1	1	1	1	1
64	1	24	1	1	1	1	1	1	1
65	1	24	1	1	1	1	1	1	1
66	1	24	1	1	1	1	1	1	1
67	1	24	1	1	1	1	1	1	1
68	1	24	1	1	1	1	1	1	1
69	1	24	1	1	1	1	1	1	1
70	1	24	1	1	1	1	1	1	1
71	1	24	1	1	1	1	1	1	1
72	1	24	1	1	1	1	1	1	1
73	1	24	1	1	1	1	1	1	1
74	1	24	1	1	1	1	1	1	1
75	1	24	1	1	1	1	1	1	1
76	1	24	1	1	1	1	1	1	1
77	1	24	1	1	1	1	1	1	1
78	1	24	1	1	1	1	1	1	1
79	1	24	1	1	1	1	1	1	1
80	1	24	1	1	1	1	1	1	1
81	1	24	1	1	1	1	1	1	1
82	1	24	1	1	1	1	1	1	1
83	1	24	1	1	1	1	1	1	1
84	1	24	1	1	1	1	1	1	1
85	1	24	1	1	1	1	1	1	1
86	1	24	1	1	1	1	1	1	1
87	1	24	1	1	1	1	1	1	1
88	1	24	1	1	1	1	1	1	1
89	1	24	1	1	1	1	1	1	1
90	1	24	1	1	1	1	1	1	1
91	1	24	1	1	1	1	1	1	1
92	1	24	1	1	1	1	1	1	1
93	1	24	1	1	1	1	1	1	1
94	1	24	1	1	1	1	1	1	1
95	1	24	1	1	1	1	1	1	1
96	1	24	1	1	1	1	1	1	1
97	1	24	1	1	1	1	1	1	1
98	1	24	1	1	1	1	1	1	1
99	1	24	1	1	1	1	1	1	1
100	1	24	1	1	1	1	1	1	1



41



taken, where feasible, included such items as shell bending radius of curvature, changes in diaphragm hoop size, shape and contour, and pressure on both sides of the diaphragm. The nature and reasons for diaphragm failure was determined subsequent to reversal testing. A summary of the diaphragm reversal test results is contained in Table 3 herein. A detailed discussion of each diaphragm test, including measurements taken, is given in section 3.3.3, which follows.

TABLE 3 - Summary of 13" Stainless Steel  
Diaphragm Cycle Test Results

Part Number	Serial Number	Description	No. of Reversals
D3745	1	25° cone angle (.094"Ø wires)	Leaked #11
	2	25° cone angle (.094"Ø wires)	Leaked #4
	3	25° cone angle (.094"Ø wires)	Leaked #8
D3747	1	25° cone angle smaller intermediate wire design. (.094" Ø and .047" Ø wires)	Leaked #6
D3767	1	25° cone angle corrugated diaphragm design (.094"Ø wires)	Leaked #4
D3798	1	25° cone angle (.125"Ø wires)	Leaked #8
D3804	1	25° cone angle (.110"Ø wires)	Leaked #12
D3769	1	17 1/2° cone angle (.094" Ø wires)	Leaked #3
D3805	1	17 1/2° cone angle (.110" Ø wires)	Leaked #6

### 3.3.3 Cycle Test Results

#### 3.3.3.1 P/N D3745 S/N 1 (Figure 8)

This 25° cone angle smooth shell diaphragm with .094"Ø reinforcing rings was the first diaphragm tested. It was used as a tooling check out unit. Prior to reversal testing, the diaphragm was GHe leak checked using the special leak check fixture TD-10156 (figure 22). During this leak checking the diaphragm flange to cone radius at the equator region was straightened out somewhat due to the 15 psi internal pressure differential across the diaphragm. This increased the "developed height" of the diaphragm causing interference between the diaphragm and the leak check fixture cavity which resulted in buckling of the diaphragm in the equator cone region. The leak check fixture cavity was subsequently reworked to provide clearance between the diaphragm and the cavity during the GHe leak checking operation.

The D3745 S/N 1 diaphragm was then mounted in the water actuation rig and pressurized with water to an internal pressure difference of 45 psi in an attempt to straighten out the buckles. After this pressurization, the diaphragm was reassembled in the water actuation rig in the open position and reversed with water as the pressurant using the TE 1050-21 open cycle 25° ring as shown in figure 23. Because of the interference problems, no further helium leak tests were performed on this tooling check out unit, but the actuation pressure was raised to 45 psi after each reversal to check for leaks.

The test diaphragm was disassembled from the water actuation rig after each reversal for visual and photographic observation. The diaphragm was then reassembled in the test rig and reversal cycling was continued. Actuation pressure differences across the diaphragm during reversals ranged from 3 to 7 psi.

The D3745 S/N 1 diaphragm was completely reversed ten (10) times as described above before a pin hole leak was observed during the eleventh reversal. Control of diaphragm deflection mode was good. No substantial diaphragm cocking was observed. The eleventh reversal was completed and the diaphragm disassembled from the test rig for visual inspection. The failure was in the diaphragm shell in the equator cone region near a shell buckle. Photographs of this 25° cone angle tooling check out test diaphragm after the first and tenth reversals are shown on figure 25. The diaphragm shell buckles due to the aforementioned leak check fixture interference are clearly visible. Views of the diaphragm after the eleventh reversal are shown on figure 26.

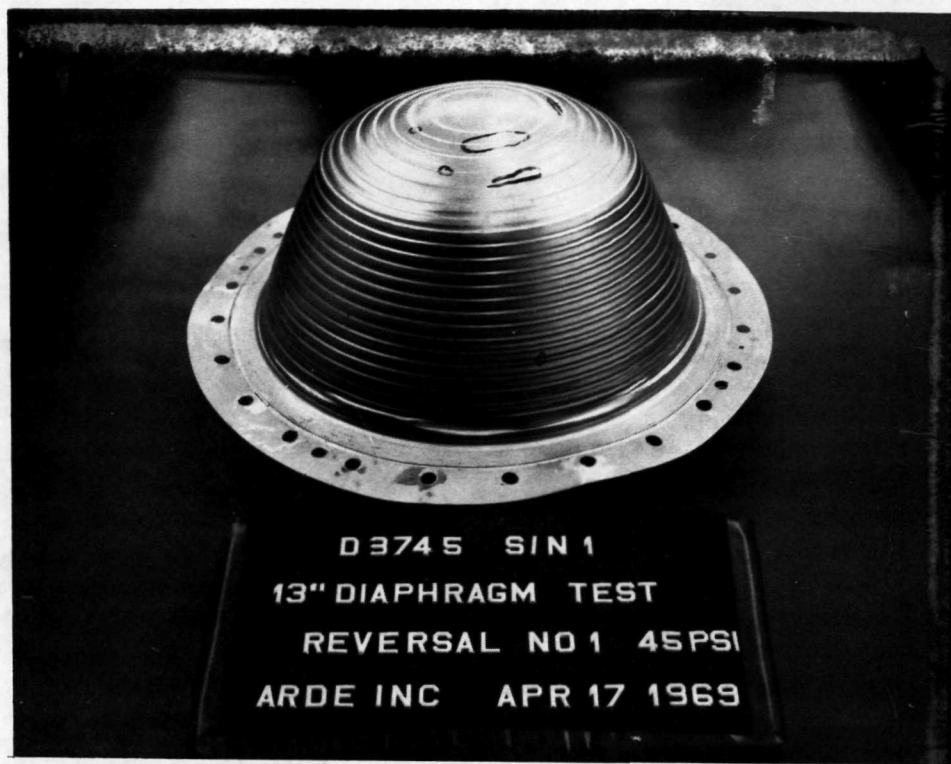


Figure 25

25° Cone Angle Diaphragm D 3745, S/N #1  
After First and Tenth Reversals



Figure 26  
25° Cone Angle Diaphragm D 3745, S/N #1  
After Eleventh Reversal

### 3.3.3.2 P/N D374S S/N 2 (Figure 8)

This second tooling verification diaphragm was reversal tested per ARDE Test Plan TP-100 (section 3.3.2) to check out the test rigs and test procedures. Figure 27 shows a view of the diaphragm and test rig during test set up prior to reversal testing. The open position of the water actuation rig (SKD-10504, figure 23) was used for the first diaphragm reversal and the closed position of the water cycling test rig (SKD-10505, figure 24) was used for all subsequent diaphragm reversals. Diaphragm condition and behavior were determined by visual and photographic means as well as by GHe leak checks and dimensional measurements. Diaphragm actuation pressure difference ( $\Delta p$ ) was sensed by a strain gage type pressure transducer and recorded by a Sanborn recorder as shown on the schematics of figures 23 and 24. Pressurant fluids were water and GN<sub>2</sub> and expelled fluids were air and water as applicable.

Interference between the tooling verification test diaphragm and the reversal test rig was noted during the first diaphragm reversal. This interference caused wire and shell buckling in the diaphragm equator area. The test rig was reworked and reversal testing followed by GHe leak checking after each diaphragm reversal was continued. P/N D3545 S/N 2 diaphragm failed (leaked) during the fourth reversal. Water was observed spraying through a "pin hole" in the diaphragm cone region. GHe leak checks after the first, second and third reversals indicated no leakage (GHe leakage  $\ll 10^{-6}$  SCC/SEC). The premature diaphragm failure during the fourth reversal was brought about by the first reversal interference with resulting equator region buckling. The failure was in the cone skin through the high local strain area of a previously formed buckle.

Figure 28 shows outside and inside views of the diaphragm after the first reversal. The buckling due to the interference problem is clearly evident. A view of the diaphragm after the second reversal is given in Figure 29 and close up photos of the diaphragm failure region after the fourth reversal are reproduced on figure 30.

The causes of the interference problem brought out during these test rig checkout tests were as follows:

- a) The diaphragm (initially smaller in diameter than the leak check fixture) took on the larger leak check fixture contour in the equator region as a result of the 15 psid



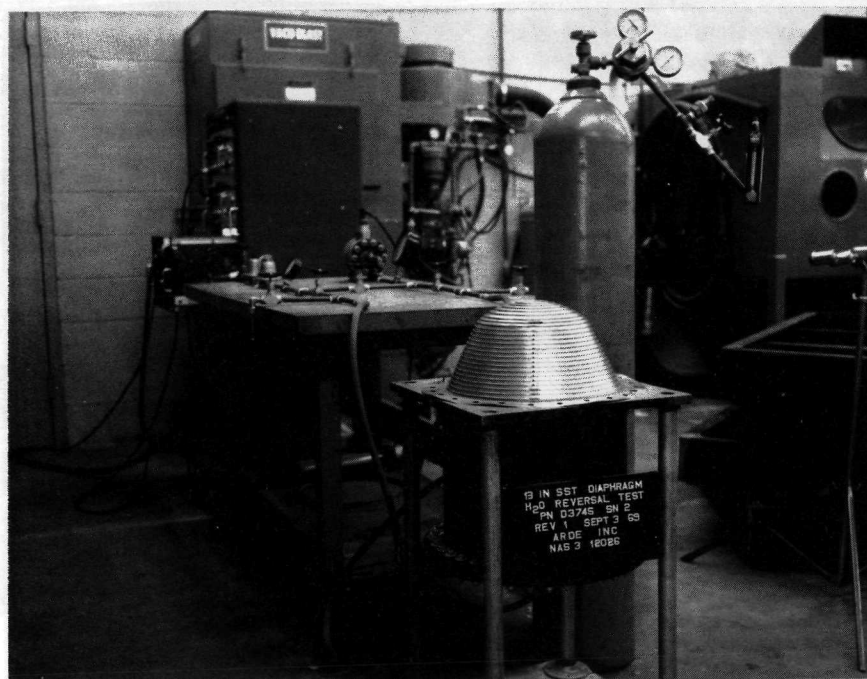
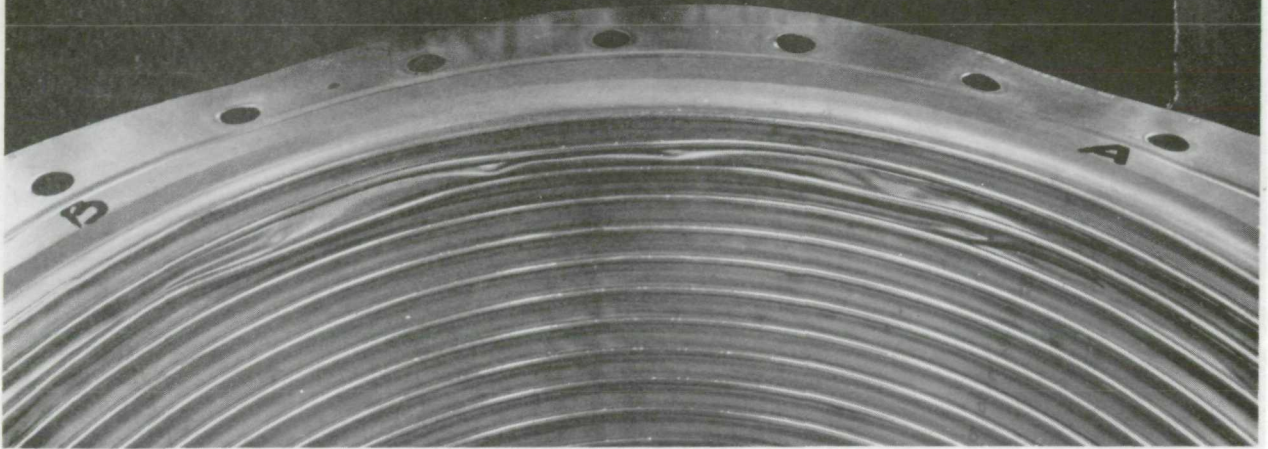


Figure 27

13" SST Diaphragm Water Reversal Test  
Reversal #1

13 IN SST DIAPHRAGM  
H<sub>2</sub>O REVERSAL TEST  
PN D3745 SN 2  
REV 1 SEPT 4 69  
ARDE INC  
NAS 3 12026



13 IN SST DIAPHRAGM  
H<sub>2</sub>O REVERSAL TEST  
PN D3745 SN 2  
REV 1 SEPT 4 69  
ARDE INC  
NAS 3 12026



Figure 28  
13" SST Diaphragm Water Reversal Test  
Reversal #1



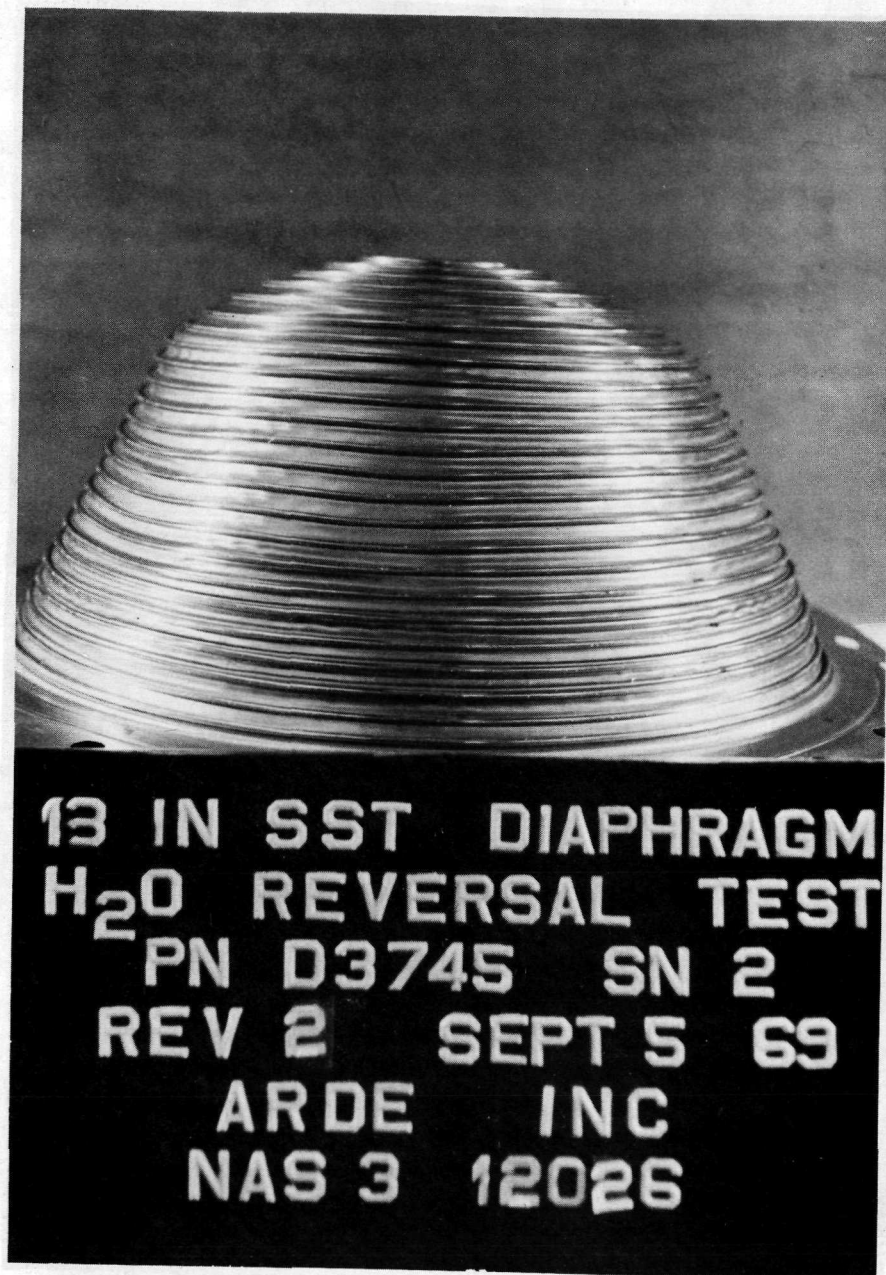


Figure 29

13" SST Diaphragm Water Reversal Test  
Reversal #2

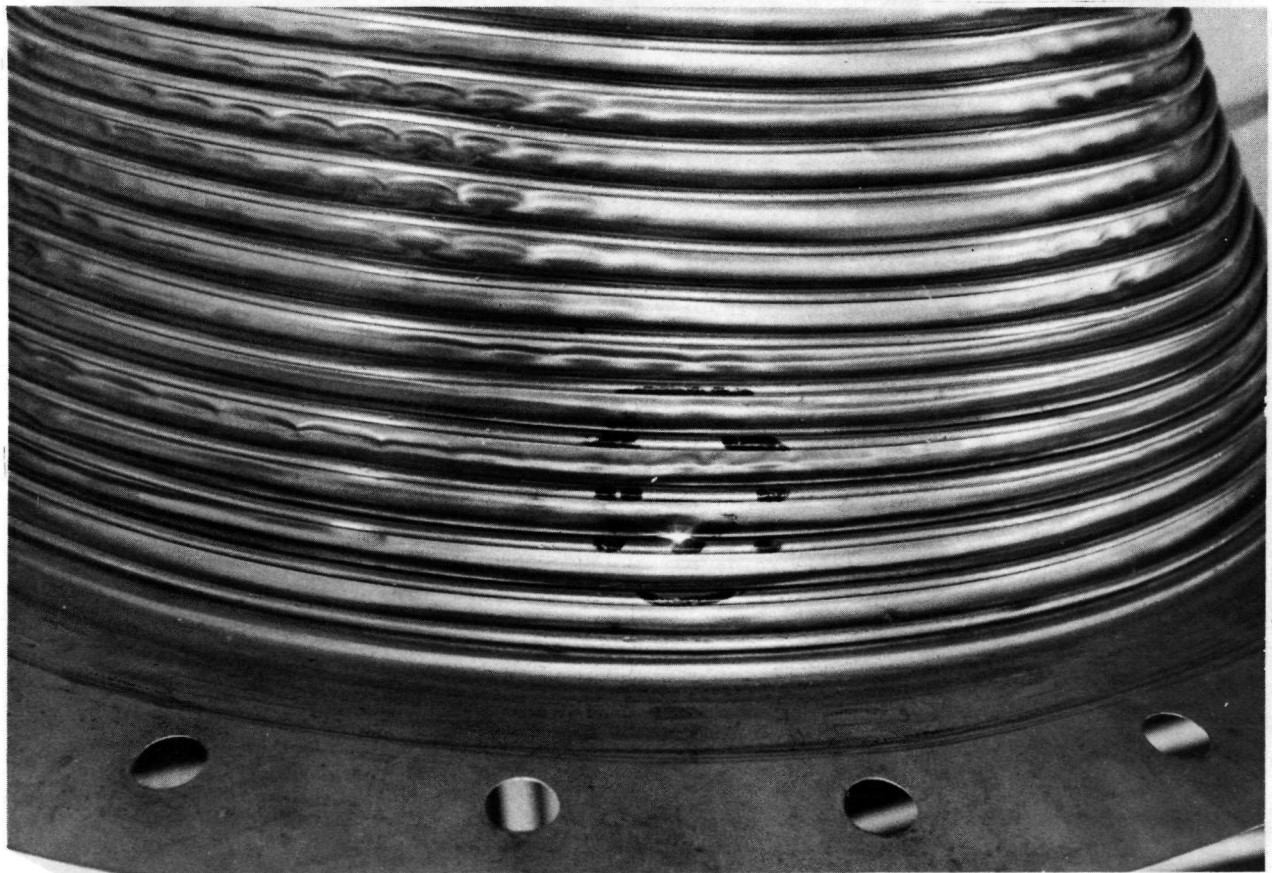
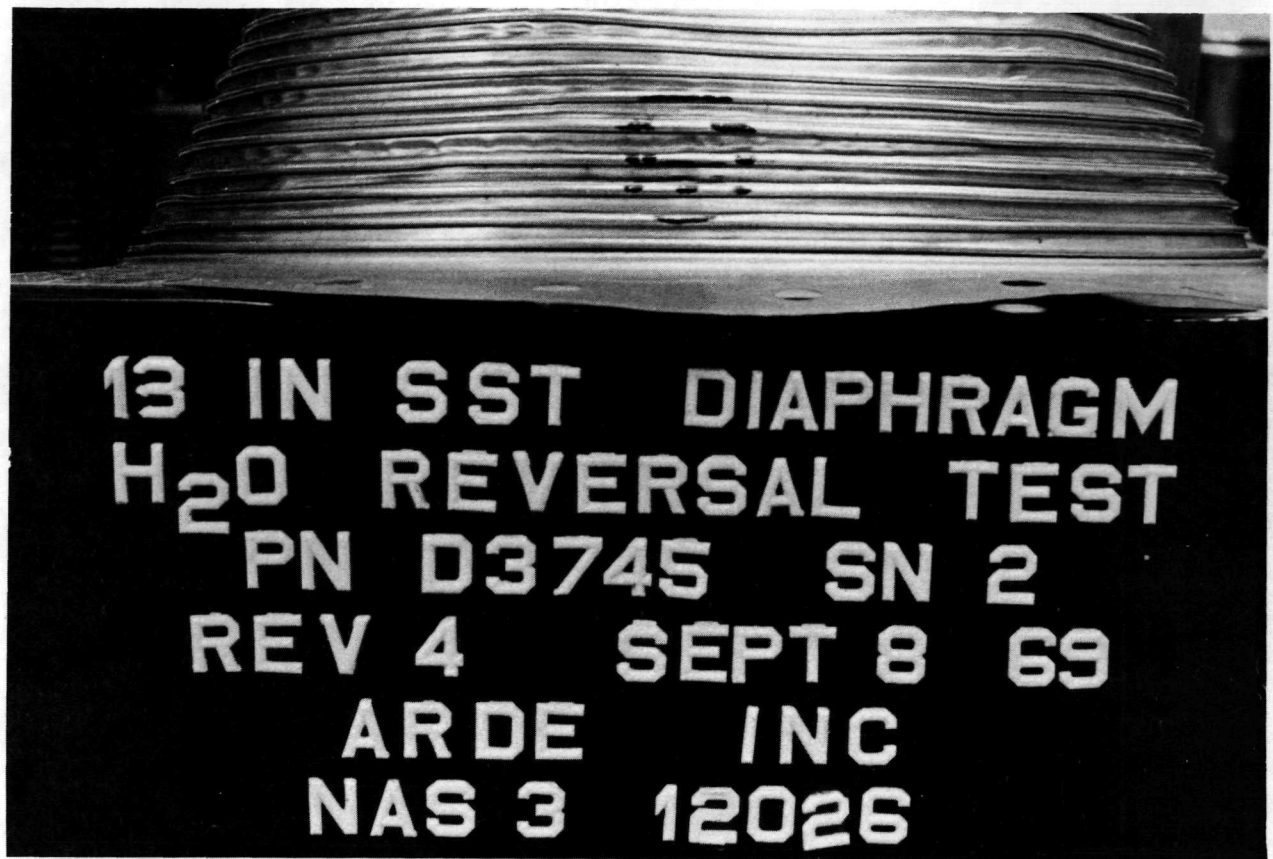


Figure 30

13" SST Diaphragm Water Reversal Test  
Reversal #4

pressure impressed across it during GHe leak checks before and after brazing. This increase in diaphragm diameter plus some out of roundness and growth due to furnace brazing, produced interference with the reversal test rig contour in the diaphragm equator area during the first reversal.

- b) At the end of the first reversal, when the diaphragm was completely reversed by the impressed pressure difference, it took on the larger contour of the reversal test rig in the diaphragm equator region. This further increase in diaphragm diameter then caused interference with the leak check fixture support ring which had to be removed to facilitate leak checking.

Corrective action taken to eliminate this problem included rework of the test rig and GHe leak checking in the rig itself as discussed in detail in section 3.3.3.3, which follows.

Dimensional measurements taken by means of micrometers prior and subsequent to diaphragm reversals verified the continuing ring (and attached shell) compression which has been previously discussed in section 3.1.3.3 and illustrated in figure 11. Table 4 gives ring outside diameter measurements for rings 1,2,3,17,18 taken initially (reversal zero) and after reversals 1 to 4. Rings 1,2,3 are located on the cone in the equator region and rings 17 and 18 are on the "knee region" (transition between the cone and hemisphere). AC and BD are two reference diameter locations 90° apart. Comparing the diameter measurements for the various rings at the same reference diameter stations, one finds residual ring compressive strains (diameter reduction/diameter) ranging from a fraction of a percent to about 2.5%. These results should be considered as qualitative since ring out of roundness and difficulty of obtaining accurate measurements on a flexible sheet metal part introduce errors.

Measurements of shell mid-span diameter changes were found not to be practical because of buckling, large shell curvatures and difficulty of getting calipers or micrometers on the shell in between the deformed rings. Measurement of ring torsional twist was also not accomplished for similar reasons.



TABLE 4 - REINFORCING WIRE DIAMETER REDUCTION DUE TO  
DIAPHRAGM REVERSAL (P/N D3745, S/N 2)

Wire No.	Rev. #0 (Initial Condition)		Rev. #1		Rev. #2		Rev. #3		Rev. #4	
	Ring Outside Diameter AC Inches	Ring Outside Diameter BD Inches	AC	BD	AC	BD	AC	BD	AC	BD
1	13.128	13.102	12.864	12.829	13.053	13.100	12.806	12.824	13.058	13.076
2	12.842	12.830	12.607		12.705	12.752	12.536	12.689	12.740	12.712
3	12.562	12.527	12.354		12.525	12.513	12.244	12.286	12.533	12.496
17	8.459	8.454			8.462	8.459			8.466	8.438
18	7.928	7.938			7.930	7.929			7.941	7.910

AC and BD are two (2) reference diameter locations 90° apart on diaphragm.

Diaphragm shell curvature during and after reversal was monitored by means of casts (or molds) of diaphragm contour made from dental wax. These molds were sectioned, mounted in plastic, polished and photographed using a microscope to give enlarged views. Curvatures were then obtained by curve fitting techniques. Circles of radii  $\rho$  were passed through groups of three (3) points on the magnified local shell contour. Figure 31 shows a magnified view (50X) of the diaphragm contour at wire number 1 during the first reversal, obtained by the aforementioned dental wax mold method. The lighter region is the wax mold and the darker area is the plastic. A magnified view (50X) of the diaphragm contour at the failure region after the fourth reversal is given on figure 32. Bending curvatures,  $K=1/\rho$ , obtained from these wax molds ranged from about 25 to 50 ( $\text{in}^{-1}$ ) for figures 31 and 32, respectively. These curvatures correspond to bending strains,  $\epsilon = K t/2$  (in/in), where  $t/2$ , half the shell thickness, is the distance from the neutral axis to the extreme shell fiber. For diaphragm shell thickness  $t=8$  mils, the local bending strains derived from the wax mold technique varied from about 10% at the wire number 1 region to 20% at the failure region. Using low cycle fatigue results, section 6.2, with the 20% strain at four reversal failure, one obtains,  $N = .16/\epsilon^2$ , as the number of reversals versus plastic strain correlation for stainless steel.

The wax mold technique utilized for monitoring diaphragm local curvature changes worked out quite well. It would appear to have applications to monitoring large local strains of other types of structures.

Actuation pressures for the tooling verification diaphragm (P/N D3745, S/N 2) varied from about 3 to 10 psid. Figure 33 shows part of the actuation pressure trace ( $\Delta p$  across the diaphragm) during the first reversal. The sharp pressure rise at the end of the pressure trace signifies the completion of the reversal because the fluid volume is approaching zero. The "peaks" and "valleys" on the pressure trace also have significance relative to diaphragm behavior during reversal. The pressure rises to the "peak" value required to yield the shell in bending and roll the wire. After the shell has yielded and the wire and attached shell has rolled as illustrated in figure 2, the actuation pressure difference drops to the "valley" value corresponding to the volume change brought about by the diaphragm rolling displacement. Each peak and valley pressure magnitude on the pressure trace corresponds to each diaphragm wire region. The "gross" behavior of the diaphragm during reversal can therefore be monitored from the recorded actuation pressure difference traces.

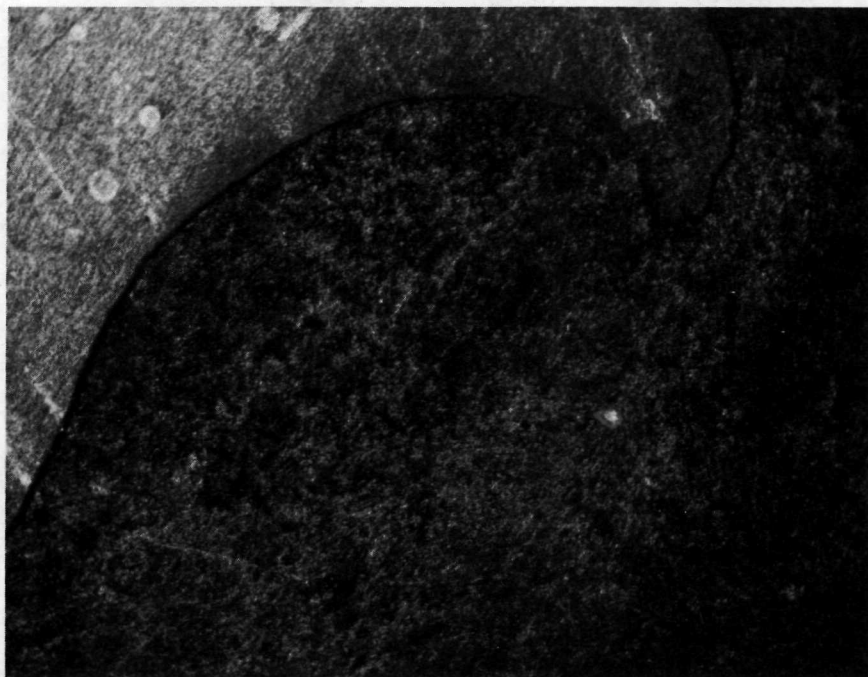


Figure 31  
Diaphragm Contour at Wire Number 1  
During First Reversal

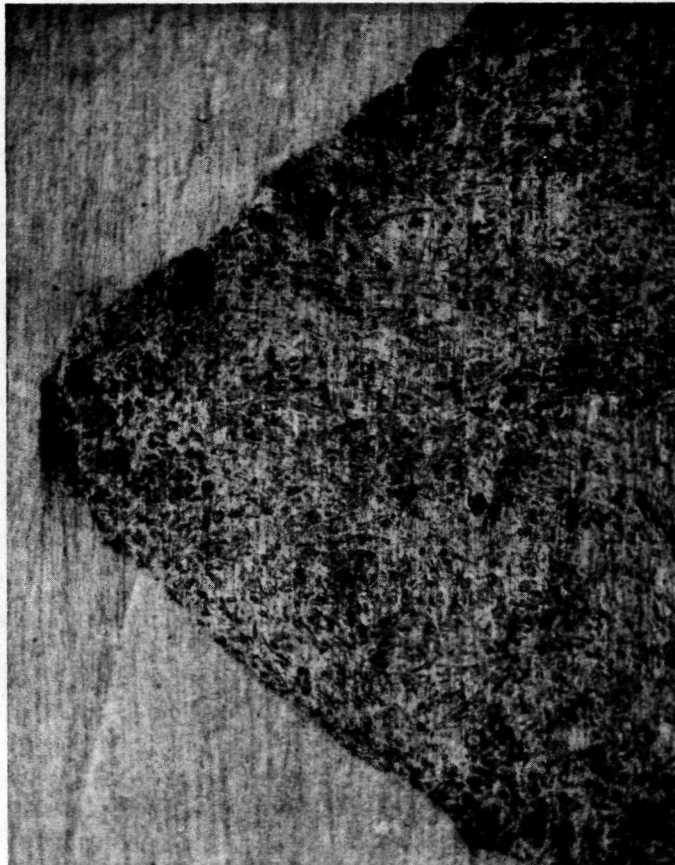


Figure 32

Diaphragm Contour at Failure Region  
After Fourth Reversal



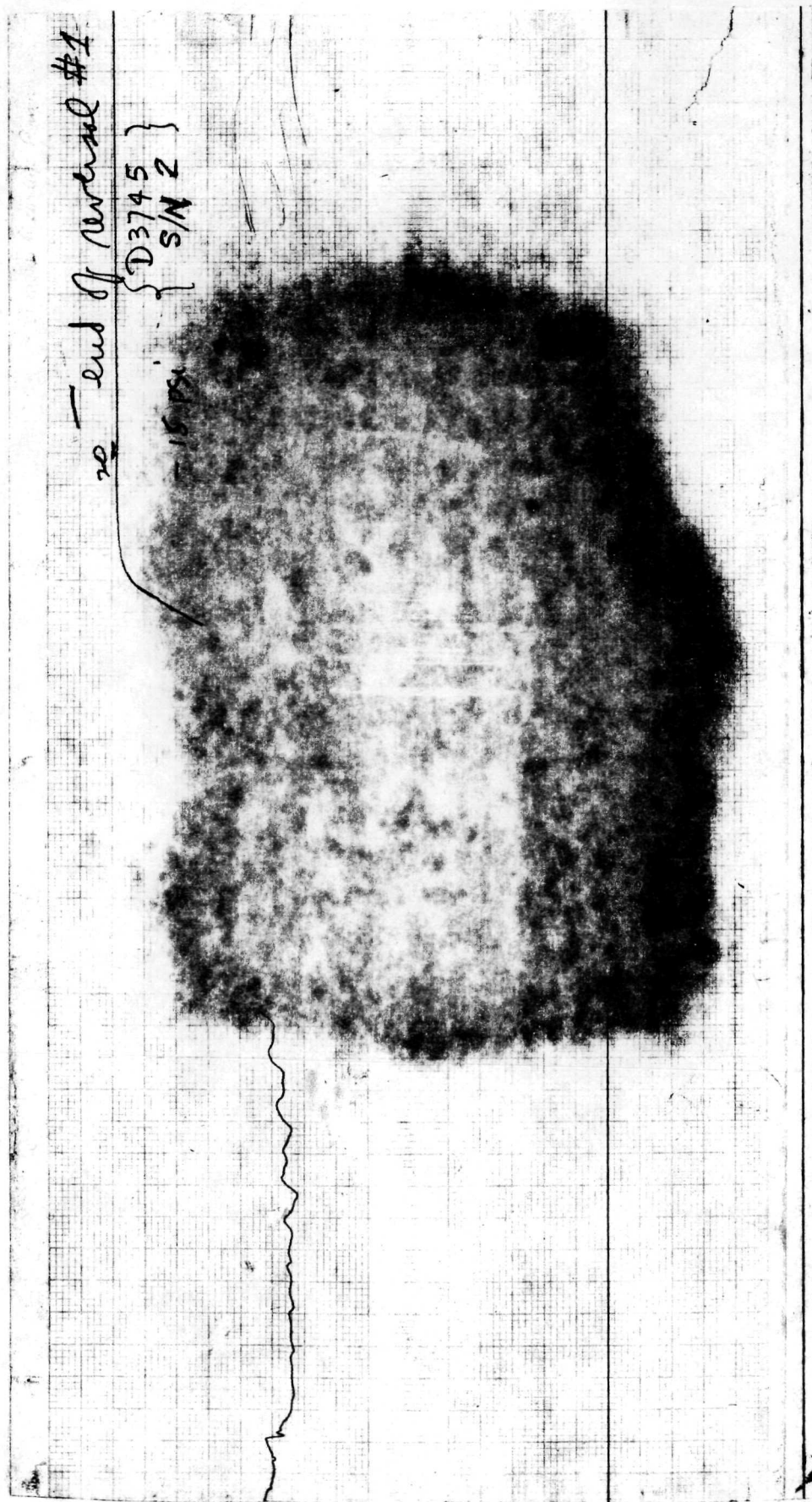


Figure 33  
Actuation  $\Delta P$  Trace  
P/N D 3745, S/N 2 (Reversal #1)



### 3.3.3.3 P/N D3745 S/N 3 (Figure 8)

Prior to reversal testing P/N D3745 S/N 3 diaphragm, corrective actions were taken to eliminate the diaphragm test rig interference problems brought out by the tooling checkout test of S/N 1 and S/N 2 diaphragms described in the previous sections herein.

- a) The S/N 3 diaphragm was leak checked in the special leak check fixture (figure 22) before and after brazing as part of the diaphragm fabrication procedure. The diaphragm contour was increased in diameter in this operation. The diaphragm took on the larger diameter of the leak check rig cavity due to the 15 psid pressure used for GHe leak checking.
- b) The reversal test rig contour diameter (figure 24) was increased to provide sufficient clearance to accommodate the diaphragm dimensional changes that were due to step (a) above.
- c) All subsequent diaphragm GHe leak checking was performed in the reversal test rig (figure 24) as described in TOP-101, (Appendix 3). Reversal test rig leak tightness was checked prior to each diaphragm GHe leak check operation. The test rig was purged with  $\text{GN}_2$  after each GHe leak check operation. The diaphragm was disassembled from the reversal test rig for visual and dimensional inspection as required. The diaphragm was then assembled into the test rig for continued reversal testing.

No further diaphragm and test rig interference problems were encountered during reversal testing. The above procedure was followed on all subsequent diaphragm reversal tests.

The D3745 S/N 3 diaphragm was reversal tested for seven (7) complete reversals without any indication of leakage. GHe leak checks after each reversal showed leakage to be much less than  $10^{-6}$  SCC/SEC. Cocking with some accompanying wire buckling was encountered on the diaphragm cone region during the second reversal. The diaphragm was then overpressured to 45 psid at the end of the second and subsequent reversals to "straighten out" the diaphragm. No further cocking and wire buckling occurred

after this overpressuring.

Diaphragm "pin hole" leakage was observed midway through the eighth diaphragm reversal. The leakage was in the diaphragm shell in the cone region between the ninth and tenth wire. The failure was through a shell buckle in the previously cocked and buckled diaphragm cone region. The eighth diaphragm reversal was continued until all the fluid was expelled from the reversal test rig.

Figure 34 shows the D3745 S/N 3 diaphragm prior to testing and after the fifth complete reversal. Views of this diaphragm after the eighth reversal are given on the photographs of figure 35. The effects of the cocking and wire buckling during the second reversal are clearly shown in these figures, particularly in the close up of the failure region given on figure 35.

Actuation pressure differences during diaphragm reversal varied from about 3 to 10 psid. Figure 36 shows a portion of the actuation pressure trace during and at the end of the eighth reversal.

Diaphragm ring compression during reversal was again verified by dimensional measurements. Table 5 gives wire outside diameter measurements before testing and after the fifth diaphragm reversal. Wire locations 2 and 3 are in the equator cone region and wires 17 and 18 are in the knee region. Diaphragm ring (and attached shell) compression strain varied from about zero to approximately 0.4% as determined by this dimensional change data. As discussed in section 3.3.3.2, this data should be viewed as qualitative information because of measurement difficulties.

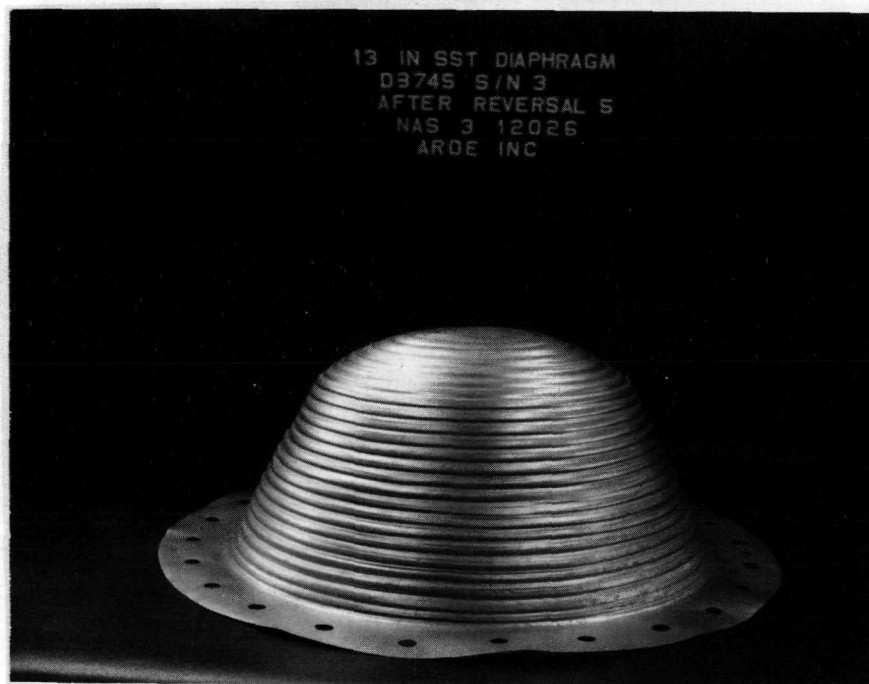


Figure 34  
13" SST Diaphragm  
Reversals 1 & 5

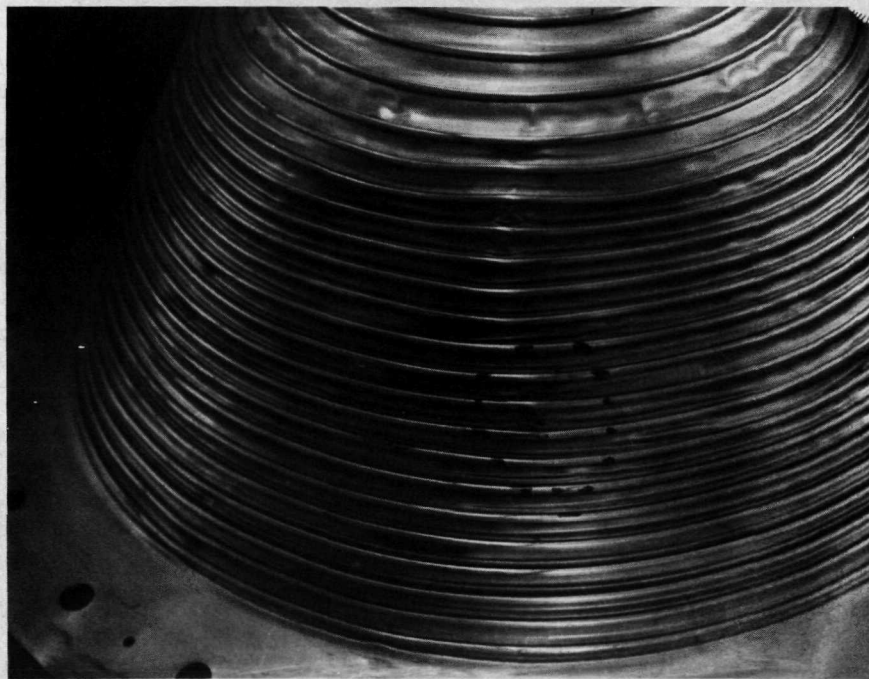


Figure 35  
13" SST Diaphragm After Reversal #8



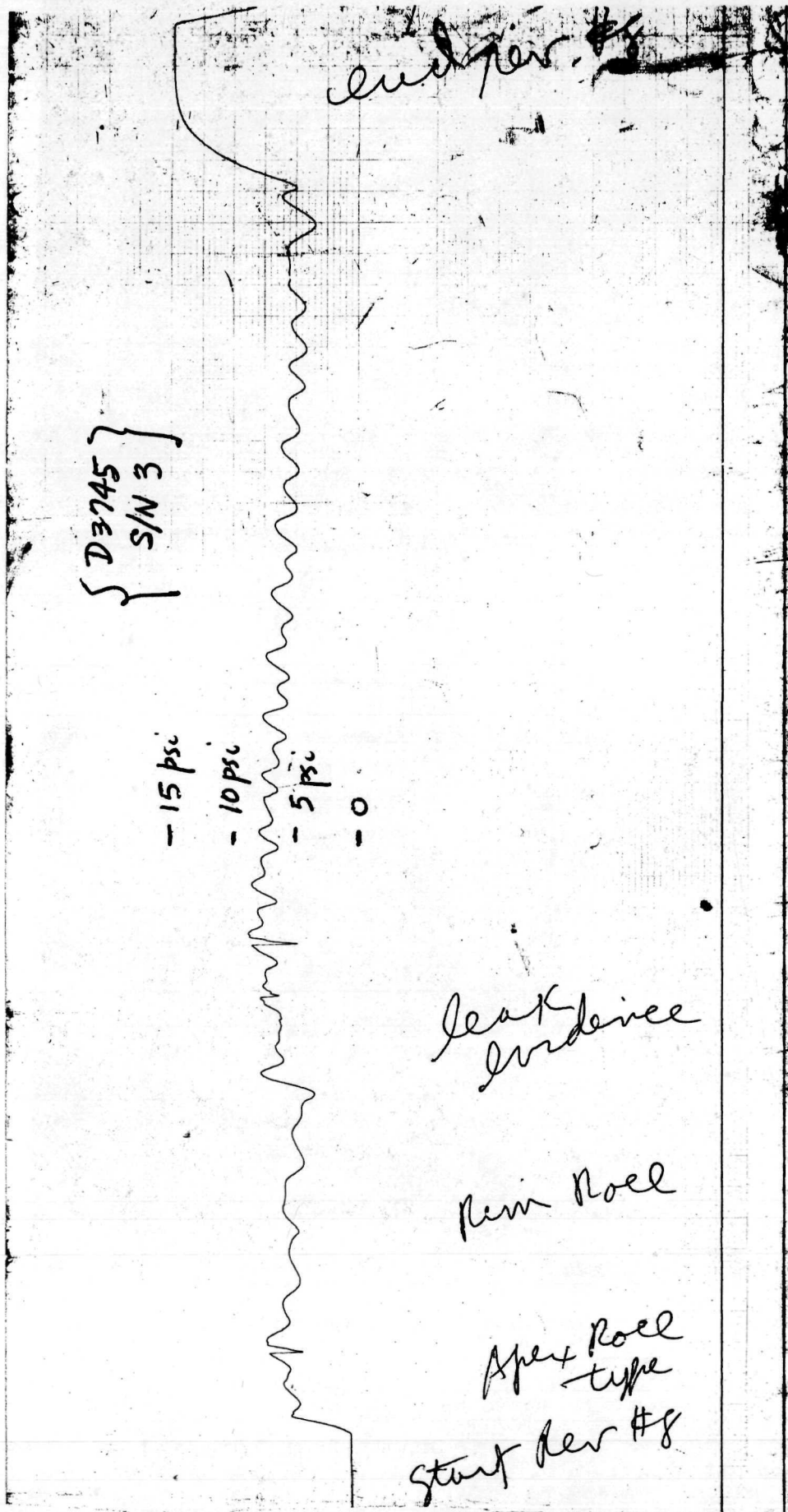


Figure 36

Actuation  $\Delta P$  Trace  
P/N D 3745, S/N 3 (Reversal #8)

TABLE 5 - Reinforcing Wire Diameter  
Reduction Due to Diaphragm  
Reversal (P/N D3745 S/N 3)

Wire No.	Initial Condition Rev.0		Rev.5	
	Ring Dia.	Ring Dia.		
	AC (inches)	BD (inches)	AC	BD
2	12.857	12.848	12.832	12.796
3	12.571	12.559	12.552	12.546
17	8.523	8.525	8.506	8.504
18	8.048	8.053	8.046	8.028

AC and BD are two (2) reference diameters  
located 90° apart on the diaphragm.

#### 3.3.3.4 P/N D3747 S/N 1 (Figure 12)

P/N D3747 S/N 1 diaphragm was reversal tested using the open position of the water actuating rig (figure 23) for the first reversal and the closed position of the water cycling test rig (figure 24) for all subsequent diaphragm reversals. This 25° Cone angle diaphragm had smaller (.047" cross-sectional diameter) intermediate wires between the primary .094" cross-sectional diameter reinforcing wires. The purpose of the smaller intermediate reinforcing wires was to suppress "diamond-shaped" buckles in the diaphragm shell as previously discussed in section 3.1.3.3.

The P/N D3747 S/N 1 diaphragm was completely reversed five (5) times without any leakage being detected by GHe leak checks with a mass spectrometer after each reversal. Pin hole leakage was observed during the sixth diaphragm reversal. Diaphragm deflection mode control was not particularly good. The smaller wires could not control diaphragm cocking between the larger wires and in some instances the smaller wires, buckled and went out of action. Some rather pronounced cocking and wire buckling occurred in the diaphragm cone region during the second reversal.

Figure 37 shows views of the P/N D3747 S/N 1 diaphragm after the sixth reversal. The failure was in the cone region through one of the shell buckles which were initiated by the cocking during the second reversal. Actuation pressures during diaphragm reversal varied in the range of 3 to 12 psid. The actuation pressure trace during the fifth reversal is reproduced on figure 38.

Reinforcing wire compressive strain was again noted by measurements of reinforcing wire diameter reductions after reversals. Table 6 gives comparative data for the zero and second reversals. Compressive strains (diameter reduction divided by initial diameter) ranging from about zero to 0.7% are indicated by this data. Measurement difficulties were experienced due to wire buckling and shell deformation. This data should therefore be viewed as only indicating the trend of wire compression after reversals.

A magnified view of the diaphragm contour in the immediate vicinity of the first wire during reversal number one is shown on figure 39. The dental wax mold technique previously discussed in section 3.3.3.2 was utilized. The lighter area is the wax and the darker area is the plastic used to encapsulate the mold for photographic purposes. A local diaphragm shell curvature of about  $25 \text{ (in}^{-1}\text{)}$ , corresponding to a plastic bending strain of 10%, was

13 IN SST DIAPHRAGM  
P/N D3747 SN 1  
AFTER REVERSAL 6  
NAS 3 12026  
ARDE, INC.

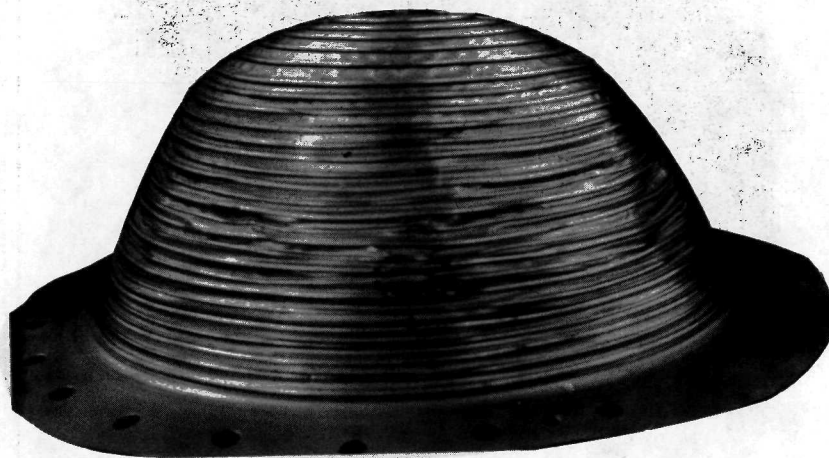


Figure 37

13" SST Diaphragm After Reversal #6



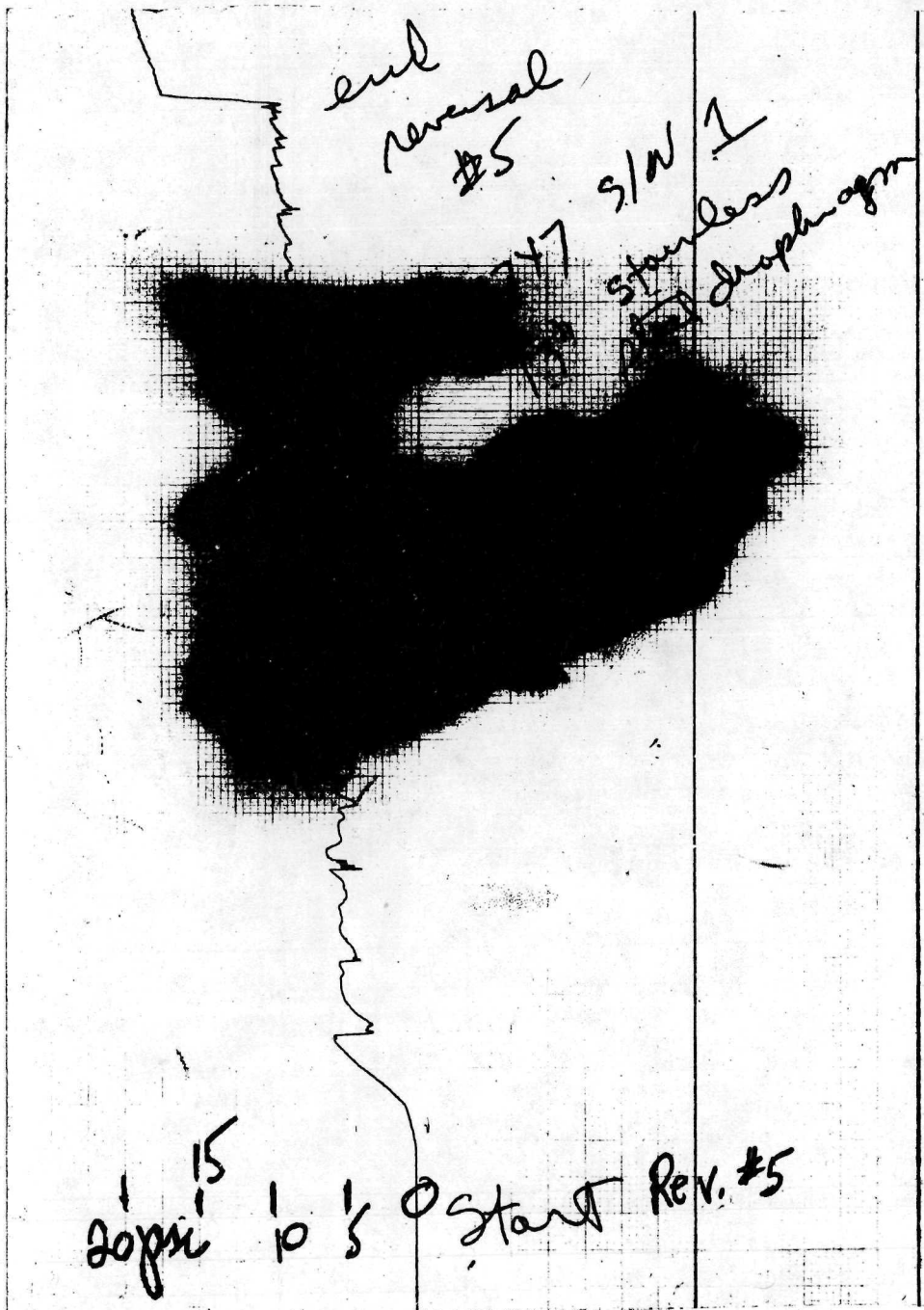


Figure 38

Activation  $\Delta P$  Trace  
P/N D 3747, S/N 1 (Reversal #5)

estimated from this magnified contour view. This strain is the same magnitude as measured at wire number 1 region of P/N D3745 S/N 2 diaphragm (figure 31).

TABLE 6 - Reinforcing Wire Diameter  
Reduction Due to Diaphragm  
Reversal (P/N D3747 S/N 1)  
(Dimensions In Inches)

Wire No.	Wire Dia.	Initial Condition Rev.0		Rev.2	
		AC	BD	AC	BD
1	.094	13.125	13.105	13.114	13.020
2	.047	12.815	12.780	12.754	12.714
3	.094	12.672	12.635	12.709	12.596
4	.047	12.344	12.312	----	12.276
5	.094	12.199	12.171	----	12.155
6	.047	11.877	11.850	-----	----

### 3.3.3.5 P/N D3767 S/N 1 (Figure 15)

This 25° cone angle diaphragm with the corrugated shell was reversal tested in the water cycling test rig (figure 24) using the closed position mode of operation. Water and GN<sub>2</sub> were expelled on alternate diaphragm reversals. This diaphragm was completely reversed three (3) times without any leakage indication as determined by GHe mass spectrometer leak checks after each reversal. Leakage was visually observed during the middle of the fourth reversal. Deflection mode control was good. The wires plus corrugations prevented diaphragm cocking. The failure was in the cone region shell, about halfway up the cone from the equator. Figure 40 shows views of the diaphragm prior to first reversal and after the fourth reversal.

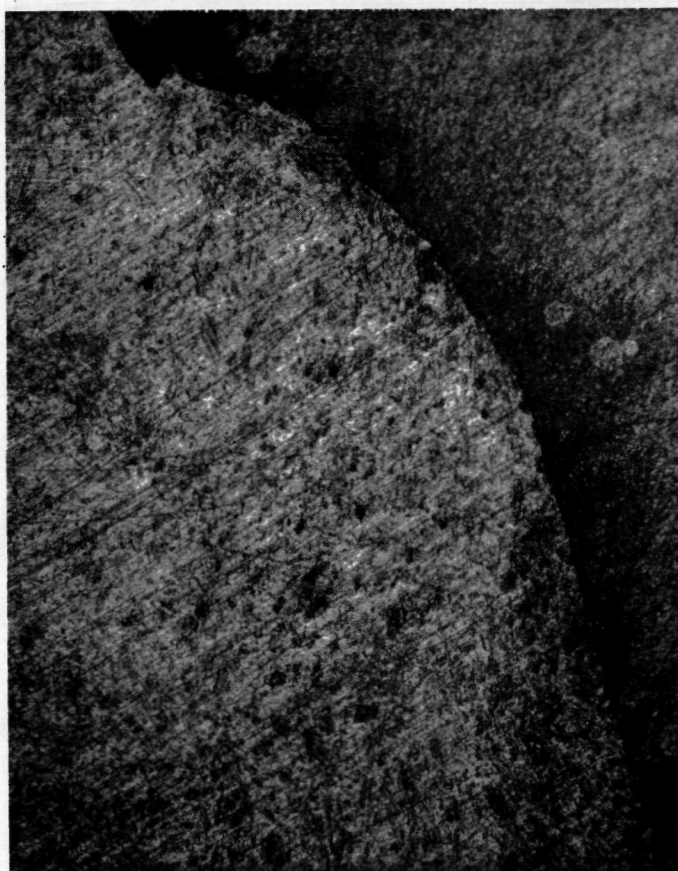


Figure 39

Diaphragm Contour in Vicinity of First Wire  
During First Reversal

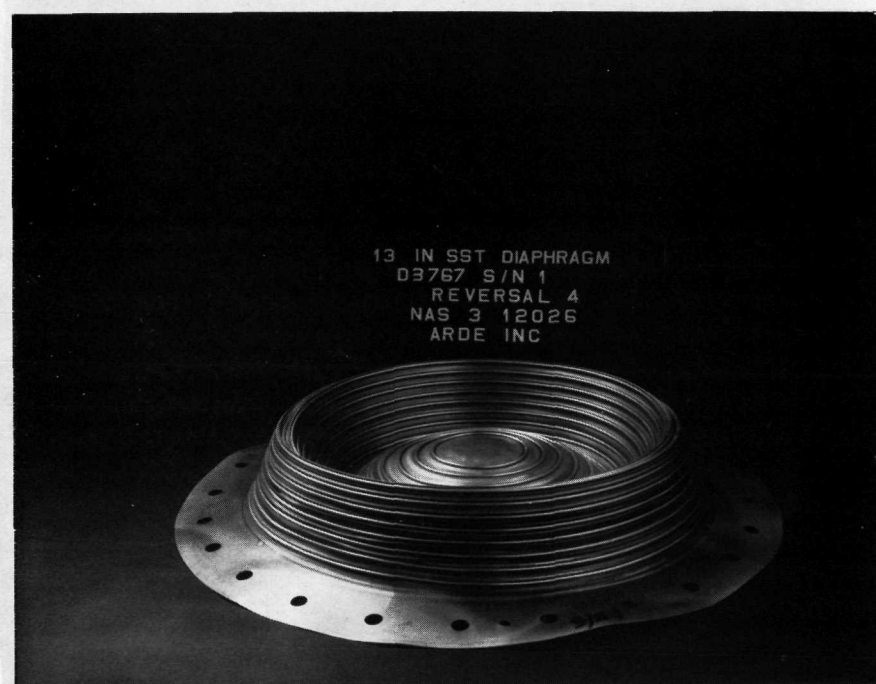


Figure 40  
13" SST Diaphragm  
Reversals 1 & 4



The corrugated shell construction was used to reduce the strain due to wire rotation by moving the wire center of gravity to the midplane of the diaphragm shell as previously discussed in detail in section 3.1.3.4. This objective was met, but at the expense of increased shell bending strain due to the stiffening effect of the corrugations. The corrugations, because of their greater distance from the centroid of bending of the median plane of the shell, were very rigid in bending compared to the uncorrugated shell regions and this offered increased restraint to shell rotation with accompanying amplification of shell bending strain. The failure in the diaphragm cone shell was in this high strain region of a corrugation.

Actuation pressure differences during diaphragm reversal were in the range of 3 to 12 psid. A portion of the actuation pressure difference trace during the second reversal is reproduced on figure 41.

#### 3.3.3.6 P/N D3798 (Figure 17)

This 25° cone angle diaphragm configuration had 1/8" cross-sectional diameter reinforcing wires to provide increased deflection mode control during reversal. Reversal testing was performed using the water cycling test rig in the closed mode of operation (figure 24). The diaphragm was completely reversed seven (7) times without any helium leak indication. Leak checking was performed in the test rig after each reversal per TOP-101 (see Appendix 3, section 6.3). Pin hole leakage was observed visually during the eighth reversal. The failure was in the diaphragm shell cone near the equator region. Figure 42 shows views of the diaphragm prior to testing and after the eighth reversal.

Control of diaphragm mode shape was excellent. The heavier 1/8" diameter reinforcing wires forced controlled rolling modes without any cocking. Diaphragm displacement took place in an orderly manner with rolling through the wires occurring one wire at a time, in sequence until each reversal was completed. The failures were a series of small cracks spaced essentially uniformly around the hoop circumference of the shell. This indicated uniform strain conditions around the circumference and attested to the uniformity and control of the diaphragm deflection mode.

Diaphragm actuation pressure differences ranged from 3 to 15 psid during diaphragm reversal. The strain gage differential pressure transducer malfunctioned during reversal testing so no recorded pressure difference traces were obtained for tests

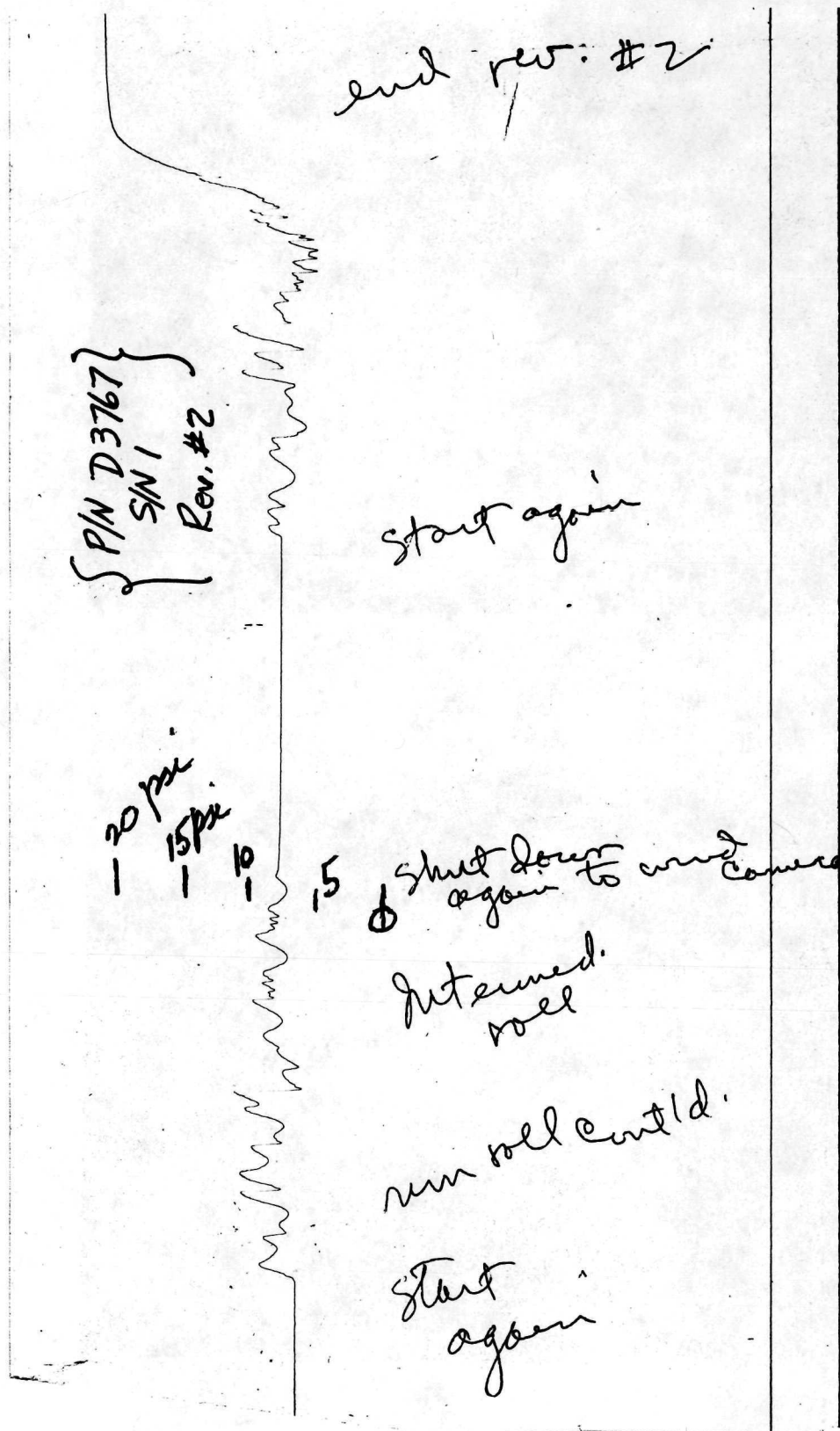


Figure 41

Actuation  $\Delta P$  Trace

P/N D 3767, S/N 1 (Reversal #1)

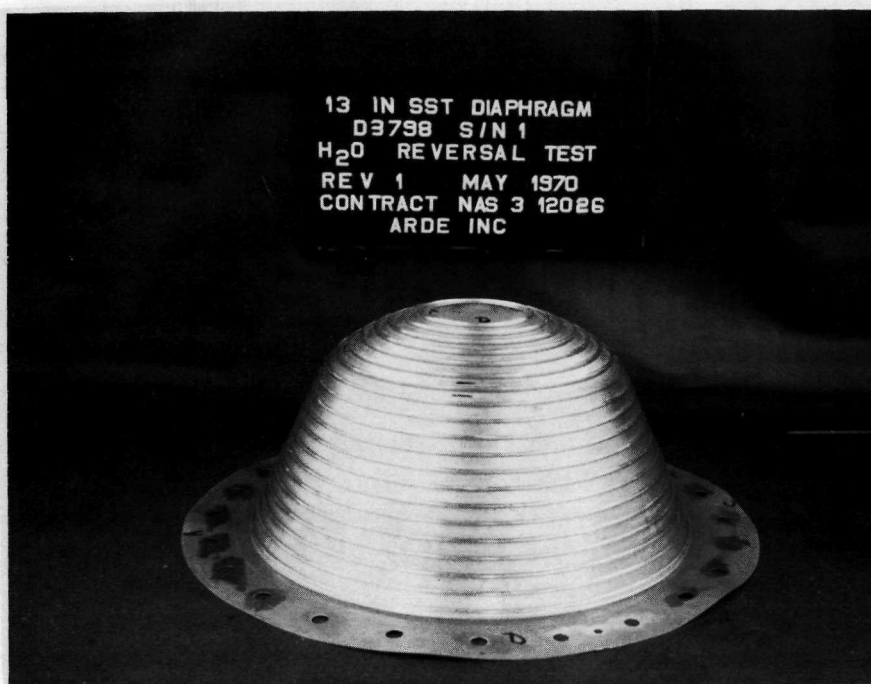


Figure 42  
13" SST Diaphragm  
Reversals 1 & 8

of P/N D3798 S/N 1 diaphragm. Actuation pressures were monitored visually by a mechanical pressure difference gage interposed in the reversal test rig circuit.

The reversal test results for P/N D3798 S/N 1 diaphragm demonstrated the trade off between the beneficial effect of increased deflection mode control brought about by use of the heavier 1/8" diameter reinforcing wires and the detrimental effect of the accompanying increased wire restraint to shell rotation as previously detailed in section 3.1.3.5. Better diaphragm deflection mode control eliminates shell strain amplification due to cocking. On the other hand, increased restraint to shell rotation increases shell bending strain. Based on this test data, the 1/8"  $\emptyset$  wires appeared to be too stiff. The .110"  $\emptyset$  wire cross-sectional diameter configurations, discussed in following sections, were thus evolved.

#### 3.3.3.7 P/N D3804 S/N 1 (Figure 18)

The water cycling test rig (figure 24) was used in the closed mode to reversal test the P/N D3804 S/N 1, 25° cone angle diaphragm with .110" cross-sectional diameter reinforcing wires. The choice of this wire size was a compromise between the conflicting requirements of increased wire stiffness for diaphragm deflection mode control and reduced wire stiffness for lower restraint against shell rotation. Reversal test results, detailed in previous sections, indicated that the 1/8"  $\emptyset$  wires offered excessive restraint against shell rotation and the less stiff .094"  $\emptyset$  wires were at marginal value of the lower bound of stiffness required for good deflection mode control. The .110"  $\emptyset$  reinforcing wire configurations were thus evolved.

The P/N D3804 S/N 1 diaphragm was completely reversed eleven (11) times without any evidence of leakage being detected by the helium mass spectrometer leak checks after each reversal. Leakage was visually observed during the twelfth reversal. The failure was in the diaphragm shell cone region. Testing was then continued until all the fluid was expelled, completing the twelfth reversal. Deflection mode control was very good. No cocking at all occurred and the reversals proceeded in an orderly manner, with the rolling deflection mode occurring one wire at a time, in sequence until each reversal was completed.

Figure 43 shows a view of the diaphragm after the twelfth reversal. The condition of the diaphragm was excellent. The reinforcing wires were still round and parallel to each other and



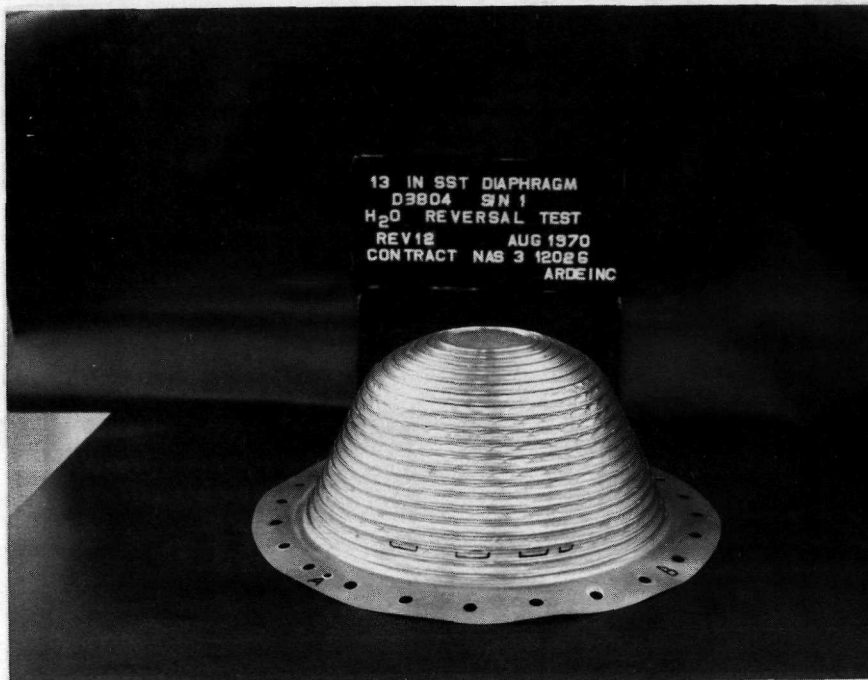


Figure 43  
13" SST Diaphragm  
Water Reversal Test  
Reversal #12

unbuckled. This P/N D3804 S/N 1 diaphragm showed the best cycle life results of all the diaphragms tested. The validity of the selection of the .110"Ø reinforcing wires as a good design trade off for this configuration was thus verified.

Actuation pressure differences varied in the range of 3 to 10 psid. Figures 44 and 45 give the actuation pressure traces during the eleventh and twelfth reversals, respectively. The diaphragm was overpressured to 45 psid at the end of each reversal prior to GHe leak checking to pick up any "visual" leak indications.

#### 3.3.3.8 P/N D3769 S/N 1 (Figure 6)

This 17 1/2° cone angle diaphragm with .094"Ø reinforcing wires was a "scale down" of the 6-7 reversal cycle life 23" diaphragm previously demonstrated by ARDE for the Air Force, references 7, 18. It was projected for use on the present program as a reference datum point diaphragm configuration. Fabrication difficulties were encountered during construction of this diaphragm. Contamination of the brazing furnace occurred which led to a faulty copper braze. A copper burn out cycle plus a rebraze attempt was also unsuccessful. Finally, the copper was stripped off with acid, new braze material applied, and the part was then successfully rebrazed. The diaphragm after this fabrication processing (four brazing cycles and one shell annealing cycle) was in a high temperature environment (1700 to 2050°F) for about four to five hours. This led to growth of large grains in the thin diaphragm shell and significant diffusion of copper braze material into the parent shell material. Both of these factors reduced available elongation of the as fabricated diaphragm. This destroyed the usefulness of P/N D3769 S/N 1 diaphragm as a reference cycle life configuration.

Reversal testing of P/N D3769 S/N 1 diaphragm was performed using the water cycling test rig (figure 24) in the closed mode. Leakage was observed during the third reversal cycle. The failure was in the diaphragm shell near the equator region. Figure 46 shows views of P/N D3769 S/N 1 diaphragm prior to testing and after the third reversal. The premature failure of this diaphragm was caused by significantly reduced shell elongation capability brought about by the excessively long time at elevated temperatures as discussed above.

#### 3.3.3.9 P/N D3805 S/N 1 (Figure 19)

P/N D3805 S/N 1 17 1/2° cone angle diaphragm

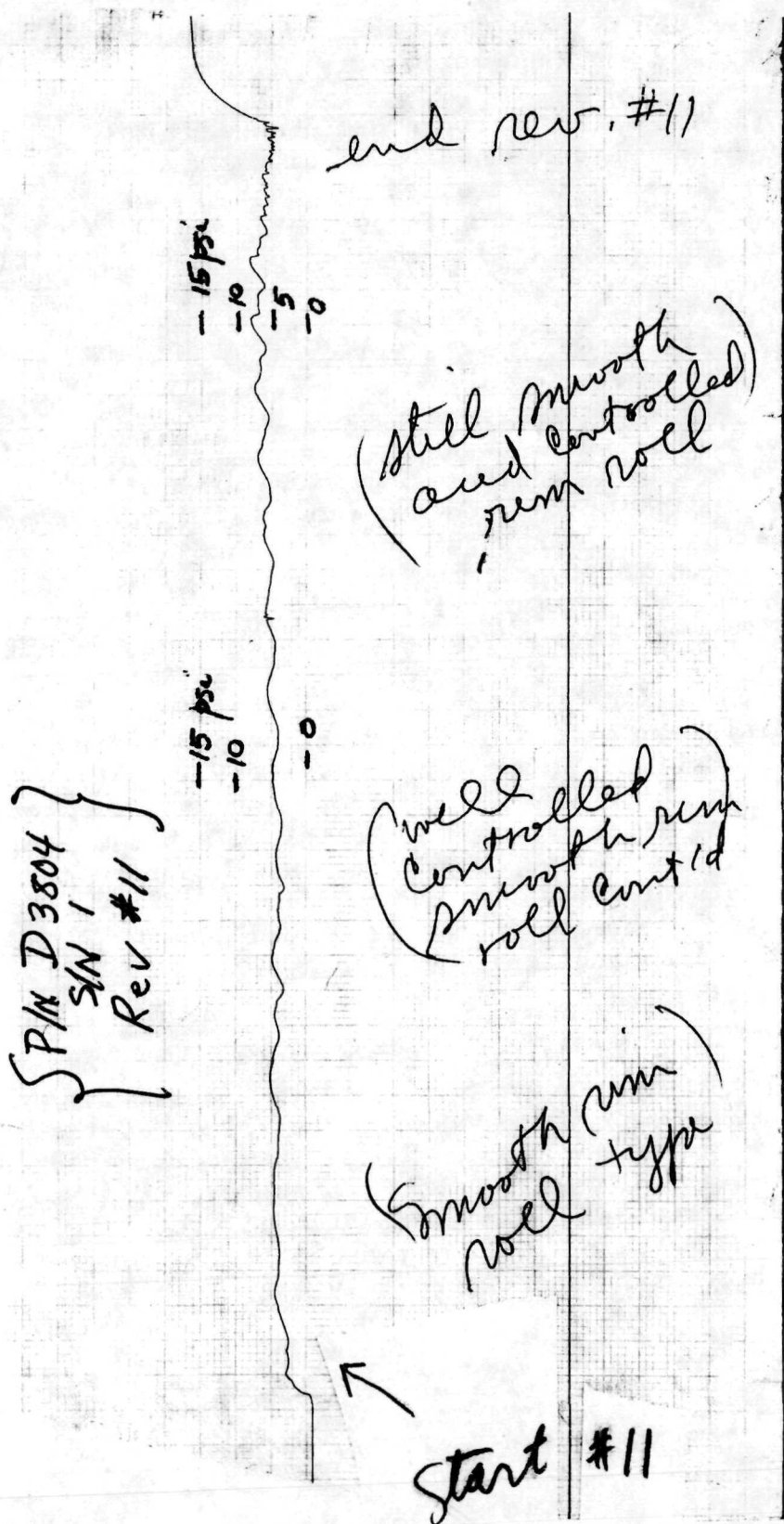


Figure 44  
 Actuation  $\Delta P$  Trace  
 P/N D 3745, S/N 2 (Reversal #1)

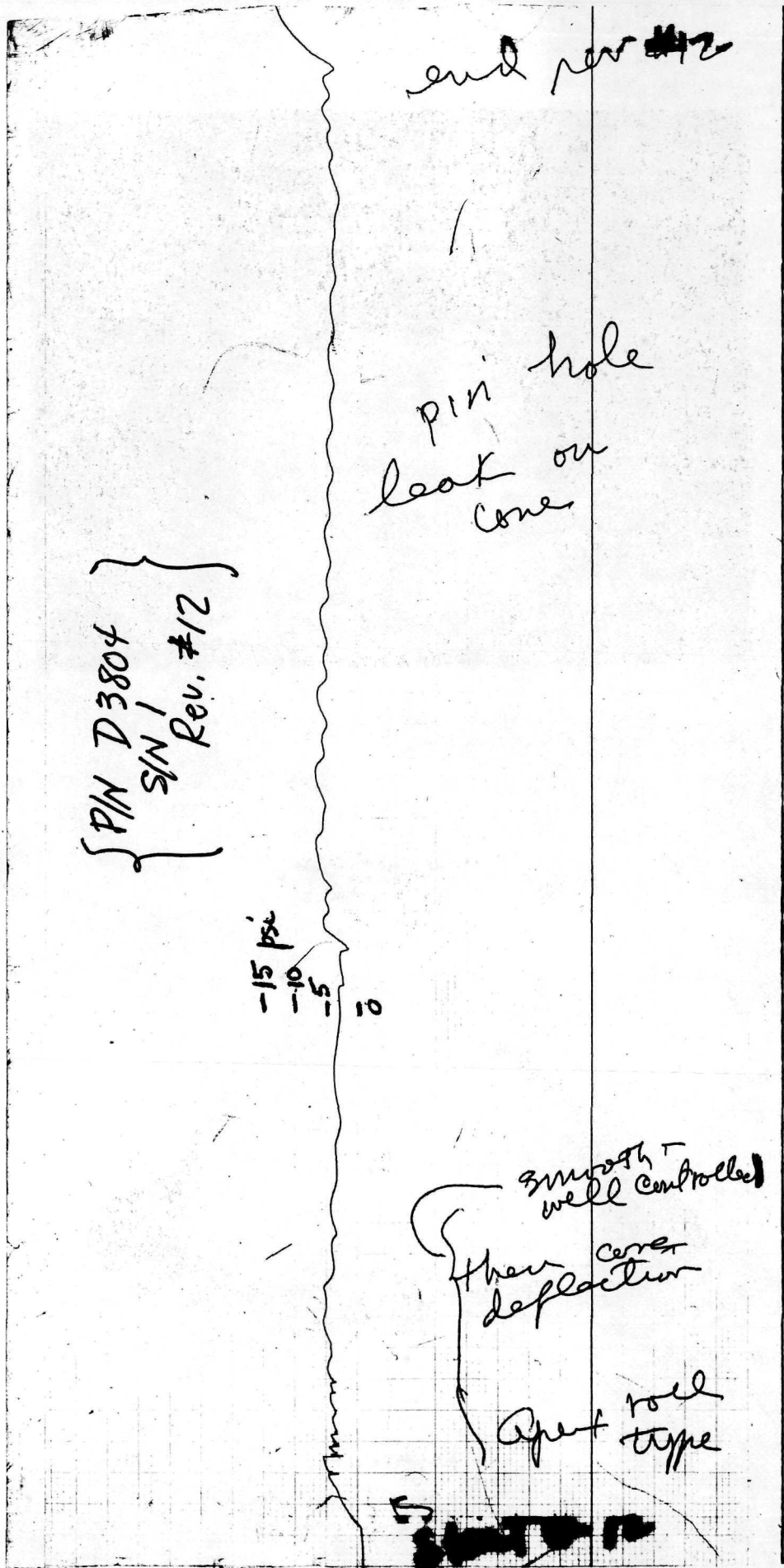
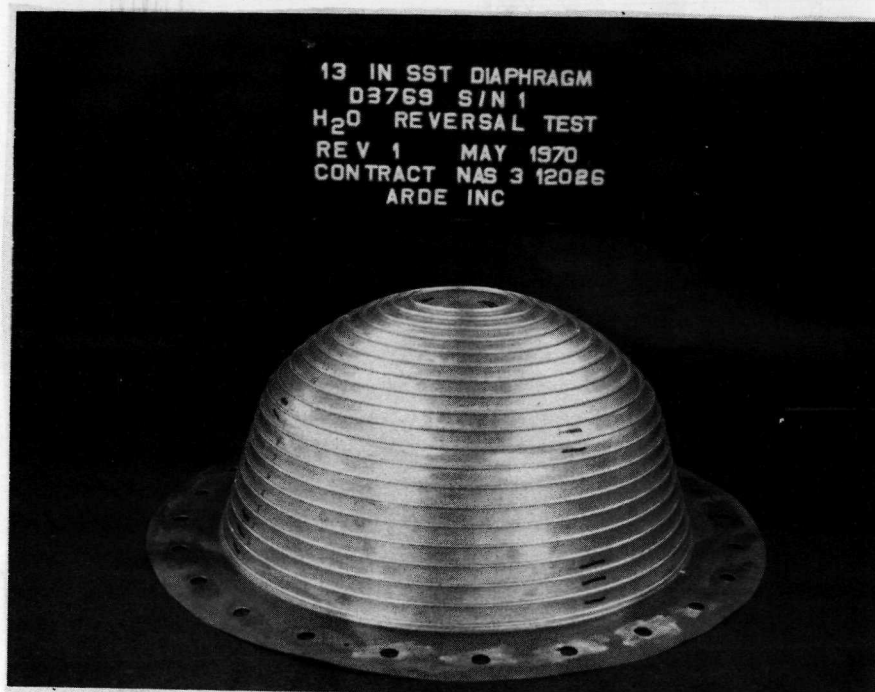


Figure 45

Actuation  $\Delta P$  Trace  
P/N D 3804, S/N 1 (Reversal #1)





13 IN SST DIAPHRAGM  
PN D3769 SN 1  
AFTER REVERSAL 3  
NAS 3 12026  
ARDE, INC.

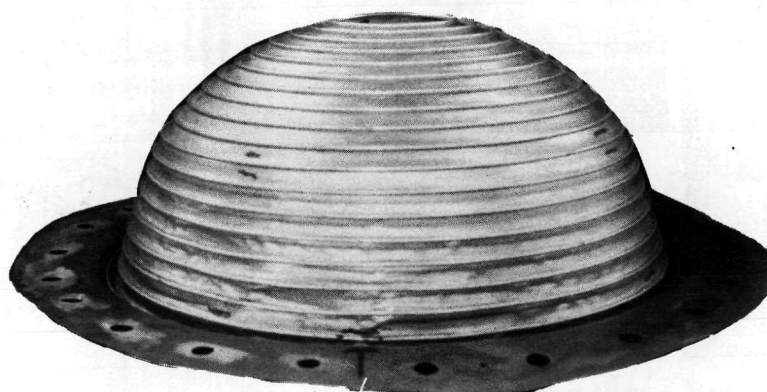


Figure 46  
13" SST Diaphragm  
Reversals 1 & 3

was reinforced with the "optimum" stiffness, .110"Ø wires. Reversal testing was performed using the closed mode configuration of the water cycling test rig (figure 24). Deflection mode control by the .110"Ø reinforcing wires was excellent. Actuation pressures during reversals varied between 3 and 8 psid. A portion of the actuation pressure trace during reversal 3 is shown in figure 47. Flat regions are holds for camera rewinding. GHe leak checks were performed after each reversal. In addition, the actuation pressure was raised to 45 psid at the end of each reversal as an aid to visual leak detection. The P/N D3805 S/N 1 diaphragm was reversed completely five (5) times without any leakage indications. Towards the end of the sixth reversal, pin hole leakage was observed visually. The reversal was then continued until all the fluid was expelled. The failure was in the diaphragm shell cone in the equator region. A view of the diaphragm after the sixth reversal is given in figure 48.

### 3.4 Evaluation of Stainless Steel Ring Reinforced Diaphragm Reversal Test Results

Evaluation of the diaphragm reversal test results detailed in section 3.3 indicated the following.

#### 3.4.1 Cycle Life Correlation

As anticipated, diaphragm reversal cycle life increased with increased cone angle. Reversal cycle life test results obtained on the present program with 13" diameter stainless steel diaphragms and test results for 23" diameter stainless steel diaphragms generated on a previous Air Force program, reference 18, were both correlated by the cycle life relation (See Appendix 2, section 6.2).

$$N \propto (R/t) \left\{ \frac{\sin \theta}{(\pi - 2\theta)^2} \right\} (\epsilon_N)^2 \quad - - - (3.4 - 1)$$

Here,

N=number of complete diaphragm reversals prior to failure (leakage)

R=diaphragm shell radius

t=diaphragm shell thickness

$\epsilon_N$ =strain to necking for diaphragm material

$\propto$ =proportionality factor

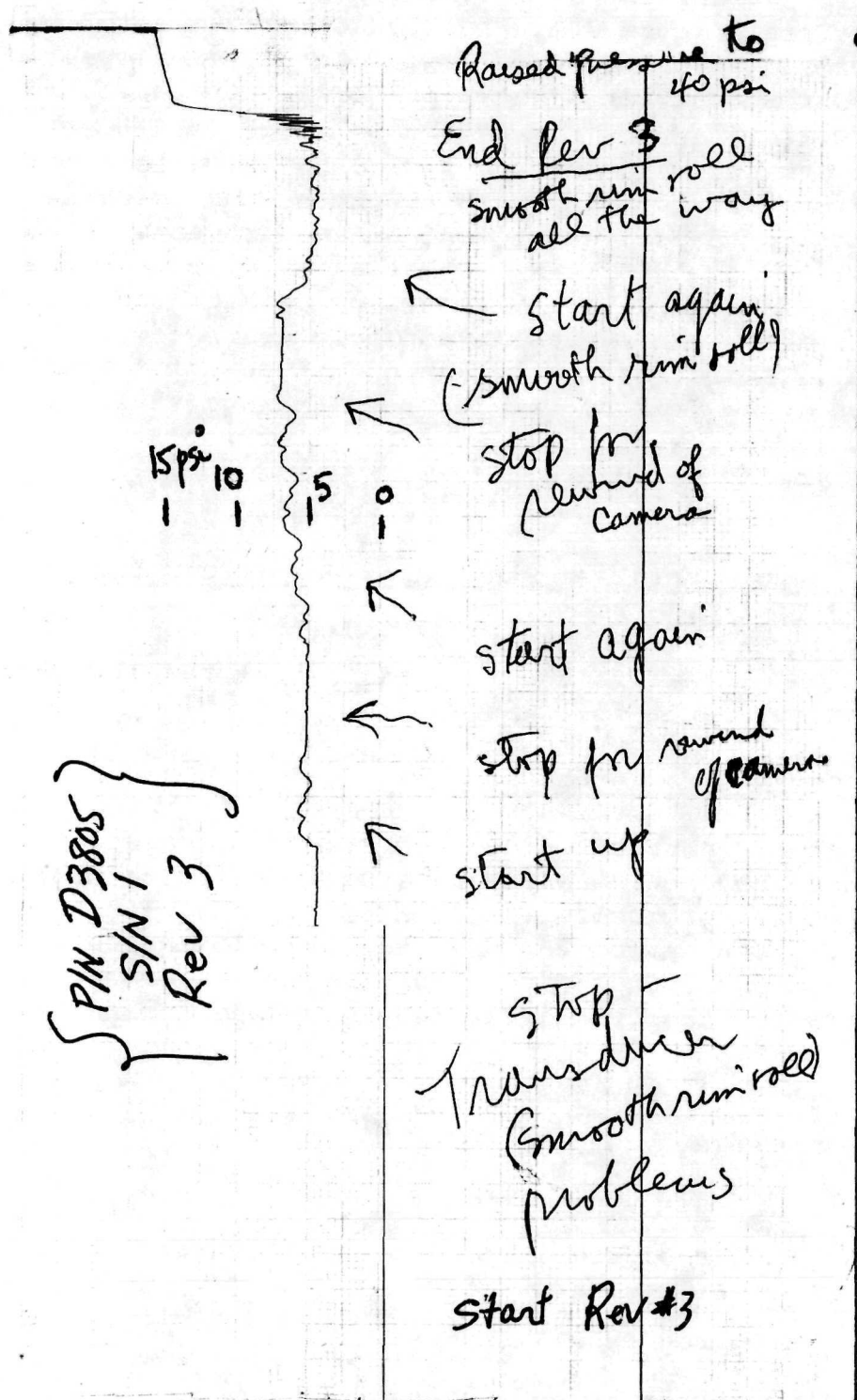


Figure 47

Actuation ΔP Trace

P/N D 3805, S/N 1 (Reversal #3)

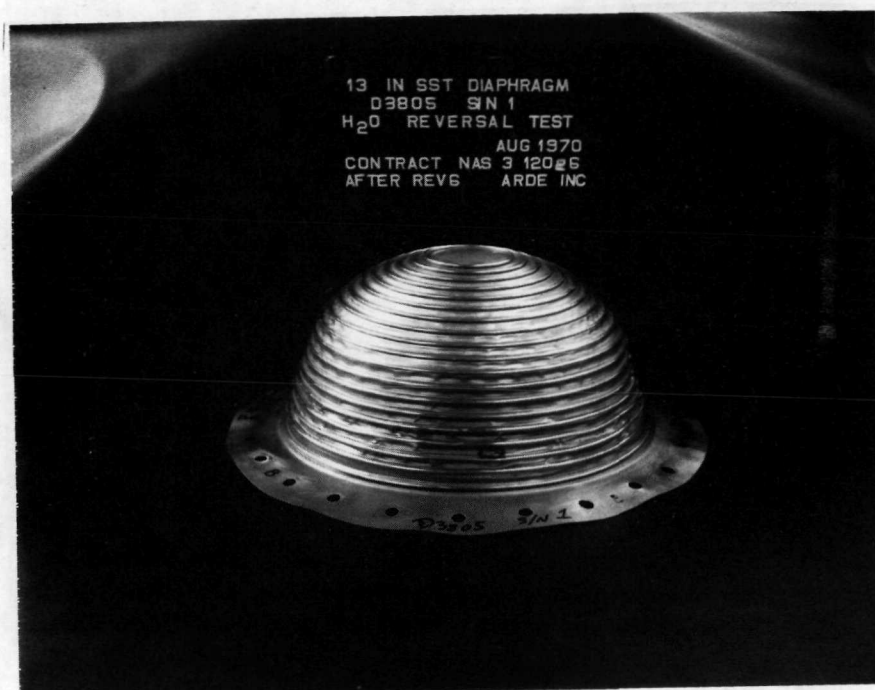


Figure 48

13" SST Diaphragm  
Water Reversal Test  
Reversal #6



$\theta$  = diaphragm cone angle (angle with cone axis of rotation)

It has been assumed that optimum ratios of ring to shell stiffness have been used when comparing reversal cycle lives of various diaphragm configurations. This explains why reinforcing ring diameter is not found explicitly in equation 3.4 - 1. When cone angle  $\theta \rightarrow \pi/2$ , or  $R/t \rightarrow \infty$  in equation (3.4 - 1), cycle life  $N$  becomes very large as one would anticipate for a flat plate. Table 7 below shows a comparison of the actual versus computed stainless steel ring reinforced diaphragm reversal cycle lives. Equation 3.4 - 1 above was used to determine the computed values. The strain to necking factor,  $\epsilon_N$ , was taken equal to unity since the diaphragm material was the same. For convenience of reference, the results have been normalized on the maximum cycle life  $25^\circ$  cone angle 13" diameter diaphragm. It is seen that the agreement between predicted and test values is good. One can thus project reversal cycle lives for modified hemispherical type ring reinforced diaphragms of various geometries and materials with a reasonable degree of certainty.

TABLE 7 - DIAPHRAGM REVERSAL CYCLE LIFE CORRELATION

R (in)	t (in)	$\theta$ ( $^\circ$ )	$\pi - 2\theta$ ( $^\circ$ )	$\sin\theta$	N(actual) (complete reversals)	N(computed) (complete reversals)
6.5	.008	17.5	145	.300	5	6
6.5	.008	25	130	.423	11	11
11.5	.010	17.5	145	.300	7	8

### 3.4.2 Diaphragm Shell Configuration and Variable Wire Size Effects

Smooth diaphragm shell configurations with constant reinforcing wire sizes developed the best cycle life performance. The corrugated diaphragm shell configuration, figure 15, which reduced ring (and shell) membrane compressive strain by putting the ring centroid at the midplane of the diaphragm shell, did not prove effective. The corrugations were too stiff compared to the uncorrugated diaphragm shell regions and induced very high bending strains in the shell, leading to substantial reduction in diaphragm cycle life. Similarly the smaller intermediate wire design, figure 12, did not yield good results. The smaller reinforcing wires put in to suppress

diaphragm shell buckling between the larger wires were not effective in controlling the diaphragm deflection mode. Cocking led to severe overstraining and reduction in cycle life.

#### 3.4.3 Reinforcing Wire Size Trade-Offs

The .094"Ø reinforcing wires provided relatively low shell rotational restraint bending strain but gave marginal diaphragm deflection mode control which reduces cycle life. The best diaphragm deflection mode control was achieved using 1/8"Ø wires. However, these stiff wires forced very high bending restraint strains in the diaphragm shell leading to lowered cycle life. The .110"Ø reinforcing wires provided a good compromise between the conflicting requirements of good diaphragm deflection mode control and low diaphragm shell rotational restraint bending strains as evidenced by the test results. The .110"Ø reinforcing wire size used on the 25° cone angle smooth shell provided the highest cycle life diaphragm configuration. Similarly, the .110"Ø reinforcing wire size diaphragm configuration showed the highest cycle life for the 17 1/2° cone angle diaphragm variations tested.

#### 3.5 Description of Aluminum Diaphragm and Cryogenic Testing Effort.

Work was performed on the program in the areas of Aluminum diaphragm fabrication investigation and cryogenic testing of diaphragms. This effort was of a limited nature since it was decided to concentrate resources on demonstrating a high cycle life stainless steel diaphragm configuration.

##### 3.5.1 Aluminum Diaphragm Fabrication Investigation

Annealed 1100 aluminum was selected as the material to be initially investigated because of its reported high elongation to necking property. The critical fabrication problem for a ring reinforced aluminum diaphragm is the attachment of the reinforcing rings to the diaphragm shell. The limited investigation conducted on this program indicated the following.

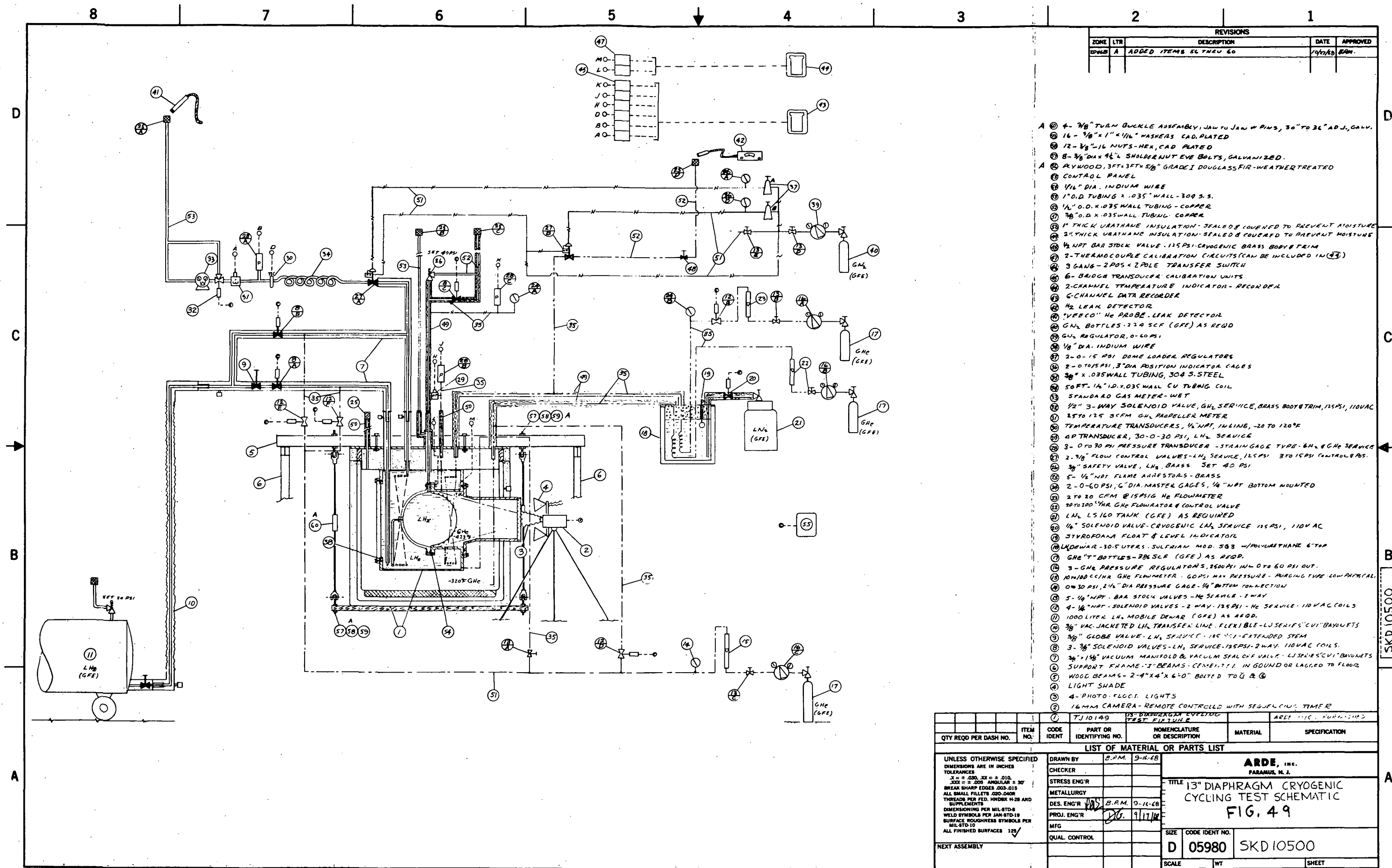
- a) Furnace brazing appears potentially to be a practical approach. Successful furnace brazing of thin members in an argon atmosphere has been reported, reference 19, and suitable fluxless brazing alloys have been identified. Use of a dry hydrogen atmosphere for brazing should give even better results.

- b) Dip brazing is also a possibility for reinforcing wire attachment although more severe distortion problems are anticipated compared to furnace brazing. Control of braze meniscus may also be more difficult.
- c) Regardless of the brazing technique, the reinforcing wires must be positioned and held to the diaphragm during the brazing operation. For stainless steel, tack welding of the reinforcing wires to the diaphragm shell has been very successful. Tack welding of aluminum reinforcing wires to the aluminum diaphragm shell needs development effort. The power requirements for tack welding are much higher compared to stainless steel because the aluminum members will be thicker and in addition, the very high thermal conductivity of the aluminum conducts the heat away from the joint rapidly. Resistance welding type of equipment will have to be used instead of capacitor discharge type employed for stainless steel. New or modified types of welding heads and tacking tooling will probably have to be employed to accommodate the geometric and thermal (burn through) constraints of the ring reinforced diaphragm configuration constructed of aluminum. Positioning and holding the wires to the shell by means of brazing fixtures is also a possibility. This technique would eliminate the need for tack welding. Some limited work indicating initial feasibility has been done on this approach using stainless steel flat plate models, reference 8. It is anticipated that the brazing fixture approach would be less difficult for aluminum since the brazing temperature is about 1000-1050°F compared to 2000-2050°F for stainless steel.

### 3.5.2 Diaphragm Reversal Testing at Cryogenic Temperatures

The effort performed during the program related to cryogenic reversal testing of stainless steel and aluminum hemispherical type ring reinforced diaphragms included:

- a) Design and preparation of 13" diaphragm cryogenic cycling test schematic, SKD 10500 (Figure 49)



- b) Design of 13" diaphragm cryogenic cycling test fixture (TJ 10149)
- c) Preparation of test plans TP-201, TP-202 and test operational procedure TOP-200, for cryogenic cycle tests of stainless steel and aluminum positive expulsion diaphragms.
- d) Preparation of work statement (WS-200) for LH<sub>2</sub> cycle testing of 13" metallic diaphragms and acceptance criteria (AC-200) for 13" diaphragm cryogenic cycling test rig.
- e) Liaison with industry sources and Government personnel regarding design and specification of cryogenic tests and test equipment as well as solicitation and evaluation of cryogenic diaphragm cycle test vendors, including supporting contract and procurement activity.

For the sake of completeness and potential value for any future cryogenic testing of ring reinforced hemispherical type metallic positive expulsion diaphragms, documents TP-201, TP-202, TOP-200, WS-200 and AC-200 are reproduced herein in Appendix 3, section 6.3.



## 4.0 Conclusions and Recommendations

### 4.1 Conclusions

4.1.1 The program objective has been achieved. A high cycle life 25° cone angle ring reinforced stainless steel modified hemispherical type positive expulsion diaphragm configuration has been identified and demonstrated by test in 13" nominal diameter size. Eleven (11) complete diaphragm reversals at room temperature were achieved before pin hole leakage was observed during the twelfth diaphragm reversal which was completed without further incident, expelling all fluid successfully. This demonstrated performance represents about a 70% increase in reversal cycle life compared to the best test results previously obtained for stainless steel ring reinforced hemispherical type positive expulsion diaphragms. Based on room temperature, LN<sub>2</sub> and LH<sub>2</sub> temperature test results obtained on a previous 23" diameter diaphragm program, reference 18, similar high cycle life performance of the 13" diameter configuration is anticipated at cryogenic temperatures.

4.1.2 The effect of increased cone angle in increasing diaphragm reversal cycle life has again been demonstrated by test results. Experimental data obtained on this 13" diaphragm program and on a previous 23" diaphragm program, reference 18, were correlated by an analytic relation which expresses the effects of cone angle, bending stiffness, and material, i.e.,  $N \propto (\pi - 2\theta)^2 \sin \theta (R/t) \times (\epsilon_N)^2$ . Here, N is number of diaphragm reversals,  $\propto$  is proportionality factor,  $\theta$  is the cone angle with the axis of rotation, R/t is the radius to thickness ratio and  $\epsilon_N$  is the strain to necking of the diaphragm material. Agreement of predicted diaphragm reversal cycle life and test results was excellent. Reversal cycle life of ring reinforced modified hemispherical type metallic diaphragms may be predicted with reasonable certainty for various sizes, thicknesses, contours and materials.

4.1.3 Ring reinforced diaphragm configurations featuring either corrugated shells or smooth shells with smaller intermediate wires between larger wires result in significantly reduced reversal cycle lives compared to smooth shell designs having properly sized constant cross-sectional diameter reinforcing wires. Excessive bending

strains result from relatively high corrugation stiffness or result from cocking due to lack of diaphragm deflection mode control of the smaller intermediate reinforcing wires.

Despite its relatively low cycle life, the corrugated diaphragm effort conducted on the program proved of value. A method for fabricating thin corrugated shells to close tolerances was developed. The technique consisted of hydroforming a smooth shell from sheet stock and then spinning in the corrugations using a split mandrel tool. Intermediate anneals are needed between forming passes.

4.1.4 The ratio of reinforcing ring torsional stiffness to diaphragm shell bending stiffness is an important parameter in determining diaphragm reversal cycle life. Since this stiffness ratio is proportional to the fourth power of ring cross-sectional diameter, small changes in ring diameter,  $d$ , can markedly influence diaphragm performance. A practical and economical fabrication technique has been demonstrated for obtaining prescribed values of ring diameter,  $d$ , to close tolerances. The fabrication method consists of centerless grinding the nearest larger standard available rod size down to the desired ring cross-sectional diameter. This technique therefore, permits one to "finely tune" the ring to shell stiffness ratio to optimum values in order to maximize diaphragm reversal cycle life.

4.1.5 A non-destructive technique for determining the local curvature (or bending strain) of the diaphragm shell, even under conditions of large strains, has been developed. The method consists of making a wax mold of the local area using quick setting dental wax. The mold is sectioned, polished and photographed under high magnification. The curvatures and/or bending strains are readily obtained from the magnified local shell contour. The technique is useful in evaluating diaphragm performance. The strains obtained by this method during the program were correlated qualitatively with the test reversal cycle lives obtained. This non-destructive curvature (strain) monitoring technique would appear to have application to other types of structures.

#### 4.2 Recommendations

Although the present program objective has been attained, additional efforts appear warranted in order to further the technology for near term applications, such as Shuttle, which require reliable and leak-tight positive expulsion devices with even higher multicycling

capability. Some areas that appear fruitful to pursue are discussed below.

#### 4.2.1 Complete the Verification of Current High Cycle Life Configurations

Diaphragms have been reversal tested clamped in mechanical jointed (flanged) test rigs. In flight type positive expulsion tank/diaphragm assemblies, the diaphragm is integrally welded at its girth, into the tank. Diaphragm reversal cycle life for welded joint construction typical of flight hardware should be verified. It is recommended that diaphragms be welded into tanks using girth weld details compatible with obtaining high cycle life. GHe leak checks, diaphragm reversal tests and tank hydrostatic tests would be used to verify the design and construction of the positive expulsion tank/diaphragm assembly. Use of 13" diameter diaphragms size is projected so as to utilize existing tooling. Demonstrated welding technology and diaphragm tank girth joint design techniques will be utilized to minimize development risk.

#### 4.2.2 Improved Reversal Cycle Life Configurations

##### a) Alternate Materials of Construction

As detailed herein, reversal cycle life is proportional to the square of the strain to necking of the diaphragm material. For significantly improved cycle life, therefore, it is recommended that alternate materials with high strain to necking values be investigated. Annealed Hastelloy B and 1100-0 aluminum, references 20, 21 reportedly have strain-to-necking values approximately 40 to 50 percent higher than annealed austenitic stainless steel, which should yield potential diaphragm cycle lives in excess of twenty reversals.

Aluminum, well suited because of fluid compatibility or weight advantage for low pressure and/or small size requirements, needs fabrication development efforts before it can be effectively utilized as a material of construction. The primary diaphragm fabrication problems which have to be resolved for aluminum are (1) attachment of the reinforcing rings to the diaphragm shell and (2) the development of suitable leak-tight diaphragm to tank girth weld joints compatible with high cycle life operation. The limited aluminum diaphragm fabrication investigation effort performed on the current program indicates that reinforcing ring attachment to the diaphragm shell by means of brazing appears potentially to be a feasible and practical technique. Continuation



of aluminum diaphragm fabrication investigation appears warranted.

In contrast to aluminum, hastelloy B on the other hand, does not appear to need any significant fabrication development effort. Brazing and tack welding techniques for reinforcing wire attachment to the diaphragm shell as well as diaphragm to tank girth weld technology which were developed for stainless steel materials, appear to be suitable. Hastelloy B is readily formable into shells from sheet stock. The alloy is available in sheet and wire form suitable for diaphragm construction. It is recommended that ring reinforced diaphragms of annealed hastelloy B be built and tested utilizing tooling available from the present program. This would appear to be a low risk and high pay off potential program.

b) Alternate Geometric Configurations

Increased diaphragm cone angle and radius to thickness ratio will also increase diaphragm reversal cycle life, as previously discussed. Increasing the diaphragm cone angle has to be interfaced with packaging efficiency trade-offs. Application to tank construction with shallow head closures could, for example, show advantages. Increased radius-to-thickness ratio diaphragms have to be evaluated in terms of diaphragm and tank fabrication considerations such as tack welding of the reinforcing wires to the shell and welding of the diaphragm into the tank girth. To be fruitful, investigation of diaphragm cycle life increases due to alternate diaphragm geometry, should be pointed towards specific application envelopes.

## 5.0 References

1. Timoshenko & Woinowski - Krieger, "Theory of Plates & Shells, Second Edition, p.468-472 and p.548, Mc Graw-Hill Book Co., 1959.
2. Rourk, R.J., "Formulas for Stress and Strain," Second Edition, p.223, Mc Graw-Hill Book Co., 1943.
3. Coffin, L.F., Jr., "A Study of the Effects of Cyclic Thermal Stresses on a Ductile Material," Trans. ASME, Vol. 76, 1954, p.923.
4. Manson, S.S., "Behavior of Materials Under Conditions of Thermal Stress," Technical Note No. 2933, NACA 1953; Report No. 1170, 1954.
5. Sachs, G., et.al., "Low-Cycle Fatigue of Pressure Vessel Materials," Proc. ASTM, Vol 60, 1960, p.512.
6. Sessler, J.G. and Weiss, V., "Low Cycle Fatigue Damage in Pressure Vessel Materials," Paper No. 62-WA-233, presented at Winter Annual Meeting of ASME in New York, N.Y., Nov. 25-30, 1962.
7. Gleich, D. and L'Hommedieu, F., "Metallic Bladders for Cryogenic Fluid Storage and Expulsion Systems," Journal of Spacecraft and Rockets, Vol. 5, No. 9, Sept. 1968.
8. Gleich, D., "Six Foot Diameter Metallic Diaphragm for Fluid Storage and Positive Expulsion Systems", AIAA Paper No. 70-683 presented at AIAA 6th Propulsion Joint Specialists Conference, San Diego, Cal., June 15-19, 1970.
9. ARDE Report No. 56001-2, "Development of Gold Brazing Technique and Design and Supply of 18" Diameter Positive Expulsion Tank Assembly", Final Report under Jet Propulsion Laboratory Contract 951898 under NAS 7-100, Feb. 1969.
10. 11 1/2" Diameter Bladder/Tank for Advanced Thrust Vector Control Application, ARDE, INC. for Aerojet General Corporation under Contract F-04-694-67-C0004, 1967.
11. 33" Diameter Conospheroid Bladder/Tank Assembly for N<sub>2</sub>O<sub>4</sub> Service, ARDE, INC. for Aerojet General Corporation under Contract AF 04 (611) 11614, 1968.

12. Sievers, R.W., and Martin, S.B., "Design Manufacture and Test of a Fluidically Controlled Hydrazine Roll Rate Control System", AIAA Paper No. 70-650 presented at AIAA 6th Propulsion Joint Specialists Conference, San Diego, Cal. June 15-19, 1970.
13. "Fluid Storage and Expulsion System", Patent 3, 339, 803, Sept. 5, 1967.
14. Krezke, M.A. and Kiernan, T.J., "The Effect of Initial Imperfections on the Collapse Strength of Deep Spherical Shells," Research and Development Rept. 1757, Feb. 1965, David Taylor Model Basin Structural Mechanics Lab., Washinton, D.C.
15. Pulos, J.G., "Structural Analysis and Design Considerations for Cylindrical Pressure Hulls," Research and Development Report 1639, April 1963, David Taylor Model Basin Structural Mechanics Lab., Washington, D.C.
16. Ball, W.E., Jr., "Formulas and Curves for Determining the Elastic-General Instability Pressures of Ring-Stiffened Cylinders," Research and Development Report 1570, Jan. 1962, David Taylor Model Basin Structure Mechanics Lab., Washington, D.C.
17. Libove, C., "Elastic Stability," Handbook of Engineering Mechanics, 1st ed., edited by W. Flugge, McGraw-Hill, FNew York, 1962, Sec.44, pp.44-1-44-42.
18. Technical Report AFAPL-TR-66-146, June 1967, ARDE, INC. under Contract No. AF 33 (657)-11314.
19. Development of High Strength, Brazed Aluminum, Honeycomb Sandwich Composites Adaptable for Both Elevated and Cryogenic Temperature Applications, Final Report 30, Sept 1966, Aeronca Inc., Middletown, Ohio, Contract No. NAS 8-5445, MSFC, Huntsville, Ala.
20. Cryogenic Materials Data Handbook, Vol I, Technical Documentary Report No. ML-TDR-64-280. Aug.1964, Air Force Materials Lot, WPAFB, Ohio, Prepared by Martin Co., Denver, Col. under Contract No. AF 33 (657)-9161.
21. Hastelloy Alloy B, Haynes Stellite Co., Kokomo, Indiana, March 1962.

## 6.0 Appendices

Appendices which supplement the discussion of the main text are contained in this section. For convenience of reference, the nomenclature used is defined below.

### Nomenclature

$C, C_1, C_2$	= constants
$d$	= ring cross-sectional diameter
$E$	= Youngs modulus (secant value for plastic strains)
$K, K'$	= constants
$M$	= bending moment
$M_r, p$	= plastic resisting moment of ring
$M_s, p$	= plastic resisting moment of shell
$N$	= number of diaphragm reversal cycles
$P_A$	= actuation pressure (pressure difference across diaphragm)
$P_A, s$	= actuation pressure due to diaphragm shell
$P_{As}, w, P_{As}, w'$	= actuation pressures due to diaphragm shell plus reinforcing ring.
$Q$	= edge shear force per unit length of diaphragm shell circumference
$R$	= diaphragm shell radius
$s$	= ring spacing
$T$	= diaphragm shell meridional membrane force per unit length of shell circumference
$Tr, p$	= plastic resisting torque of ring
$t$	= diaphragm shell thickness
$Z$	= section modulus
$Ze, r$	= ring elastic section modulus
$Zp, r$	= ring plastic section modulus
$Zp, s$	= diaphragm shell plastic section modulus

$\alpha$  = diaphragm coordinate angle

$\beta$  = diaphragm shell local bending decay parameter =  $\frac{1.285}{\sqrt{Rt}}$

$\epsilon$  = strain

$\epsilon_F$  = uniaxial strain to fracture

$\epsilon_N$  = uniaxial strain to necking

$\epsilon_\psi$  = strain due to shell rotation

$\theta$  = diaphragm shell cone angle

$\psi$  = diaphragm shell angle of rotation

$\phi$  = angle between diaphragm shell radius vector, R, and meridional tension, T.

$\sigma$  = stress

$\sigma_y$  = yield stress

## 6.1 Appendix 1 - Diaphragm Actuation Pressure Relation

The maximum moment due to edge shear  $Q$ , causing diaphragm reversal (figures A-1 and 2) is as detailed in reference 1 for Poissons ratio = 0.3 ,

$$M = \frac{.322 Q}{p} = \frac{.322 Q \sqrt{Rt}}{1.285} \quad - - - (6.1)$$

This bending moment is resisted by local bending of the diaphragm shell and twisting of the reinforcing ring. Assuming the shell and ring yielded in bending we have, references 1 and 2,

$$M = M_{s,p} + T_{r,p} = \frac{\sigma_y Z_{p,s}}{R \sin \alpha} + \frac{\sigma_y Z_{pr}}{R \sin \alpha} \quad - - - (6.2)$$

Noting that the plastic shell and ring section modulii are  $\frac{t^2}{4}$  and  $\frac{d^3}{6}$ , respectively, we find from (6.2) that

$$M = \sigma_y \left( \frac{t^2}{4} + \frac{d^3}{6R \sin \alpha} \right) \quad - - - (6.3)$$

The shell membrane meridinal force per unit length is given by, references 1,2 ,

$$T = P_A \frac{R}{2} \quad - - - (6.4)$$

From figure A-1 one observes that the edge shear is related to the meridinal membrane force by,

$$Q = T \cos \psi = T \cos \left( \frac{\pi}{2} - 2\alpha \right) = T \sin 2\alpha \quad - - - (6.5)$$

Using (6.1), (6.3), (6.4) and (6.5) we obtain, after simplification, the actuation pressure relation,

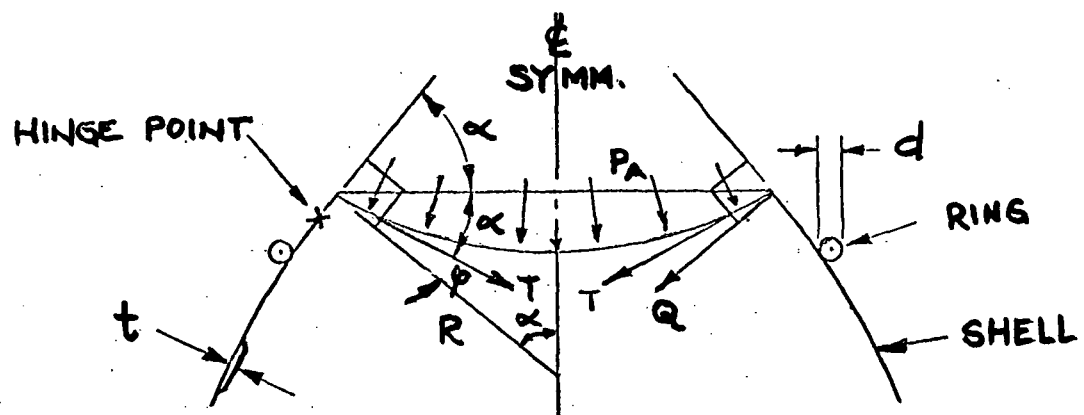


Figure A-1  
Diaphragm Actuation Pressure  
Loads and Forces

$$(6.5) - P_{A,s} \approx \frac{2\sigma_y}{(R/t)^{3/2} \sin 2\alpha} \left\{ 1 + \frac{2}{3} \frac{(d/R)^3 (R/t)^2}{\sin \alpha} \right\} = P_{A,s} \left\{ 1 + \frac{2}{3} \frac{(d/R)^3 (R/t)^2}{\sin \alpha} \right\}$$

The first term of equation (6.6),

$$P_{A,s} = \frac{2\sigma_y}{(R/t)^{3/2} \sin 2\alpha} \quad - - - (6.7)$$

is the actuation pressure due to the shell alone. The second term is the effect of the ring.

If one assumes that the shell is yielded in bending but the reinforcing ring is still elastic, noting that the elastic ring section modulus is  $\frac{\pi d^3}{32}$ , we find in a manner similar to the above

that the constant  $2/3$  in equation (6.6), becomes  $\pi/8$ . The actuation pressure relation then becomes,

$$P_{As,w'} = P_{A,s} \left\{ 1 + \frac{\pi/8}{\sin \alpha} \frac{(d/R)^3 (R/t)^2}{\sin \alpha} \right\} \quad - - - - (6.8).$$



## 6.2 Appendix 2 - Diaphragm Cycle Life Variables

An analytic relation for estimating reversal cycle life of ring reinforced hemispherical type metallic positive expulsion diaphragms has previously been developed by ARDE. This relation is evolved herein for sake of completeness.

For small cycle fatigue under completely reversed cycling investigators have shown, references 3 to 6, that cycles to failure is given by a relation of the form,

$$N = C \frac{1}{(\epsilon/\epsilon_F)^2} = C \frac{1}{(\epsilon/\epsilon_N)^2} \quad - - - (6.9)$$

Here for diaphragm application, we have replaced uniaxial tension strain to fracture  $\epsilon_F$ , by uniaxial tension strain to necking  $\epsilon_N$ .

Measurements have shown that the bending strain due to shell rotation is much larger than the hoop shell strain due to wire contraction during reversal. In estimating diaphragm cycle life, therefore, we will consider that only the plastic shell bending strain controls the cycle life. The plastic strain per cycle,  $\epsilon$  is then related to the angle of rotation,  $\psi$ , through which the diaphragm shell turns during reversal, the diaphragm shell stiffness ratio  $R/t$ , and reinforcing wire stiffness ratio,  $d/t$ , and spacing,  $S$ . The quantities  $\psi$  and  $S$  are in turn related to the cone angle,  $\theta$ . If we assume that the wire to shell stiffness ratio is "tuned" to produce maximum cycle life, as discussed in sections 3.1.3.5 to 3.1.3.7 and 4.14, the  $d/t$  wire stiffness ratio would not appear explicitly when we would estimate the cycle life ratio of two optimum wire stiffness configurations. The strain,  $\epsilon$ , then will be a function of  $\theta$ , and  $R/t$  and from (6.9) the cycle life relation would depend upon  $\epsilon_N$ ,  $R/t$  and  $\theta$  as shown below.

The diaphragm shell rotates due to an applied edge moment as discussed in section 6.1. The angle of rotation,  $\psi$ , due to an applied edge moment,  $M$ , is given by (references 1,2)

$$\frac{\psi}{\beta D} = \frac{M}{Et^3} = C \frac{M \sqrt{Rt}}{Et^3} \quad - - - (6.10)$$

From bending theory, the strain due to this moment is,

$$\epsilon_{\psi} = C_2 M/Et^2 \quad - - - (6.11)$$

and we find from (6.10) and (6.11) that,

$$\epsilon_{\psi} = (C_2/C_1) \psi (t/R)^{1/2} \quad - - - (6.12)$$

Study of figure A-1 shows that the diaphragm shell rotates through an angle  $2\alpha$  during complete reversal. Theory and tests indicate that the maximum strain occurs in the conical transition region near the diaphragm shell equator. On the conical region then,

$$\psi = 2\alpha = \pi - 2\theta \quad - - - (6.13)$$

We have then from (6.12) and (6.13),

$$\epsilon_{\psi} = (C_2/C_1) (t/R)^{1/2} (\pi - 2\theta) \quad - - - (6.14)$$

From (6.14) and (6.9) we obtain the first estimate of diaphragm cycle life,

$$N' = C \epsilon_N^2 (R/t) \quad \equiv K' \epsilon_N^2 (R/t) \quad - - - (6.15)$$

$$\frac{(C_2/C_1)^2 (\pi - 2\theta)^2}{(C_2/C_1)^2 (\pi - 2\theta)^2}$$

Wire spacing influences diaphragm cycle life. The closer the reinforcing wires are spaced, the better the diaphragm deflection mode control becomes and therefore, less shell strain due to cocking occurs. We therefore have to apply a correction factor to (6.15). To account for the effect of wire spacing, we assume that the relative cycle life of two diaphragm configurations is linearly related to the minimum permissible reinforcing wire spacing. The minimum permissible wire spacing occurs when theoretical line on line contact occurs between adjacent wires as the diaphragm reverses. This minimum permissible spacing is related to the cone angle by

$$S/d = \sin\theta \quad - - - (6.16)$$

as seen from figure A-2

Since the variation of  $d/t$  for "tuned" designs is small, we take therefore the cycle life effect of wire spacing proportional to  $\sin \theta$  and evolve finally from (6.15) the cycle life relation,

$$N = \frac{K \epsilon_N^2 (R/t) \sin \theta}{(\pi - 2\theta)^2} \quad - - - (6.16)$$

When comparing the cycle life of two designs, identified by the subscripts 1 and 2, we have then,

$$\frac{N_1}{N_2} = \left( \frac{\epsilon_{N1}}{\epsilon_{N2}} \right)^2 \left( \frac{\pi - 2\theta_2}{\pi - 2\theta_1} \right)^2 \left( \frac{\sin \theta_1}{\sin \theta_2} \right) \left( \frac{R_1/t_1}{R_2/t_2} \right) \quad - - - (6.17)$$

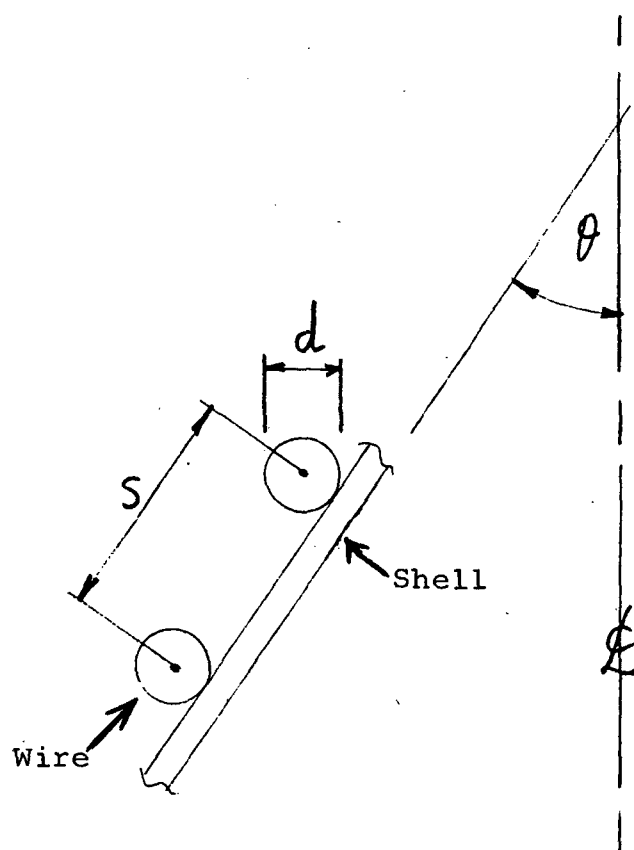


Figure A-2  
WIRE SPACING CONSIDERATIONS

### 6.3 Appendix 3 - Diaphragm Reversal Testing Documentation

This appendix contains documentation relating to room temperature and cryogenic reversal testing of diaphragms. The documents are listed below for ease of reference.

- TP-100, "Test Plan for Room Temperature Cycle Testing of 13" Stainless Steel Diaphragms".
- TOP-100, "Operation Procedures for Diaphragm Water Actuation Test
- TOP-101, "Operational Procedure for Diaphragm Water Cycling Test".
- TP-201, "Test Plan for Cryogenic Cycle Test of Stainless Steel Positive Expulsion Diaphragms".
- TP-202, "Test Plan for Cryogenic Cycle Test of Aluminum Positive Expulsion Diaphragm".
- TOP-200, "Operational Procedures for Diaphragm Cryogenic Cycle Test".
- WS-200, "LH<sub>2</sub> Cycle Testing of 13" Metallic Diaphragms"
- AC-200, "Acceptance Criteria 200, 13" Diaphragm Cryogenic Cycling Test Rig".

TEST PLAN 100

Test Plan for Room Temperature Cycle Testing  
of 13" Stainless Steel Diaphragms

Contract: NAS 3-12026, "Metallic Positive Expulsion Diaphragm",  
ARDE J/N 46002-3

1.0 TEST OBJECTIVE: To determine cycle life and/or expulsion efficiency of 13" stainless steel wire reinforced positive expulsion diaphragms while cycling at room temperature.

2.0 TEST DESCRIPTION: Diaphragms will be reversed (cycled) at room temperature as follows:

2.1 Use H<sub>2</sub>O as pressurant to reverse diaphragm per schematic SKD 10504 or,

2.2 Alternatively, use GHe as the pressurant to reverse diaphragm and expel H<sub>2</sub>O, or use H<sub>2</sub>O as the pressurant to reverse diaphragm and expel GHe per schematic SKD 10505.

3.0 DESCRIPTION OF STAINLESS STEEL TEST DIAPHRAGMS

Diaphragm Assembly Drawing No.	Type** Design- nation	Description
D3745	A'	25° Cone Angle, Constant wire size
D3747	B'	25° Cone Angle, Intermediate small wires
D3767	C'	25° Cone Angle, Corrugated Shell
*	D'	25° Cone Angle *
D3769	A	17 1/2° Cone Angle, Constant wire size (scale model of Air Force Design)
*	B	17 1/2° Cone Angle *
*	C	" *
*	D	" *

\* To be furnished subsequently, when available.

\*\* A total of eight (8) diaphragms, excluding tooling checkout units, will be tested.

#### 4.0 REFERENCE DOCUMENTATION:

- 4.1 Test Operation Procedure 100 (TOP-100) "Operation Procedures for Diaphragm Water Actuation Test".
- 4.2 Test Operation Procedure 101 (TOP-101) "Operational Procedure for Diaphragm Water Cycling Test".

#### 5.0 TEST PLAN:

##### 5.1 Types of Parameters Determined and/or Evaluated During or Subsequent to Testing

- a) Radius of curvature of shell "plastic hinge"
- b) Change in hoop size (wires and shell)
- c) Change in diaphragm shape or contour
- d) Degree and manner of twisting of hoop wire reinforcements
- e) Amplitude and pitch of local buckles
- f) Flow rate of expelled fluid
- g) Pressure on both sides of diaphragm
- h) Expulsion efficiency
- i) Changes in material properties (such as work hardening) after failure, and
- j) Nature and reasons for diaphragm failure, including helium leak rate through diaphragm.

##### 5.2 Diaphragm Identification and Inspection Prior to Test

###### 5.2.1 Data Folders

Establish separate data folder for each diaphragm to be tested. This folder(s) shall contain copies of all inspection, processing and quality assurance records for the diaphragm (dimensional, material and processing data, helium leak checks). Inspection and test data taken before, during and after testing shall also be included in the diaphragm data folder(s).

## 5.2.2 Diaphragm Identification

- 5.2.2.1 Mark part number (P/N) and serial number (S/N) on diaphragm flange as well as A, B, C, D reference diameter measurement points 90° apart. Marking to be done by vibro etch (very light) and marks-a-lot pen (manufactured by Carters Ink Company) or equivalent.
- 5.2.2.2 Number wires 1 to n with number 1 wire closest to equator flange, and carry up reference diameter measurement points A,B,C,D on wires and shell as "longitudes" to diaphragm apex. Use marks-a-lot pen for marking.
- 5.2.2.3 Mark circles (parallel to equator flange) and wires on shell in midspans between first three(3) wires nearest equator (spans 01, 12, 23) and on shell midspans adjacent to the two(2) wires(m) and (m+1) closest to "knee" region. Use marks-a-lot pen or lightly scribe over "toolmakers blue" applied to shell.
- 5.2.2.4 Mark several "ring rotation monitoring" circumferentially directed grid lines on wire outside surfaces parallel to flange in regions A,B,C,D on wires 1,2,3 and m, m+1. Identify and define angular coordinate(s) of grid lines using a protractor. Mark by lightly scribing over "toolmakers blue" on wires.

## 5.2.3 Dimensional Inspection

- 5.2.3.1 Pi ( $\pi$ ) tape wire outside diameters and measure wire outside diameters at reference measurement stations AC and BD for wires 1 through 3 and one (1) wire on each side of diaphragm knee region (wires m, m+1).



5.2.3.2 Pi ~~(m)~~ tape shell midspan diameters and measure shell midspan diameters at reference measurement stations AC and BD for spans 01, 12, 23 adjacent to first three (3) wires and spans  $(m-1, m)$ ,  $(m, m+1)$ , and  $(m+1, m+2)$  adjacent to the two (2) "knee-region" wires  $(m)$  and  $(m+1)$ .

### 5.3 Test Operational Procedures

Refer to TOP-100 and TOP-101.

### 5.4 Types of Measurements Taken During or Subsequent to Testing

Types of measurement taken during and subsequent to testing will be prescribed by program manager and/or test engineer as outlined below. Data sheets for recording data shall be provided.

Measurement Type  
Designation  
Number

Measurement Type Designation Number	Measurement Type	Method of Measurement	Remarks
1	Shell curvature at "plastic hinge"	Mold of local section (modeling clay, dental plastic or equivalent) or "feeler contour gage" type tools	Performed during first and selected other reversals on "shell open" configuration of SKD 10504 or performed subsequent to diaphragm reversal for selected number of reversals upon removal of diaphragm from test rig.
2	Change in hoop size (wires and shell) and change in diaphragm shape or contour	tape and/or micrometer calipers at same locations previously measured prior to test (refer to Section 5.2.3)	" " " "
3	Degree and manner of twisting of hoop wire reinforcements	Monitor change of angular location of circumferentially directed grid lines (refer to Section 5.2.2.4) by means of rod tool and protractor.	" " " "
4	Amplitude and pitch of local buckles in shell	Depth micrometer, calipers, scale	" " " "
5	Pressure on both sides of diaphragm	Pressure gages (refer to SKD 10504 and SKD 10505)	Performed for each reversal of each diaphragm
6	Flow rate of expelled fluid	Flowmeter	Performed only when expelling H <sub>2</sub> using SKD 10504 for selected reversals other than first reversal for selected diaphragm types (4 types total)

(continued on next page)

Measurement Designation Number	Measurement Type	Method of Measurement	Remarks
7	Expulsion Efficiency	Weight of system full and subsequent to fluid expulsion (refer to TOP-101).	Performed on one (1) diaphragm of demonstrated high cycle life configuration for each reversal number at pressure levels less than diaphragm membrane yield pressure and then for final reversal at a high overpressure corresponding to membrane plastic deformation of diaphragm simulating "full chamber pressure condition" at end of fluid expulsion.
8	Work Hardening	Bend tests of shell material specimens.	Slope of stress-strain curve measures work hardening effect.
9	Helium Leak Check of Diaphragm	Helium mass spectrometer (Veco Detector) used in conjunction with helium leak check rig (TD-10156) or water test rigs SKD 10504, SKD 10505.	Performed for each reversal of each diaphragm.

TEST OPERATION PROCEDURE 100

Operation Procedures for Diaphragm Water Actuation Test

Contract: NAS 3-12026, "Metallic Positive Expulsion Diaphragm"  
ARDE J/N 46002-3 and 46002-7

- 1.0 OBJECTIVE: To determine cycle life of a metallic diaphragm while cycling at room temperature.
- 2.0 TEST-FIXTURE: Dwg. TE 10150-1 and -2, "13" Diaphragm Water Cycling Test Fixture".
  - 2.1 Test Set-Up: Dwg. SKD 10504, "Water Actuating Rig - 13" Diaphragm Water Cycling Test".
  - 2.2 Test Diaphragms:
    - a. 25° cone, stainless steel diaphragm (Dwg. D3745 & D3747)
    - b. 17-1/2° cone, stainless steel diaphragm
    - c. 25° cone, aluminum diaphragm
    - d. 17-1/2° cone, aluminum diaphragm

Additional test diaphragm drawing numbers for items a to d above will be provided when available.

- 3.0 ASSEMBLY PROCEDURE: The following procedure describes all operations to install, leak test, and fill the test set-up.

For clarity, all items will be referenced to the water actuating rig, Dwg. SKD 10504.

The assembly procedure is as follows:

- 3.1 After inspection of the diaphragm assembly, install it in test rig assembly Item (23) (TE 10150-1 or -2) with Item (24) ring (TE 10150-21 or -22). Lubricate "O" rings prior to installation and assembly. Torque all flange bolts equally.
- 3.2 Place test fixture assembly on side to bleed air and fill with water. Connect water hoses (8) per SKD 10504.
- 3.3 Fill lines with water by closing drain valve (7), opening valves (6), (9), (10), and cracking water supply valve (1). Note: No pressure should be indicated on pressure gage (4).
- 3.4 After bleeding all air, close valve (1) and erect test rig assembly on its feet in an upright position.

- 3.5 Open  $\Delta P$  transducer (12) bleed to vent air from its line.
- 3.6 Close vent valve (10) and valves (6) and (9). Open bypass valve (5).
- 3.7 To calibrate, open  $\Delta P$  transducer (12) bleed valve slightly. Zero out and calibrate Sanborn recorder (13) to approximately 2 psi per centimeter on recorder chart.
- 3.8 Set water regulator at zero psi, crack water supply valve (1) slightly, re-set water regulator at 2 psi, 4 psi, 6 psi, 8 psi, and 10 psi and adjust Sanborn recorder to read 1 cm = 2 psi. Leave water regulator set at 15 psi.
- 3.9 Close valves (1) and (5) and open valve (6) and (9). Close  $\Delta P$  transducer (12) bleed. System is now ready for test. Note: Leave Sanborn recorder power on.

#### 4.0 TEST PROCEDURE:

- 4.1 Check camera (21) to be sure it is loaded, focus camera and turn on flood lamps.
- 4.2 Turn on Sanborn recorder (13) chart to a speed of 1"/minute and turn on camera.
- 4.3 Open water supply valve (1) to actuate diaphragm. Set water flow rate for about a 10 minute expulsion rate as judged from the movement of the diaphragm. Record the pressure at  $P_1$  (11).
- 4.4 Detailed instructions for diaphragm inspection and measurement will be provided in the test plan. To shut down for inspections and measurements during reversal, shut off water valve (1), Sanborn chart (13), movie camera (21) and flood lights (22). For visual inspection and contour cast of the diaphragm shell, the water does not have to be drained from the diaphragm. If it is desired to measure the wire diameters, it will be necessary to open the vent valve (10) and drain water using valve (7).
- 4.5 Water leaks may be detected by visual observation. To measure the rate of leakage the diaphragm must be run to the end of its stroke, removed, and measured with a "Veeco" leak detector (26) in a special set-up (diaphragm leak check fixture). Alternatively, one may use the test rig by attaching the  $\Delta P$  water line to the expelled side of the diaphragm, closing off valves (6) and (7), connecting leak detector (26) to air vent line, and opening valve (10). Connect He purge line to the pressurization side of the diaphragm and pressurize to 2 psig. Start leak detector (26) and measure leak rate.

- 4.6 To restart the reversal when the shut down is to take a cast of diaphragm shell or other measurements not requiring rig disassembly or water drain, open valve (1) until expulsion movement (about 1"/minute) is obtained. If shut down for wire diameter or leak measurements, proceed per 4.1 through 4.3.
- 4.7 When the pressure begins to rise to 10 psi on the recorder (10) and  $P_1$  (11), close off valve (1), shut off camera (21), lights (22), and recorder (13). Observe diaphragm for leaks and take external measurements or diaphragm shell contour cast. Relieve pressure by opening valves (7) and (10).
- 4.8 To reverse diaphragm, remove ring (24), and remove diaphragm for measurements. Sponge and dry test fixture (23) re-install diaphragm, install expulsion head (25), connect water hoses (8) to expulsion head (25), open valves (10) and (6), and close valve (7).
- 4.9 Fill with water by cracking valve (7) until water flows out of air vent. Close valve (7) and air vent valves (10).
- 4.10 Dry up all external water, place camera (21) and flood lights (22) below test rig, focus and load camera (21), and turn on flood lights (22). Diaphragm is ready for reversal.
- 4.11 Turn on camera (21) and recorder (13).
- 4.12 Open water valve (1) until diaphragm moves about 1"/min.
- 4.13 Water collecting on window indicates a leak. If a leak is detected, shut down per 4.4 and measure per 4.5.
- 4.14 Restart per 4.6
- 4.15 When pressure begins to rise to 10 psi on recorder (10) and  $P_1$  (11), close off valve (1), shut off camera (21), lights (22) and recorder (13).
- 4.16 Drain water by opening valves (7) and (10).
- 4.17 Check for leakage by attaching water lines to test rig (23), closing valves (7), (6), (9). Connect leak detector to air vent with valve (10) open. Connect He purge supply to head (25), plug all holes in head (25) and apply 2 psi with regulator (16) with valves (18) open and (19) closed. Use detector (26) to determine leak rate.
- 4.18 Open valve (7), remove leak detector (26), shut off valve (18), and open valve (19).
- 4.19 Remove purge line (20), head (25) and diaphragm.
- 4.20 Inspect and measure diaphragm.
- 4.21 Re-install diaphragm in test fixture (23) using ring (24).

- 4.22 Place camera (21) and lights above rig.
- 4.23 Repeat reversals per 4.1 through 4.22 as directed by test engineer.

5.0 SHUT DOWN PROCEDURE:

- 5.1 When a leak is detected or at the direction of the test engineer, terminate the test.
- 5.2 Close off valve (1), remove film from camera (21), shut power off Sanborn recorder (13), turn off lights (22).
- 5.3 Open valves (10), (7), & (19).
- 5.4 Turn off GHe supply valves (15) and open valves (18), (6), (7), (5), and (9).
- 5.5 Remove hoses (8) and hose (20) from test rig.
- 5.6 Remove head (25) or ring (24) and test diaphragm.
- 5.7 Dry rig and lubricate all exposed steel surfaces on test rig TE 101501, Item (23).



TEST OPERATION PROCEDURE 101

Operational Procedure for Diaphragm Water Cycling Test

Contract: NAS 3-12026, "Metallic Positive Expulsion Diaphragm"  
ARDE J/N 46002-3 and 46002-7

- 1.0 OBJECTIVE: To determine cycle life of a metallic diaphragm while cycling at room temperature and the volumetric expulsion efficiency of the diaphragm and simulated vessel assembly.
- 2.0 SET-UP:
- 2.1 Test fixture: Dwg. TE 10150-1 or -2 "13" Diaphragm Water Cycling Test Fixture" less open cycle rings, TE 10150-21 & -22.
  - 2.2 Test Set-Up: Dwg. SKD 10505, "13" Diaphragm Water Cycling Test Rig"
  - 2.3 Test Diaphragms:
    - a. 25° cone, stainless steel diaphragm (Dwg. D3745 & D3747)
    - b. 17-1/2° cone, stainless steel diaphragm
    - c. 25° cone, aluminum diaphragm
    - d. 17-1/2° cone, aluminum diaphragm

Additional test diaphragm drawing numbers for items a to d above will be provided when available.

- 3.0 ASSEMBLY PROCEDURE: The following procedure describes all operations required to install, leak test, measure tare volume, purge and fill the test fixture in the test set-up.

For clarity, all items will be referenced to the test rig schematic, Dwg. SKD 10505.

The assembly procedure is as follows:

- 3.1 After inspection of diaphragm assembly, install diaphragm in water cycling test fixture (23) with the 25° (25A) or 17-1/2° (25B) expulsion head. Lubricate all "O" rings prior to installation. Torque all flange bolts equally to 150 in. #.
- 3.2 Place test fixture on its side to bleed air and fill with water.
- 3.3 Connect water lines, per SKD 10505, purge air, and place

rig in upright position. Note: Water lines will be flexible hoses to test fixture.

- 3.4 Connect GHe supply to rig per SKD 10505.
- 3.5 Open vent valve (10), close drain valve (7) and open valves (6), (5) and (9).
- 3.6 Crack water supply valve, bleed  $\Delta P$  transducer (12) and vent air through valve (10).
- 3.7 To calibrate, turn off valve (1), (6), and (9). Leave P transducer (12) bleeding slightly. Zero out and calibrate Sanborn recorder (13) to approximately 2 psi per centimeter on chart.
- 3.8 Set water regulator 2 at zero psi and crack valve (1), reset regulator (2) at 2 psi, 4 psi, 8 psi, and 10 psi. Adjust sensitivity on Sanborn recorder (13) to read 1 cm = 2 psi. Leave water regulator set at 15 psi. Close valves (1) and (5) open valves (6) and (9), close P transducer (12) bleed and vent valve (10).

Note: Leave Sanborn recorder (13) power on to keep it warmed up. Recalibrate recorder every time its power is shut off.

#### 4.0 TEST PROCEDURE:

- 4.1 Weigh test rig on scale (24) and record data.
- 4.2 Load film in camera (21), focus, and turn on flood lamps (22).
- 4.3 Set Sanborn recorder (13) chart at 1"/min. speed.
- 4.4 With drain valve (7), vent valve (19), GHe valve (18) closed, set GHe regulator (16) to 10 psi.
- 4.5 Open GHe valve (18) to pressurize system at 10 psi.
- 4.6 Leak check (23) and (25) test fixture assembly using GHe detector (27) to sniff around flanges, connections and window. If leak indicated, directions for proceeding will be given by test engineer. If test fixture is leak tight, proceed with test as described below.
- 4.7 When system is leak tight, turn on camera and recorder chart and actuate test diaphragm by opening drain valve (7) until flow meter (8) reaches about 0.5 gpm. Note pressures  $P_1$  and  $P_2$  and record data.
- 4.8 When pressure differential begins to increase to 10 psi at end of run, increase GHe regulator to 15 psi and shut off valve (18). Turn off camera, lights, and chart recorder. Weigh test set-up and record weight. Change

of weight from initial tare reading (para. 4.1) is water expelled. As a double check the water drained out during the run will also be weighed.

- 4.9 Test rig shut down for inspection, measurement or observation for leaks will be as directed by the test engineer. Detailed diaphragm inspection and measurement information will be supplied as part of the test plan.
- 4.10 To shut down for inspection or observation for leaks, turn off gas valve (18), camera (21), flood lights 22, and recorder (13) chart. Leakage indications are a drop in gas pressure and gas bubbles coming through flow meter (8). When water has been drained, close valves (7), (6), and (9). To measure gas leak rate, connect leak detector (27) to air vent and open vent valve (10).
- 4.11 To start up again, repeat 4.2, 4.3, 4.4, 4.5, and 4.7. If diaphragm is disassembled and re-installed, repeat 4.6.
- 4.12 After GHe actuated reversal 4.8 has been completed, diaphragm cycling can be continued as follows using water as the pressurant. Turn on camera, lights, and recorder chart. Close valves (10), (7), (18), and (19). Start diaphragm reversal by opening valve (19) until about 75 SCFM flow is indicated on GHe flow meter (26).
- 4.13 If water is observed coming through diaphragm or  $\Delta P$  across diaphragm drops in a manner different from the usual  $\Delta P$  rise and fall associated with diaphragm reversal, leakage is indicated. Close valve (1) and open valves (7) and (19) to vent pressure. Remove diaphragm for inspection and leak check in leak check fixture.
- 4.14 To restart a water actuated reversal, repeat 4.12.

## 5.0 GENERAL SHUT DOWN PROCEDURE

- 5.1 When a leak has been established or at the direction of the test engineer, terminate the diaphragm actuation for diaphragm inspection.
- 5.2 Close off valves (18), (7), and (1).
- 5.3 Open valve (19) to relieve  $\text{GH}_2$  pressure to zero.
- 5.4 Drain water by opening valves (7) and (10).

- 5.5 Shut off camera (21) , lights (22) , and recorder (13) .
- 5.6 Close off GHe bottle (15) .
- 5.7 Remove head (25) , clamp ring, TE 10150-11, to remove diaphragm.
- 5.8 Dry and lubricate all exposed surfaces on test fixture.

TEST PLAN 201

Test Plan for Cryogenic Cycle Test of Stainless  
Steel Positive Expulsion Diaphragms

Contract: NAS 3-12026, "Metallic Positive Expulsion Diaphragm"  
ARDE J/N 46002-3

1.0 OBJECTIVE OF TEST PROGRAM:

Twenty (20) reversals of a stainless steel expulsion diaphragm assembly at liquid hydrogen temperatures (-423°F). Four (4) designs of the diaphragm will be cycled until failure occurs or 20 reversals are completed. The expulsion efficiency and differential pressures across the diaphragm will be obtained by test measurements.

2.0 TEST SPECIMENS:

The four (4) diaphragm assemblies that will be cryogenically tested in this program will be similar to those described by ARDE drawings D3745 and D3747, 13" SST Diaphragm Assy. Types A' and B', respectively. A 17 1/2 degree cone angle may be used instead of the 25° angle shown.

3.0 TEST SET UP:

The 13" Diaphragm Cryogenic Test Set up is described as follows:

3.1 Test Set Up Schematic:

Refer to Drawing SKD 10500 "13" Diaphragm Cryogenic Cycling Test Schematic".

3.2 Test Fixture:

Refer to Drawing TJ 10149 and Bill of Material TJ 10149, titled "13" Diaphragm Cryogenic Cycling Test Fixture." Note that TJ 10149 Type I fixture is to be used for 25° cone diaphragm assemblies and TJ 10149 Type II is to be used for 17 1/2° diaphragm assemblies.

#### 4.0 TEST PROCEDURE:

#### 4.1 Initial Inspection of Diaphragm Assemblies (Arde Inc.)

##### 4.1.1 Dimensional Inspection

Measurements will be made of the following assembly dimensions of each test specimen:

- a. Outside diameter of each wire hoop brazed to the diaphragm.
- b. Layout, marking, and measurement of inside surfaces of diaphragm (expulsion side) to be used for purposes of dimensional inspection during reversals.
- c. Concentricity measurements of the wire hoop reinforcements.

##### 4.1.2 Leak Test

Each diaphragm will be tested for leaks in a special leak test fixture prior to any cycle testing. If there is a leak, it will be located and repaired.

##### 4.1.3 Photographs

Each diaphragm will be photographed prior to cycling to record any repair work that may have to be done on it prior to test.

#### 4.2 Test Procedure: (Test Subcontractor)

Test Operational Procedure 200 describes the set up, assembly and operational procedure for diaphragm cryogenic cycling test.

#### 4.3 Post Test Inspection: (Arde Inc.)

##### 4.3.1 Dimensional Inspection

Dependent on the condition of the tested diaphragm assembly, the following dimensional will be made:

- a. Outside diameter of critical wire hoop if external to shell.
- b. Inside diameter of critical wire hoop if internal to shell.

#### 4.3.1 Dimensional Inspection (Continued)

- c. Outside or inside diameter of inspection points of expulsion side of shell.
- d. Cast of failed area to determine bend radius when a cast can be made.

#### 4.3.2 Leak Test

In addition to the three leak checks during cycling, a leak test will be conducted on a diaphragm assembly that has passed the 20 cycle reversal test. On failed diaphragms, the leak test will be used to determine the order of magnitude of the leak. On massive failures this test will be unnecessary.

#### 4.3.3 Failure Analysis (ARDE)

Each failed diaphragm will be sectioned in the area of the failure to determine bend radius and local hardness of the material.

### 5.0 PHOTOGRAPHY:

#### 5.1 Motion Pictures (Test Subcontractor)

16 mm time sequence movies will be made of the brazed wire hoop side of each diaphragm assembly. These movies will record each reversal of the diaphragm assembly. Film will be developed and re-produced by ARDE.

#### 5.2 Still Photographs

##### 5.2.1 Test Set Up (Test Subcontractor)

The following still photographs will be made of the test set up.

- a. Three (3) photos showing assembly of test diaphragm assembly into TJ 10149 Test Fixture (no Polaroids).
- b. Three (3) photos showing the assembly of the TJ 10149 Test Fixture into the SKD 10500 "Test set up schematic system". (No Polaroids)

5.2.1 Test Set Up (Continued)

- c. Three (3) photos showing the test set up prior to test (different views). (No Polaroids)
- d. Three (3) photos showing the test set up during test (different views). (No Polaroids)

5.2.2 Test Specimen (Test Subcontractor)

Two (2) black and white photographs, 4" x 5" of each tested bladder and a minimum of one (1) photo of the failure area shall be taken. (No Polaroids)

5.2.3 Sections of Test Specimens (Arde Inc.)

Micro-photographs will be made of any failure analysis sections that are cut from the diaphragm assemblies.

5.2.4 Reproduction of Photographs (Test Subcontractor)

Each photograph will have two (2) glossy prints made and one (1) negative for reproduction.

6.0 TEST REPORTS:

6.1 Intermediate Test Reports

At the conclusion of each cryogenic cycling test of a diaphragm assembly, the following information will be made available.

6.1.1 Test Data (Test Subcontractor)

This data will include the following:

- a. Three (3) copies of the original data sheets.
- b. Three (3) copies of the recordings.
- c. Three (3) copies of inspection data between runs.
- d. Photograph of the test diaphragm and its failure.
- e. Undeveloped movie film of each cycle.
- f. The test diaphragm assembly.



6.1.2 Failure Analysis (Arde, Inc.)

The failure analysis will consist of the following:

- a. Copy of original data.
- b. Copy of test data.
- c. Final inspection data.
- d. Photograph of failure.
- e. Conclusion as to causes of failure.

6.2 Final Report

6.2.1 Test Subcontractor's Report

The test subcontractor will submit three (3) copies of a final report to ARDE that will include the following: (Note to prevent duplication, this report will include the work under Test Plan 202 "Cycling of Aluminum Positive Expulsion Diaphragms".)

- I Objective
- II Test Set Up Description
  - a. Schematic
  - b. Bill of Materials
  - c. Still Photographs (negative plus 3 prints)
- III Test Procedures
- IV Test Results of Each Test
  - a. Test Data (original plus 2 copies)
  - b. Inspection Data (original plus 2 copies)
  - c. Photographs (negative plus 3 prints)
  - d. Failure Report (Description of Failure)
  - e. Instrument Calibrations

6.2.2 Final Report (Arde Inc.)

The testing phase will be described in detail in the final report submitted by ARDE to NASA in compliance with the requirements of Contract NAS 3-12026.

TEST PLAN 202

Test Plan for Cryogenic Cycle Test of Aluminum  
Positive Expulsion Diaphragm

Contract: NAS 3-12026, "Metallic Positive Expulsion Diaphragm"  
ARDE J/N 46002-7

1.0 OBJECTIVE OF TEST PROGRAM:

Twenty (20) reversals of an aluminum expulsion diaphragm assembly at liquid hydrogen temperatures (-423°F). One design of the diaphragm will be cycled until failure occurs or 20 reversals are completed. The expulsion efficiency and differential pressures across the diaphragm will be obtained by test measurements.

2.0 TEST SPECIMENS:

The diaphragm assembly that will be cryogenically tested in this program will be chosen on the basis of the results of the cycling test conducted under Test Plan 201 and water cycling test on aluminum diaphragm. On this basis a 25° or 17 1/2° cone angle will be chosen for the test diaphragm.

3.0 TEST SET UP:

The 13" Diaphragm Cryogenic Test Set Up is described as follows:

3.1 Test Set Up Schematic

Refer to Drawing SKD 10500 "13" Diaphragm Cryogenic Cycling Test Schematic".

3.2 Text Fixture

Refer to Drawing TJ 10149 and Bill of Material TJ 10149, titled "13" Diaphragm Cryogenic Cycling Test Fixture". Note that TJ 10149 Type I fixture is to be used for 25° cone diaphragm assembly, or the TJ 10149 Type II is to be used for 17 1/2° diaphragm assembly.

#### 4.0 TEST PROCEDURE:

##### 4.1 Initial Inspection of Diaphragm Assemblies (Arde Inc.)

###### 4.1.1 Dimensional Inspection

Measurements will be made of the following assembly dimensions of the test specimen:

- a. Outside diameter of each wire hoop brazed to the diaphragm.
- b. Layout, marking, and measurement of inside surfaces of diaphragm (expulsion side) to be used for purposes of dimensional inspection during reversals.
- c. Concentricity measurements of the wire hoop reinforcements.

###### 4.1.2 Leak Test

The diaphragm will be tested for leaks in a special leak test fixture prior to any cycle testing. If there is a leak, it will be located and repaired.

###### 4.1.3 Photographs

The diaphragm will be photographed prior to cycling to record any repair work that may be done on it prior to test.

##### 4.2 Test Procedure (Test Subcontractor)

Procedure 200 describes the set up assembly and operational procedure for diaphragm cryogenic cycling test.

##### 4.3 Post Test Inspection (Arde Inc.)

###### 4.3.1 Dimensional Inspection

Dependent on the condition of the tested diaphragm assembly, the following dimensions will be made:

#### 4.3.1 Dimensional Inspection (continued)

- a. Outside diameter of each wire hoop if external to shell.
- b. Inside diameter of each wire hoop if internal to shell.
- c. Outside or inside diameter of inspection points of expulsion side of shell.
- d. Cast of failed area to determine bend radius when a cast can be made.

#### 4.3.2 Leak Test

In addition to the three leak checks during cycling, a leak test will be conducted on the diaphragm assembly that has passed the 20 cycle reversal test. On a failed diaphragm, the leak test will be used to determine the order of magnitude of the leak. On massive failures this test will be unnecessary.

#### 4.3.3 Failure Analysis (ARDE)

The failed diaphragm will be sectioned in the area of the failure to determine bend radius and local hardness of the material.

### 5.0 PHOTOGRAPHY:

#### 5.1 Motion Pictures (Test Subcontractor)

16 mm time sequence movies will be made of the brazed wire hoop side of the diaphragm assembly. These movies will record each reversal of the diaphragm assembly. Film will be developed and reproduced by ARDE.

#### 5.2 Still Photographs

##### 5.2.1 Test Specimen (Test Subcontractor)

Two (2) black and white photographs, 4"x5" of the tested bladder and a minimum of one (1) photo of the failure area shall be taken. (No Polaroids)

##### 5.2.2 Sections of Test Specimen (ARDE)

Micro-photographs will be made of any failure analysis sections that are cut from the diaphragm assembly.

### 5.2.3 Reproduction of Photographs (Test Subcontractor)

Each photograph will have two glossy prints made and one negative for reproduction.

## 6.0 TEST REPORTS:

### 6.1 Intermediate Test Reports

At the conclusion of the cryogenic cycling test of the aluminum diaphragm assembly, the following information will be made available.

#### 6.1.1 Test Data (Test Subcontractor)

This data will include the following:

- a. Three (3) copies of the original data sheets.
- b. Three (3) copies of the recordings.
- c. Three (3) copies of inspection data between runs.
- d. Photograph of the test diaphragm and its failures.
- e. Undeveloped movie film of each cycle.
- f. The test diaphragm assembly.

#### 6.1.2 Failure Analysis (Arde Inc.)

The failure analysis will consist of the following:

- a. Copy of original data.
- b. Copy of test data.
- c. Final inspection data.
- d. Photograph of failure.
- e. Conclusion as to cause of failure.

## 6.2 Final Report

### 6.2.1 Test Subcontractor's Report

The test subcontractor will submit three (3) copies of a final report to ARDE that will include the following: (Note:

6.2.1 Test Subcontractor's Report (Contd.)

to prevent duplication, this report will be included in the work under Test Plan 201 "Cycling of Stainless Steel Positive Expulsion Diaphragm").

- I Objective
- II Test Set Up Description
  - a. Schematic
  - b. Bill of Materials
  - c. Still photographs (negative plus 3 prints)
- III Test Procedures
- IV Test Results of Each Test
  - a. Test Data (original plus 2 copies)
  - b. Inspection Data (original plus 2 copies)
  - c. Photographs (negative plus 3 prints)
  - d. Failure Report (Description of Failure)
  - e. Instrument Calibrations

6.2.2 Final Report (Arde Inc.)

This test report will summarize the results of all test, design calculations, pull test, and water actuation test. A summary of all testing, as reported under Item 6.2.1 of Test Plans 201 and 202, will be included.

TEST OPERATIONAL PROCEDURE 200

Operational Procedures for Diaphragm Cryogenic  
Cycle Test

Contract: NAS 3-12026, "Metallic Positive Expulsion Diaphragm"  
ARDE J/N 46002-3 and 46002-7

1.0 OBJECTIVE:

To determine cycle life of 13" metallic positive expulsion diaphragms at liquid hydrogen temperatures.

2.0 SET-UP:

2.1 Test Fixture: Dwg. TJ10149-I and II, "13" Diaphragm Cryogenic Cycling Test Fixture"

2.2 Test Set-up: Dwg. SKD 10500, "13" Diaphragm Cryogenic Cycling Test Schematic"

2.3 Test Diaphragms:

- a. 25° cone, stainless steel diaphragms (Dwg. D3745 & 3747)
- b. 17 1/2° cone, stainless steel diaphragms
- c. 25° cone aluminum diaphragms
- d. 17 1/2° cone aluminum diaphragms

Additional test diaphragm drawing numbers for items a to d above will be supplied when available.

3.0 ASSEMBLY PROCEDURE:

The following procedure describes operations to install, leak test, and purge the test set-up.

For clarity, all items will be referenced to the test schematic SKD 10500 and individual test fixture assembly items will be referred to as follows:

Item TJ10149-I & II Items

- A Head Expulsion, 25° cone - TJ10149-1 and 17 1/2° cone - TJ10149-58
- B LH<sub>2</sub> cryostat - TJ10149-2
- C Cryostat - 30" I.D. - TJ10149-16
- D Photo Tube Assembly consisting of items TJ10149-13, 39, 43, 44, 45, 46, 47, 48, 54, 55 and 56.
- E Indium - 1/16" wire Item TJ10149-6

The assembly procedure is as follows:

- 3.1 Install inspected diaphragm assembly in cryogenic test fixture, TJ10149, by assembling diaphragm between Items B & A with Indium (E) seals. Torque bolts 225 in. lbs.  
Note: Obtain internal tare volume of vessel with demineralized water at this point. Drain vessel and dry before proceeding (first cycle test only).
- 3.2 Check expulsion side of assembly for leaks by pressurizing internally with 5 psig He and sniffing with leak detector around the O.D. of the flange and vent fitting. Leave pressurized at 5 psig.
- 3.3 Install Item D, photo tube assembly, with indium seals. Torque bolts 80 in. lbs.
- 3.4 Pressurize gas side of assembled test fixture to 2 psig with GHe and sniff all flanges, seals, and connections for leaks. Release pressure on this side and then release pressure on expulsion side of diaphragm. Install TJ10149-3 with Indium seal (38). Torque bolts 225 in. lbs.
- 3.5 Place complete rig, excluding Item C, cryostat, in vacuum chamber with GHe purge lines attached to all charging lines. Leave gas pressurization line open. Evacuate chamber.
- 3.6 Shut off vacuum pump and purge slowly with GHe until chamber pressure reaches atmospheric pressure.
- 3.7 Remove test fixture assembly and cap all lines.



- 3.8 Install test fixture at test site using Items (5) & (6) SKD 10500.
- 3.9 Remove Item D and purge slowly with GHe via diaphragm pressurization circuit with valves (27) and (48) open.
- 3.10 Install Item C over test fixture assembly with Items (56), (57), (58), and (59) and turn on GHe purge using Items (16C) and (12D). Re-install Item D with new Indium seal and insulate. Torque bolts 80 in. lbs.
- 3.11 Open all vents and disconnect LH<sub>2</sub> transfer line, Item (10) from LH<sub>2</sub> dewar. Purge by opening items (12D), (E), (F) to all lines and set maximum purge rate with Item (15) and (13C).
- 3.12 Reconnect Item (10) to dewar.
- 3.13 Shut off all purge lines using solenoid valves (12D), (E), (F) & (G).
- 3.14 Close off all vent lines, Items (27A) & (B) and Item (8C). Note Item (32) is normally by-passing Item (33), wet gas meter.
- 3.15 System is now ready to start test procedure.
- 4.0 TEST PROCEDURE:
- 4.1 Mount camera (2), lights (4), and light shade 3 as shown. Check out camera (2) and lights (4).
- 4.2 Check out all instrument circuits, Items (28), (29), (30), (31), (33), (45), (47), (43), (44), (42), & (41).
- 4.3 Fill LN<sub>2</sub> cryostat (18) by opening solenoid valve (20) and adjusting fill rate with (19) and valve on (21).
- 4.4 Start cool down by purging cryostat, Item C, with -320°F GHe using Item (22) for control.
- 4.5 When temperature at M reaches -200°F, crack LH<sub>2</sub> dewar valve and begin to purge LH<sub>2</sub> cryostat, Item B, with LH<sub>2</sub>.

- 4.6 Crack LH<sub>2</sub> control valve (27A), and open solenoid valves (8A), (B) and (C) to start cool down and purge of system with LH<sub>2</sub>.  
Note: GHe pressurization system is vented and its supply is closed off; Valve (27B) open and valves (13B) and (12G) closed.
- 4.7 When temperature at L reaches -420°F, and LH<sub>2</sub> is being vented from the vent lines, adjust globe valve (9) to regulate rate of LH<sub>2</sub> flowing from vent.
- 4.8 Check gas flow rate through flow meter (31) and temperature (30) and pressure (28A) in the discharge line. The temperature should be near ambient and the pressure should be near atmosphere. GH<sub>2</sub> should be coming out of flame arrestor (25A). Shut off flow control valve (27A) on LH<sub>2</sub> line. Take tare readings on (33). (Temp and dials)
- 4.9 When temperature at L reaches -420°F and liquid comes out of the flame arrestor (25C) start recorders and shut off LH<sub>2</sub> vent valve (8C) and supply valve (8B).
- 4.10 Close GHe vent valve (27B) and start pressurization of diaphragm with -423°F GHe by opening solenoid valve (12G) and bar stock valve (13B). Set pressure to 15 psig with regulator 16A. Turn on camera and flood lights. By-pass 3-way valve 32 through wet gas meter (33).
- 4.11 Crack LH<sub>2</sub> flow control valve (27A) open until flow rate reaches about 75 SCFM on flow meter (31).
- 4.12 Record GHe flow on (23) and pressure on both pressure gages (24A) (8B).
- 4.13 Check for GHe leak with leak detector (41) throughout test run.
- 4.14 When a pressure on LH<sub>2</sub> side of diaphragm drops down to zero and the ΔP chart reading increases to 15 psig, by-pass wet gas meter (33) with 3-way valve (32). Shut off camera and recorders. Turn off flood lights.

- 4.15 Record total flow and temperature of wet gas meter (33) .
- 4.16 If no leak has occurred, proceed with reversal of bladder by closing off LH<sub>2</sub> control valve (27A) .
- 4.17 Turn on recorders, camers, and lights.
- 4.18 Open LH<sub>2</sub> solenoid valve (8B) .
- 4.19 Close off GHe solenoid valve (12G) .
- 4.20 Open GHe vent flow control valve (27B) and control vent rate with valve (48) for 10 to 12 minute run. Observe pressures on both sides of diaphragm pressure gages (24A) & (B) .
- 4.21 Sniff GHe vent for H<sub>2</sub> leak with detector (42) throughout test run.
- 4.22 When pressure on GHe side of bladder approaches zero and ΔP approaches 20 psig, shut off LH<sub>2</sub> supply, valve (8B) and vent to atmosphere, valve (8C) .
- 4.23 When LH<sub>2</sub> is expelled from LH<sub>2</sub> vent, repeat cycle, operations 4.7 through 4.22 until a leak is indicated. Check camera after each reversal to assure film loading.

#### 5.0 SHUT DOWN PROCEDURE:

In the event of failure, leak or inspection, the shut down procedure is as follows:

- 5.1 Shut off camera, light, and recorders.
- 5.2 LH<sub>2</sub> supply is closed off at the dewar.  
Note: Cryostat solenoid valve (8A) , globe valve (9) , and LH<sub>2</sub> vent valve (8C) must remain open.
- 5.3 GHe purge valves (12D) , (E) , (8F) and (13A) are opened and valves (20) , (22) , and GHe expulsion valve 12G are closed. LH<sub>2</sub> and GHe flow valves (27A) & (B) are opened to prevent expanding gases from pressurizing during warm up.

- 5.4 Purge slowly for about two hours then remove camera and lights.
- 5.5 Remove photo tube assembly, Item D.
- 5.6 Remove cryostat, Item C.
- 5.7 Turn off all purges.
- 5.8 Remove cover plate on  $\text{LH}_2$  cryostat, Item B.
- 5.9 Remove expulsion head, Item A.
- 5.10 Inspect diaphragm.
- 5.11 Remove test rig to shop for removal of diaphragm.
- 5.12 Remove diaphragm, inspect and measure leakage rate by installing in Arde Inc. leak test fixture.
- 5.13 After inspection reassemble per 3.1 thru 3.15 if the diaphragm has not failed or completed 20 reversals.

- 4.15 Record total flow and temperature of wet gas meter (33) .
- 4.16 If no leak has occurred, proceed with reversal of bladder by closing off  $\text{LH}_2$  control valve (27A) .
- 4.17 Turn on recorders, camers, and lights.
- 4.18 Open  $\text{LH}_2$  solenoid valve (8B) .
- 4.19 Close off GHe solenoid valve (12G) .
- 4.20 Open GHe vent flow control valve (27B) and control vent rate with valve (48) for 10 to 12 minute run. Observe pressures on both sides of diaphragm pressure gages (24A) & (B) .
- 4.21 Sniff GHe vent for  $\text{H}_2$  leak with detector (42) throughout test run.
- 4.22 When pressure on GHe side of bladder approaches zero and  $\Delta P$  approaches 20 psig, shut off  $\text{LH}_2$  supply, valve (8B) and vent to atmosphere, valve (8C) .
- 4.23 When  $\text{LH}_2$  is expelled from  $\text{LH}_2$  vent, repeat cycle, operations 4.7 through 4.22 until a leak is indicated. Check camera after each reversal to assure film loading.

#### 5.0 SHUT DOWN PROCEDURE:

In the event of failure, leak or inspection, the shut down procedure is as follows:

- 5.1 Shut off camera, light, and recorders.
- 5.2  $\text{LH}_2$  supply is closed off at the dewar.  
Note: Cryostat solenoid valve (8A), globe valve (9), and  $\text{LH}_2$  vent valve (8C) must remain open.
- 5.3 GHe purge valves (12D), (E), & (F) and (13A) are opened and valves (20), (22), and GHe expulsion valve 12G are closed.  $\text{LH}_2$  and GHe flow valves (27A) & (B) are opened to prevent expanding gases from pressurizing during warm up.

- 5.4 Purge slowly for about two hours then remove camera and lights.
- 5.5 Remove photo tube assembly, Item D.
- 5.6 Remove cryostat, Item C.
- 5.7 Turn off all purges.
- 5.8 Remove cover plate on  $\text{LH}_2$  cryostat, Item B.
- 5.9 Remove expulsion head, Item A.
- 5.10 Inspect diaphragm.
- 5.11 Remove test rig to shop for removal of diaphragm.
- 5.12 Remove diaphragm, inspect and measure leakage rate by installing in Arde Inc. leak test fixture.
- 5.13 After inspection reassemble per 3.1 thru 3.15 if the diaphragm has not failed or completed 20 reversals.

WORK STATEMENT WS-200

LH<sub>2</sub> CYCLE TESTING OF 13" METALLIC DIAPHRAGMS

Contract NAS 3-12026 - J/N 46002-3 and -7

The following four (4) tasks shall be performed as described below:

<u>Task No.</u>	<u>Description of Task</u>
-----------------	----------------------------

- |   |   |
|---|---|
| 1 | <u>Design, fabrication, assembly, pre-test check out and dry run on the LH<sub>2</sub> Diaphragm cycle test rig</u> |
|---|---|

The Arde Inc. test subcontractor will be responsible for all plumbing, instrumentation, indium wire, and support frame for the cycling test. Referring to SKD 10500, Arde Inc. will furnish the test subcontractor with items (1), (5), (56), (57), (58), (59) and (60). GH<sub>e</sub> and LH<sub>2</sub> will be Government Furnished. Arde Inc. Drawing TJ 10149 (Item 1) also includes the mating female bayonet fittings on the two vacuum jacketed LH<sub>2</sub> lines. All interfaces will be indicated on the TJ 10149 drawings and bills of material.

The following items on this task must be approved and accepted by ARDE:

- a. Test schematic drawing and associated drawings.
- b. Equipment bill of materials.
- c. Test Operation Procedure (including position of all valves for each operational step).
- d. Dry run of cycle test rig using LH<sub>2</sub> as the cryogenic fluid. ARDE will furnish a diaphragm assembly and an observer for this test. Acceptance will be determined by ease of operation, leakage rates, cool down rates, and safety of the operation.

<u>Task No.</u>	<u>Description of Task</u>
1(Cont)	All instrumentation must be calibrated to standards and capable of performing their task efficiently and accurately. One (1) copy of check out test data is to be furnished to ARDE.

Drawing SKD 10500 "13" Diaphragm Cryogenic Cycling Test Schematic", and Test Operational Procedure 200 "Operational Procedures for Diaphragm Cryogenic Cycle Test" are to be used as a guide in preparation and design of the cycle test rig for this task. The test subcontractor can and should utilize his own equipment and facilities wherever feasible providing that it is economical and the objectives of the test program can be met in their entirety. ARDE will consider any alternatives that will improve the test set up, increase safety, and produce operating economies.

2      "13" Stainless Steel Diaphragm Cycling Test"

Ref. Test Plan 201, D3745 Diaphragm (typical) and Test Operational Procedure 200 (TOP 200).

Four (4) stainless steel diaphragms will be cycle tested to failure or until 20 reversals are completed. Each diaphragm cycling test will have three (3) intermediate shut downs for inspection and re-start of the test. All  $GH_e$ ,  $LH_2$ ,  $LN_2$  and  $GN_2$  will be government furnished.

The following information will be obtained from each test:

1. Expulsion efficiency measurement.
2.  $LH_2$  flow rates-recorded.
3. Differential pressure across diaphragm-recorded and measured.
4. Static pressures,  $GH_e$ ,  $LH_2$  and  $GH_2$ -recorded and measured.



<u>Task No.</u>	<u>Description of Task</u>
2 (Cont)	<ol style="list-style-type: none"><li>5. Temperatures, <math>LH_2</math>, <math>GH_2</math> and <math>GH_e</math>-recorded and measured.</li><li>6. Leak detection of <math>GH_e</math> and <math>GH_2</math> across diaphragm.</li><li>7. Inspection of the diaphragms during test will be conducted at the discretion of the Arde Inc. observer. A total of twelve (12) test shut-down inspections will be made other than failure or completion of 20 reversal run post-test inspections. The shut-down inspection during testing will consist of the following:<ol style="list-style-type: none"><li>a. Cast of the diaphragm surface to determine bend radius.</li><li>b. Pi-tape outside diameter or caliper inside diameter of reinforcing wire hoops.</li><li>c. Pi-tape outside diameters of diaphragm shell at various gage heights.</li><li>d. Measure amplitude and span of circumferential buckles between the reinforcing wires of the diaphragm shell. Cast may be used to obtain this information.</li><li>e. Leak rate measurement across diaphragm.</li></ol></li><li>8. Post-test inspections after test completion will consist of the following:<ol style="list-style-type: none"><li>a. Photographs (black and white) to be taken of all failures and the diaphragm assembly after test.</li><li>b. Visual report is to be made of the nature of the failure.</li><li>c. The diaphragm assembly is to be shipped immediately after (a) and (b) are completed to Arde Inc. for their inspection.</li></ol></li></ol>

The test subcontractor will have to provide and supply the following services and materials under this task:

<u>Task No.</u>	<u>Description of Task</u>
2 (Cont)	<ul style="list-style-type: none"><li>a. Preliminary check out, calibration, drying and purging of all equipment.</li><li>b. Diaphragm installation, sealing (indium), insulation of lines, movie film, photographs, and recording paper.</li><li>c. Assembly personnel also technicians and test engineer for conducting test.</li><li>d. Stand by services: Vacuum pumps, vacuum chamber instrument lab, test site, assembly area, inspection area, and a test set-up storage area (between test).</li><li>e. Reproduction of the test results, recorded data, photographic coverage (16 mm films plus stills) and inspection data after each cycling test.</li><li>f. Return of test diaphragm to ARDE for inspection.</li></ul>
3	<p><u>"13" Aluminum Diaphragm Cycling Test"</u></p> <p>Ref. Test Plan 202 and TOP 200.</p> <p>One (1) aluminum diaphragm will be cycle tested to failure or until 20 reversals are completed.</p> <p>Three (3) intermediate shut downs for inspection and re-start will be necessary during this test. <math>\text{GH}_e</math> and <math>\text{LH}_2</math> will be Government Furnished.</p> <p>The test subcontractor will have to provide the same services and materials as outlined in Task 2, with exception that only one test instead of four will be conducted.</p>
4	<p><u>Final Report: Three (3) copies</u></p> <p>This task will include a summary test report of all testing conducted under this contract. This report will include the following:</p>

<u>Task No.</u>	<u>Description of Task</u>
4 (Cont)	I Objective
	II Test Set Up
	a. Schematic
	b. Bill of Materials
	III Test Procedures
	IV Test Results of Each Test
	a. Test Data (original plus 2 copies)
	b. Inspection Data (original plus 2 copies)
	c. Photographs
	d. Failure Report
	e. Instrumentation Calibrations

19 February 1969

ACCEPTANCE CRITERIA 20013" Diaphragm Cryogenic Cycling Test Rig

Contract: NAS 3-12026, "Metallic Positive Expulsion Diaphragm"  
Arde J/N 46002-3 and 46002-7

1. GENERAL:

The 13" metallic diaphragm cryogenic test rig shall be acceptance tested by the test subcontractor using liquid hydrogen as the cryogenic fluid. Arde, Inc. will furnish a test diaphragm assembly and an observer for the acceptance test(s). Acceptance of the cryogenic test set up will be determined by ease of operation, leakage rates, cool down rates, measurement accuracies, safety of operation, photographic coverage, etc. as defined herein.

Prior approval by Arde of the subcontractor furnished test schematic drawings, Equipment Bill of Materials, and Test Operation Procedure must be obtained before acceptance testing of the cryogenic cycling test set up can begin.

2. DESIGN APPROVAL AND RELATED ITEMS:

The test contractor shall supply Arde, Inc. with a complete schematic of the cryogenic cycling test set up similar to Arde, Inc. schematic SKD 10500. All items and components on this schematic shall be identified and coded for operational procedures. A complete bill of material shall be supplied giving component description, size, rating, manufacturer, range accuracy, and model number. All equipment and components purchased under funding for this contract shall be identified for material accountability.

The minimum accuracy of all instrumentation shall be  $\pm 1\%$  of full scale reading and this accuracy must be verified and certified by calibration within six months prior to test.

18 February 1969

All components must meet the environmental conditions required by the cycling test; i.e., temperature, pressure, fluid or gas medium, and be capable of operating continuously in a satisfactory manner for at least twenty (20) fifteen (15) minute cycles of running time and after resetting or reloading for a total number of one hundred fifty (150) diaphragm reversals. The camera can be reloaded after each diaphragm test or test inspection.

The test contractor shall be responsible for selecting the type of 16 mm movie camera used so as to assure good motion picture photographic coverage of diaphragm reversals under cryogenic test conditions. A camera with a focal plane of approximately three (3) feet with a depth of field of  $\pm$ seven (7) inches about its focal plane is suggested. Flood lighting shall be white light. The camera must be sequenced by an intervalometer to conserve the amount of movie film used per test (400 ft. preferred). All recording equipment should have adjustable paper speeds to regulate the amount of paper used per diaphragm reversal to about 1 or 2 inches per minute.

The following data must be recorded continuously:

1.  $\text{LH}_2$  temperature.
2.  $\text{LH}_2$  diaphragm pressure.
3.  $\text{GH}^e$  temperature.
4.  $\text{GH}^e$  diaphragm pressure.
5.  $\Delta P^e$  across diaphragm.
6.  $\text{GH}_2$  temperature (at flow meter).
7.  $\text{GH}_2$  pressure (at flow meter).
8.  $\text{GH}_2$  flow rate.

The following data must be observed and noted on data sheets:

1. Purge flow rates
2. Tare readings of wet meter
3. Final readings of wet meter
4.  $\text{GH}^e$  detector readings
5.  $\text{GH}_2$  detector readings

6.  $\text{GH}_e$  expulsion pressure gage reading  
(observed only)
7.  $\text{LH}_2$  level readings (observed only)
8. Time
9. Film serial number, diaphragm part and  
serial number, reversal number, date

3. TEST OPERATION PROCEDURE DESCRIPTION: (Including position of all valves for each operational step)

This procedure will describe step by step the assembly of the diaphragm into the test rig and the test set up, purging of the rig, cool down, start up, shut down for inspection, start up, shut down for failure and disassembly.

4. ACCEPTANCE TEST CRITERIA:

The following criteria will be used for acceptance of the test rig.

- a) Visual inspection of the test rig prior to assembly including check off of circuit and components versus schematic and bill of material.
- b) Inspection of all instrumentation for date of last calibration.
- c) Check off of assembly procedure to assure the following:
  - 1) No leaks in cryogenic lines, interfaces, and diaphragm and test rig seals. Use  $\text{GHe}$  leak detector for this purpose.
  - 2) Check out all control functions.
  - 3) Dry run of movie camera and check to assure a good picture.
  - 4) Time the cool down and hold liquid without cycling for fifteen (15) minutes to be sure that  $\text{LH}_2$  will not flash during run. The test set up shall be

19 February 1969

capable of cooling down and heating cryogenic liquids and gases to the following temperatures:

1.  $\text{LH}_2$ , - 423°F  $\begin{matrix} +10^\circ\text{F} \\ - 0^\circ\text{F} \end{matrix}$
2.  $\text{GH}_e$ , - 423°F  $\begin{matrix} +10^\circ\text{F} \\ - 0^\circ\text{F} \end{matrix}$
3.  $\text{GH}_2$ , 10°F below ambient room temperature  
(at  $\text{GH}_e$  flow meter)

d) Reverse diaphragm and take all measurements and photographs.

e) Reverse diaphragm and shut down test.

f) Check operation of all instrumentation to assure  $\pm 1\%$  recording accuracy.

g) Review film for good photographic coverage.

5. CONDITIONS OF ACCEPTANCE:

a) The test contractor shall correct any deficiency in his part of the test set up (not including ARDE furnished equipment).

b) Any rework that is done to ARDE furnished equipment must be approved by or done by direction of ARDE. Examples of the afore-said rework are the insertions of  $\text{LH}_2$  level probes into the test fixture or changes that may be required for better photography.

c) Deviations from the Approved Test Procedure must be approved and amended by both parties at no extra cost to ARDE.

d) The acceptance test date notice shall be given at least one week in advance to ARDE and the test shall be conducted on schedule.

e) ARDE reserves the right to direct that remote solenoid valves be used for manual valves if the timing for opening and closing the valves are critical and personnel are endangered by operating in this manner. This revision will be made at no extra expense to ARDE.

7.0 DISTRIBUTION LIST FOR FINAL REPORT - NASA CR-72775

Contract NAS 3-12026

ARDE, INC.

No. of Copies

National Aeronautics & Space Administration  
Lewis Research Center  
21000 Brookpark Road  
Cleveland, Ohio 44135

Attention: Contracting Officer, MS 500-313	1
Liquid Rocket Technology Branch, MS 500-209	5
Technical Report Control Office, MS 5-5	1
Technology Utilization Office, MS 3-16	1
AFSC Liaison Office, MS 501-3	2
Library, MS 60-3	1
Office of Reliability & Quality Assurance MS 500-111	1
D. L. Nored, MS 500-209	1
R. F. Lark, Project Manager, MS 49-1	25
E. W. Conrad, MS 500-204	1
R. H. Kemp, MS 49-1	1
R. H. Knoll, MS 501-2	1

National Aeronautics & Space Administration  
Washington, D. C. 20546

Attention: A. O. Tischler, Director, Shuttle Technology Office	1
D. Ginter, Director, Technology Applications Office	1
W. Woodward, Director, Propulsion & Power Division	1
G. Deutsch, Director, Materials & Structures Division	1

National Aeronautics & Space Administration  
Ames Research Center  
Moffett Field, California 94035

Attention: Library	1
C. A. Syvertson	1

National Aeronautics & Space Administration  
Flight Research Center  
P. O. Box 273  
Edwards, California 93532

Attention: Library	1
--------------------	---



National Aeronautics & Space Administration  
Goddard Space Flight Center  
Greenbelt, Maryland 20771

Attention: Library

1

National Aeronautics & Space Administration  
John F. Kennedy Space Center  
Cocoa Beach, Florida 32931

Attention: Library

1

National Aeronautics & Space Administration  
Langley Research Center  
Langley Station  
Hampton, Virginia 23365

Attention: Library

1

National Aeronautics & Space Administration  
Manned Spacecraft Center  
Houston, Texas 77001

Attention: Library

1

National Aeronautics & Space Administration  
George C. Marshall Space Flight Center  
Huntsville, Alabama 35812

Attention: Library

1

Keith Chandler

1

Leon J. Hastings

1

Harry L. McDaris

1

Jet Propulsion Laboratory  
4800 Oak Grove Drive  
Pasadena, California 91103

Attention: Library

1

L. Toth

1

NASA Scientific & Technical Information Facility  
P. O. Box 33  
College Park, Maryland 20740

15

Director, Technology Utilization Division  
Office of Technology Utilization  
National Aeronautics & Space Administration, Headquarters  
Washington, D. C. 20546

1

Defense Documentation Center .  
Cameron Station  
Building 5  
5010 Duke Street  
Alexandria, Virginia 22314

Attention: TISIA 1

Office of the Director of Defense Research  
and Engineering  
Washington, D. C. 20301

Attention: Office of Assistant Director (Chem. Technology) 1

Arnold Engineering Development Center  
Air Force Systems Command  
Tullahoma, Tennessee 37389

Attention: Library 1  
AEOIM 1

Advanced Research Projects Agency  
Washington, D. C. 20525

Attention: D. E. Mock 1

Aeronautical Systems Division  
Air Force Systems Command  
Wright-Patterson Air Force Base,  
Dayton, Ohio 45433

Attention: Library 1  
J. K. Sieron (MANE) 1

Air Force Missile Test Center  
Patrick Air Force Base, Florida

Attention: Library 1

Air Force Systems Command  
Andrews Air Force Base  
Washington, D. C. 20332

Attention: Library 1

Air Force Rocket Propulsion Laboratory  
Edwards, California 93523

Attention: Library 1  
J. Brannigan 1

No. of Copies

Air Force Office of Scientific Research  
Washington, D. C. 20333

Attention: Library 1

Space & Missile Systems Organization  
Air Force Unit Post Office  
Los Angeles, California 90045

Attention: Technical Data Center 1

Office of Research Analyses (OAR)  
Holloman Air Force Base, New Mexico 88330

Attention: Library - RRRD 1

U. S. Air Force  
Washington, D. C.

Attention: Library 1

Commanding Officer  
U. S. Army Research Office (Durham)  
Box CM, Duke Station  
Durham, North Carolina 27706

Attention: Library 1

U. S. Army Missile Command  
Redstone Scientific Information Center  
Redstone Arsenal, Alabama 35808

Attention: Document Section 1

U. S. Naval Ordnance Systems Command  
Department of the Navy  
Washington, D. C.

Attention: Library 1

Commander  
U. S. Naval Weapons Center  
China Lake, California 93557

Attention: Library 1

U. S. Naval Ship Research & Development Laboratory  
Annapolis, Maryland 21402

Attention: C. Hershner, Code A-731 1

No. of Copies

Commanding Officer  
Naval Research Branch Office  
1030 East Green Street  
Pasadena, California 91101

Attention: Library

1

Director (Code 6180)  
U. S. Naval Research Laboratory  
Washington, D. C. 20390

Attention: Library

1

Picatinny Arsenal  
Dover, New Jersey 07801

Attention: Library

1

I. Forsten

1

Air Force Aero Propulsion Laboratory  
Research & Technology Division  
Air Force Systems Command  
United States Air Force  
Wright-Patterson AFB, Ohio 45433

Attention: RPRP (Library)

1

R. Quigley

1

Propulsion Division  
Aerojet-General Corporation  
P. O. Box 15847  
Sacramento, California 95803

Attention: Technical Library 2484-2015A

1

Aeronutronic Division of Philco-Ford Corporation  
Ford Road  
Newport Beach, California 92663

Attention: Technical Information Department

1

Boeing Company  
Space Division  
P. O. Box 868  
Seattle, Washington 98124

Attention: Library

1

Chemical Propulsion Information Agency  
Applied Physics Laboratory  
8621 Georgia Avenue  
Silver Springs, Maryland 20910

Attention: T. Reedy 1

Curtiss-Wright Corporation  
Wright Aeronautical Division  
Woodridge, New Jersey

Attention: Library 1

University of Denver  
Denver Research Institute  
P. O. Box 10127  
Denver, Colorado 80210

Attention: Security Office 1

Fairchild Stratos Corporation  
Aircraft Missiles Division  
Hagerstown, Maryland

Attention: Library 1

Research Center  
Fairchild Hiller Corporation  
Germantown, Maryland

Attention: Library 1

General Dynamics/Convair  
P. O. Box 1128  
San Diego, California 92112

Attention: Library 1

Missiles and Space Systems Center  
General Electric Company  
Valley Forge Space Technology Center  
P. O. Box 8555  
Philadelphia, Pennsylvania 19101

Attention: Library 1

General Electric Company  
Flight Propulsion Laboratory Department  
Cincinnati, Ohio

Attention: Library 1

Martin-Marietta Corporation  
Baltimore Division  
Baltimore, Maryland 21203

Attention: Library 1

Martin-Marietta Corporation  
Denver Division  
P. O. Box 179  
Denver, Colorado 80201

Attention: Library 1

R. Fearn 1

Rocketdyne Division  
North American Rockwell, Inc.  
6633 Canoga Avenue  
Canoga Park, California 91304

Attention: Library, Department 596-306 1

Space & Information Systems Division  
North American Rockwell  
12214 Lakewood Boulevard  
Downey, California 90241

Attention: Library 1

Northrop Space Laboratories  
3401 West Broadway  
Hawthorne, California

Attention: Library 1

Radio Corporation of America  
Astro-Electronics Products  
Princeton, New Jersey 08540

Attention: Library 1

Y. Brill 1

TRW Space Systems, Inc.  
One Space Park  
Redondo Beach, California 90278

Attention: Technical Library Document Acquisitions 1

TRW, Incorporated  
TAPCO Division  
23555 Euclid Avenue  
Cleveland, Ohio 44117

Attention: Library 1

No. of Copies

United Aircraft Corporation  
Corporation Library  
400 Main Street  
East Hartford, Connecticut 06108

Attention: Library

1

United Aircraft Corporation  
Pratt & Whitney Division  
Florida Research & Development Center  
P. O. Box 2691  
West Palm Beach, Florida 33402

Attention: Library

1

United Aircraft Corporation  
United Technology Center  
P. O. Box 358  
Sunnyvale, California 94038

Attention: Library

1

Vought Astronautics  
Box 5907  
Dallas, Texas

Attention: Library

1

Garrett Corporation  
AiResearch Division  
Phoenix, Arizona 85036

Attention: Library

1

Garrett Corporation  
AiResearch Division  
Los Angeles, California

Attention: Library

1

Grumman Aircraft Engineering Corporation  
Bethpage, Long Island, New York

Attention: Library

1

Honeywell, Inc.  
Aerospace Division  
2600 Ridgeway Road  
Minneapolis, Minnesota

Attention: Library

1

IIT Research Institute  
Technology Center  
Chicago, Illinois 60616

Attention: Library

1

Kidde Aer-Space Division  
Walter Kidde & Company, Inc.  
675 Main Street  
Belleville, New Jersey

Library

Ling-Temco-Vought Corporation  
P. O. Box 5907  
Dallas, Texas 75222

Attention: Library

1

Lockheed Missiles and Space Company  
P. O. Box 504  
Sunnyvale, California 94087

Attention: Library

1

Aerospace Corporation  
2400 East El Segundo Boulevard  
Los Angeles, California 90045

Attention: Library-Documents

1

Astropower Laboratory  
McDonnell-Douglas Aircraft Company  
2121 Paularino  
Newport Beach, California 92163

Attention: Library

1

ARO, Incorporated  
Arnold Engineering Development Center  
Arnold AF Station, Tennessee 38389

Attention: Library

1

Susquehanna Corporation  
Atlantic Research Division  
Shirley Highway and Edsall Road  
Alexandria, Virginia 22314

Attention: Library

1



Battelle Memorial Institute  
505 King Avenue  
Columbus, Ohio 43201

Attention: Report Library, Room 6A

1

Beech Aircraft Corporation  
Boulder Facility  
Box 631  
Boulder, Colorado

Attention: Library  
D. Pope

1

1

Bell Aerospace Company  
P. O. Box 1  
Buffalo, New York 14205

Attention: Library  
L. Thompson

1

1

Commander  
U. S. Naval Missile Center  
Point Mugu, California 93041

Attention: Technical Library

1

Commander  
U. S. Naval Weapons Center  
China Lake, California 93557

Attention: Library

1

U. S. Atomic Energy Commission  
Technical Information Services  
P. O. Box 62  
Oak Ridge, Tennessee

Attention: A. P. Huber, Code ORGDP

1